STUDY OF LASER SPECKLE REDUCTION FOR LASER DISPLAY
APPLICATIONS

STUDY OF LASER SPECKLE REDUCTION FOR LASER DISPLAY
APPLICATIONS

BY Qianli Ma, B.Sc.

A Thesis Submitted to the School of Graduate Studies in Partial Fulfillment of the

Requirement for the Degree Doctor of Philosophy

McMaster University © Copyright by Qianli Ma, August 2018

DOCTOR OF PHILOSOPHY (2018)   McMaster University

(Engineering Physics)   Hamilton, Ontario

TITLE: Study of Laser Speckle Reduction for Laser Display Applications

AUTHOR: Qianli Ma,

B.Sc. (University of Science and Technology of China)

SUPERVISOR: Professor Chang-qing Xu

NUMBER OF PAGES: xiv, 131

Abstract

Laser-based projection displays have been under active development over last few years. Lasers are considered as the next generation light sources for projection due to advantages including wide color gamut, high brightness, long lifetime and high electric-optic efficiency. However, speckle phenomenon caused by the coherence of lasers can greatly influence the quality of projected images. A cost effective, easy setup and robust speckle reduction system for laser projection is still very challenging.

The aim of this thesis is to investigate practical speckle reduction solutions for laser projection system. The system is divided into different modules and for each module, speckle reduction methods are studied. The study includes a low speckle laser source, an optical engine with integrated speckle reduction methods and a low speckle engineered screen. A standard speckle measurement system corresponding to human perception is also presented.

For low speckle laser source, a theoretical model that describes wavelength diversity in speckle reduction is established. The speckle contrast ratio (SCR) of the system can be simulated. The result is experimentally verified. Guidelines for optimized wavelength/power selection for lasers to generate reduced speckle are proposed. After this, a low cost, high compact and high-efficiency speckle reduction optical system using an electric elastomer actuator is studied. Both theoretical analysis and experimental work are

presented and a SCR as low as 3.7% was achieved. Besides these two parts, an engineered screen that utilizes micro lens array (MLA) which can greatly reduce speckle is studied. A comprehensive theoretical model was established for the simulation and optimization of MLA in speckle reduction. The simulated results agree well with reported values. Guidelines in MLA selection for laser projection are presented.

In the last part, a standard measurement setup of speckle in a laser projection system that matches the human perception is studied. Conditions including camera F/#, focal length, integration time and measuring geometry are discussed and suitable setups are proposed.

Acknowledgements

As for me, the experience of Ph.D. studying is like a road trip. The destination is not the only purpose, the people who you met, the things you experienced, the mountains that you conquered, all these together, give the full meaning of this Ph.D. trip.

When look back, there are many people and things that I really want to show my gratitude and appreciation. Firstly, I would like to thank my supervisor Dr. Chang-Qing Xu, who has offered me great encouragement, expert guidance and enormous support in both academic and personnel development through my entire Ph.D. program. I will not have such a positive and enriching experience in McMaster without his patience and support. I am truly fortunate to have him as my supervisor.

Also, I would like to show special thanks to Dr. Adrian Kitai and Dr. Qiyin Fang, who gave me many remarkable academic suggestions regarding my research as my supervisory committee members for the entire Ph.D. study. Thanks all the professors in the Department of Engineering Physics for their valuable suggestions on my research. Thanks Peter Jonasson and Doris Stevanovic for all their help in the lab. Thanks also to Marilyn and Nico for their help in the Engineering Physics office. I would like to express my gratitude to all members of Department of Engineering Physics and McMaster staff that helped me.

Thanks Dr. Yi Gan, Dr. Tianyi Guo for their suggestions and discussions related to my research. I also would like to thank my colleagues, Bin Zhang, Mahmoud Talaat and

Yushan Zhang. It is a very pleasant experience to know you and work with you.

I also want to say thank you to my parents for their support and encouragement. I would never have the chance to work on Engineering Physics without them. In the end, I want to show my deepest gratitude to my wife Xiaoshuo Gao. She is the source of power for me to keep moving forward and she is the best partner ever.

Table of Contents

List of Figures

List of Tables

CHAPTER 1

Introduction

1.1. An Overview of Laser Projection

Display technology is a key technology that people use frequently in their daily lives. The need for better color, higher resolution, and more brightness provide the driving force for the development of display technology. Laser display technology has multiple characteristics that meet the previous trend. These days, laser display technology is developing rapidly. Particularly in the projection field, laser projection is considered as the next generation of projection technology, after lamp and LED-based projection.

Arc lamps are the major light sources of today's projectors. The lamps are available in a wide range of powers, from about 50W to 900W [1]. They have an acceptable lifetime of over 1,000 hours [2], which can meet the minimal requirements for projection applications. However, as metals are used in the lamps and they will react with electrodes and form compounds, the spectrum of the lamps will change slowly over their lifetime, introducing color mismatch in projection [1]. Other than that, these lamps have a wide spectrum, which means color filters have to be used in order to get red, green and blue

primary colors. This results in a very low lumen efficiency [3].

Light emitting diodes (LEDs) are a mature technology and have been widely used in projectors. Compared to arc lamps, they do not require warm-up time, as they are small and can be switched fast. Also, they are available in all of the primary colors, which is a major advantage over lamps.

Although LEDs have many advantages, they also have some limits. First, the brightness of LEDs will drop slowly over their lifetime [4]. Second, they have a large étendue because of their large emission angles. Thus, the light collection within the projector can be challenging. Third, the brightness of LEDs (per unit emission area) is much lower than lamps [5]. This disadvantage prevents LEDs used in applications like in cinemas and conferences that require high power.

Compared to traditional light sources, projectors using lasers as a light source have many advantages. One of the biggest advantages is the wide gamut. Due to extremely narrow linewidth, lasers can be considered as a quasi-monochromic light source. Compared to primary colors from traditional light sources, which usually have a linewidth of 40nm-50nm, lasers can provide a much narrower linewidth, usually less than 3nm. Thus, in the visible range, when using lasers as primary colors, maximum gamut range can be covered.

Figure 1.1 shows the gamut range of different technologies [6]. It can be seen that lasers can provide a much bigger gamut range compared to a CRT, lamp or LED light source. In 2012, the International Telecommunication Union (ITU) published the latest recommendation standard, BT.2020, for ultra-high-definition television with standard dynamic range and wide color gamut [7]. Lasers are the only light source that can provide

more than 95% gamut coverage of BT.2020 in projection display.
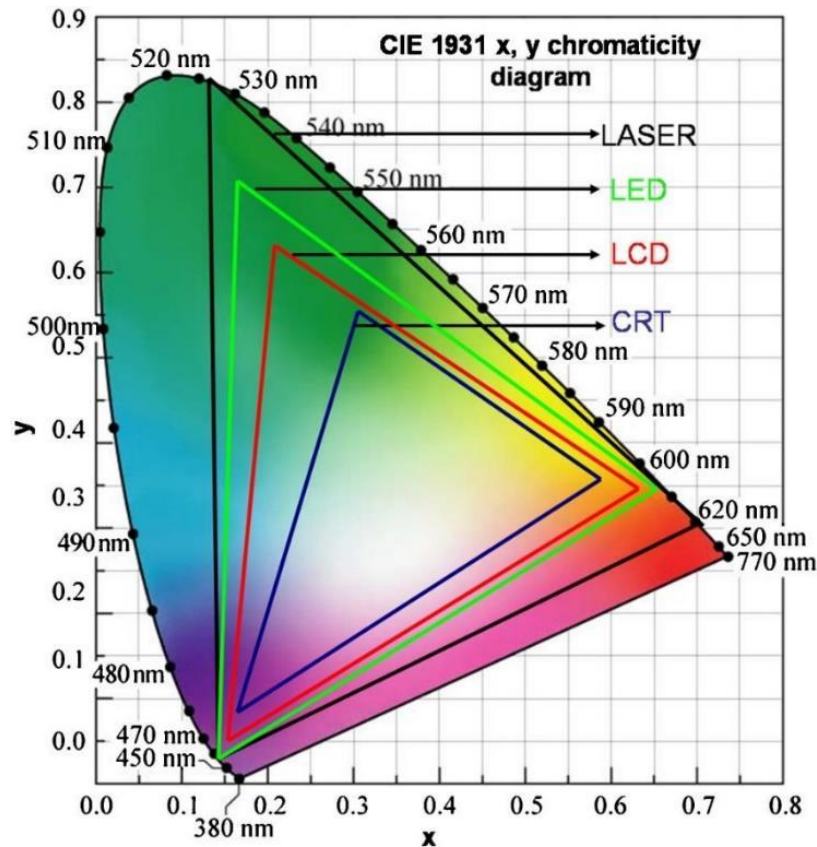
Figure 1.1 Gamut area of different display technologies [6] (Adapted with permission)

Other than wide color gamut, lasers also provide a much longer lifetime (up to 50,000 hours) [8]. This can greatly reduce the maintenance cost of projectors. Moreover, the emitting wavelengths of lasers will not shift with the increasing operation time, whereas lamps will gradually shift [1] and require color recalibration, which will also add extra cost.

Another big advantage of laser projection is high efficiency. The laser light comes from stimulated emission in the gain material of lasers. Compared to the spontaneous emission of phosphor light or heat illumination, it has a much higher energy efficiency. The

electric-opto efficiency of laser diodes can exceed 30% [9]. Also, lasers have a very narrow linewidth; by selecting the correct wavelengths, almost all light from the laser source can be utilized. This is very different from a lamp-based projector where color filters have to be used to get red, green and blue primary colors [1]. A substantial amount of light has to be filtered out. Also, the lamp emits light within the infrared range as well, which is wasted completely.

Also, lasers have higher brightness and smaller étendue [10]. These advantages give lasers the opportunity to be widely used and to have high profit.

Figure 1.2 Christie RGB laser projector (copyright: Christie)

In recent years, many companies have been trying to work on laser display technology. In 2008, Mitsubishi published the first laser television "LaserVue", which has a screen size of 65 inches, a brightness of $500cd/m^2$, and a continuous working lifetime of

more than 20,000 hours [11]. Microvision also provided a pico-laser projector the size of a cellphone in 2009 [12]. For theater and conference applications, Christie built the first cinema laser projector with 4K resolution in 2014, which is shown in Figure 1.2. It utilizes a multimode fiber bundle for laser coupling and has a brightness output of up to 120,000 lumen, which is much higher than a traditional lamp-based cinema projector with an average lumen of around 25,000 lm [13].

1.2. Speckle Issue in Laser Projection

Although after long development, laser projection is at the dawn of large-scale application, it still has several technical barriers that need to be solved. One of the biggest issues is speckle phenomenon.

Speckle is a special physical phenomenon caused by high coherence of the laser source. Generally speaking, it is a random intensity pattern caused by random interference of laser light. The speckle pattern will greatly degrade image quality in projection and result in loss of image information [14]. Figure 1.3 is an example of an image with and without a speckle pattern.

<div align="center">(a)   (b)</div>

Figure 1.3 a) Original image without speckle and b) with speckle

In order to evaluate speckle level in a laser projection system, the concept of speckle contrast ration (SCR) is often used. The SCR is defined as:

$$\text{SCR} = \frac{\sigma_I}{\bar{I}} \tag{1.1}$$

where σ_I is the standard derivation of intensity fluctuation of the speckle field and $\bar{I}$ is the average intensity of the speckle field. SCR value often lies within the range of 0 to 1, where 0 means no speckle at all and 1 means maximum speckle. In recent years, studies have shown that when the SCR value is below 5%, people can hardly notice the existence of speckle for blue lasers [15]. For green lasers, this value is lower, as human are more sensitivity to green color. People usually consider projection with SCR less than 4% as speckle-free projection.

Multiple methods have been studied to reduce speckle in laser projection. In this section, the origin of speckle and the statistical properties of speckle will be discussed, as well as some typical speckle reduction methods.

1.2.1 Origin of Speckle

In the 1960s, right after the invention of continuous wave lasers, researchers noticed that after the laser beam encounters a diffuser, a granular pattern with random intensity fluctuation can be observed. This pattern is called "speckle".

People realized this random intensity fluctuation is generated from the random surface roughness of the diffuser. In our world, when measured with wavelength scale, the surfaces of many objects can be considered as "rough". These optical rough surfaces provide random phase fluctuations to the wave front of laser beams. These random phase elements overlap and interfere with each other at the image plane and form the random intensity fluctuation as speckle (as in Figure 1.4).
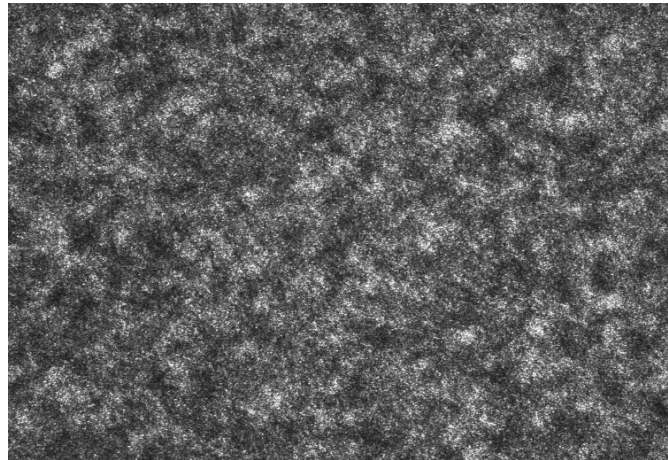
Figure 1.4 A typical speckle pattern

When we look in detail at the origin of speckle, it can be divided into two different categories: 1) objective speckle and 2) subjective speckle [18]. These two types are identified by the different ways a laser beam is propagated.

Figure 1.5(a) shows the origin of objective speckle. The light is reflected/transmitted from an optical rough object and then propagated freely in space. The point at the image plane has a contribution from all elements at the object plane. Due to the random phase introduced by the rough object, random interference will occur at the image plane and generate speckle.

Figure 1.5(b) shows the origin of subjective speckle. Different from objective speckle, in this case, the light is propagated in an imaging system. Limited by the diffraction limits of the optic system, each point on the image plane is only contributed to by elements from the objective plane within the point spread function (PSF) area of the imaging system. Similar as is discussed above, all these elements from the objective plane have random phase fluctuations and will generate random interference, which causes intensity fluctuation at the image plane.
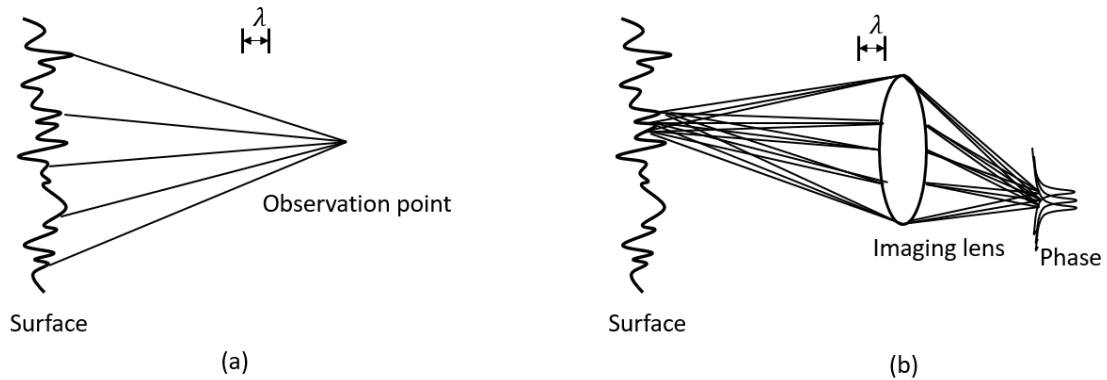
Figure 1.5 Origin of (a) Objective speckle; (b) Subjective speckle

In a practical laser projection system, there will be multiple components that can generate speckle. One of the most common ones is a projection screen. In order to diffuse the light to a large viewing angle, the screen is usually very rough and will act as the random object in Figure 1.5. Also, sometimes diffusers/multimode fibers are used for the purpose of light homogenization; they will also introduce random phases.

As shown in the origin of speckle, the amplitude of a point on the image plane is the summation of N random elements from the objective plane. In most cases, when the number of random elements is very large, where N can be considered as infinite, we say speckle meets this requirement as Gaussian speckle. If N is a limited number, the speckle in this case is called non-Gaussian speckle.

In a laser projection system, most speckle that observers come across is Gaussian speckle. However, in some special cases, non-Gaussian speckle can be generated and have some specific applications. All speckle in this thesis without a special description will be Gaussian speckle.

1.2.2 Statistical Properties of Speckle

In this section, the statistical properties of speckle are discussed. One characteristic of speckle is that we can only measure the intensity distribution of it, rather than amplitude. Thus, the statistical properties of its intensity are studied here. However, the intensity is generated by interference from amplitude. So the analysis will start from amplitude.

As discussed in Section 1.2.1, both subjective speckle and objective speckle are generated by multiple random amplitude elements. A complex element is defined with the following expression:

$$A_n = a_n e^{i\phi_n} \tag{1.2}$$

where a_n is the amplitude of this complex element and ϕ_n is its phase. The summation of N complex elements can be expressed as:

$$A = a e^{i\phi} = \frac{1}{\sqrt{N}} \sum_{n=1}^{N} a_n e^{i\phi_n} \tag{1.3}$$

where A is a phasor representing local light amplitude. N is the number of random complex elements that contribute to A. a and ϕ are amplitude and phase respectively. For a typical speckle generated in laser projection, we can make following assumptions [16]:

1.   For any specific complex element, its amplitude is independent to its phase.

2.   For any two complex elements, their amplitudes and phases are independent to each other.

3.   For random phase ϕ, it has a uniform distribution over range $(-\pi, \pi)$.

When N is infinite, the joint probability density function of amplitude a and phase ϕ can be expressed as[18]:

$$P_{a,\phi}(a, \phi) = \frac{a}{2\pi\sigma^2} \exp\left(-\frac{a^2}{2\sigma^2}\right) \tag{1.4}$$

where σ^2 equals to:

$$\sigma^2 = \sum_{n=1}^{N} \frac{E[a_n^2]}{2} \tag{1.5}$$

And we can get the probability density of amplitude:

$$P_a(a) = \int_{-\pi}^{\pi} P_{a,\phi}(a, \phi)\, d\phi = \frac{a}{\sigma^2} \exp\left(-\frac{a^2}{2\sigma^2}\right) \tag{1.6}$$

which is a Rayleigh distribution. The probability density of phase can also be calculated:

$$P_\phi(\phi) = \int_{0}^{+\infty} P_{a,\phi}(a, \phi)\, da = \frac{1}{2\pi} \tag{1.7}$$

The intensity distribution of A then can be expressed as:

$$P_I(I) = \frac{1}{2\sqrt{I}} P_a(\sqrt{I}) = \frac{1}{2\sigma^2} \exp\left(-\frac{I}{2\sigma^2}\right) \tag{1.8}$$

The Eq.1.5 follows a negative exponential distribution. The expectation of I is:

$$\bar{I} = \int_{0}^{+\infty} P_I(I)\, I dI = 2\sigma^2 \tag{1.9}$$

Thus the distribution can be written as:

$$P_I(I) = \frac{1}{2\sqrt{I}} P_a(\sqrt{I}) = \frac{1}{\bar{I}} \exp\left(-\frac{I}{\bar{I}}\right) \tag{1.10}$$

The Eq.1.10 follows a negative exponential distribution. And second order moment

is:

$$\overline{I^2} = \int_0^{+\infty} P_I(I)\, I^2 dI = 8\sigma^4 \qquad (1.11)$$

Thus the standard derivation of I is:

$$\sigma_I = \sqrt{\overline{I^2} - \overline{I}^2} = 2\sigma^2 = \overline{I} \qquad (1.12)$$

Combined with Equation 1.1, the SCR under this condition is 1. Speckle here is called "fully developed speckle". It is clear that fully developed speckle is very serious and has to be reduced.

As mentioned above, fully developed speckle has to be suppressed. Thus, it is worth discussing the statistical properties of the overlapping of N independent fully developed speckle patterns.

As the overlapping of amplitude will not cause any reduction for the SCR, the overlapping of independent, fully developed speckle patterns is on intensity bases.

The average intensity of the overall image is:

$$\overline{I_{overall}} = \sum_{n=1}^{N} \overline{I_n} \qquad (1.13)$$

where $\overline{I_n}$ is the average intensity of nth speckle pattern. The standard derivation is desired in order to calculate SCR. Thus, the second order moment should be calculated:

$$\overline{I_{overall}}^2 = \sum_{n=1}^{N} \sum_{m=1}^{M} \overline{I_n I_m} = \sum_{n=1}^{N} \overline{I_n}^2 + \sum_{n=1}^{N} \sum_{m \neq n}^{M} \overline{I_n I_m} \qquad (1.14)$$

An assumption is used here, which is when $m \neq n$, different speckle patterns are independent with each other. They all follow negative exponential distribution and have

$$\overline{I_n^{\,2}} = 2\,\overline{I_n}^{\,2}.$$

Thus Eq.1.14 can be written as

$$\overline{I_{overall}^{\,2}} = \sum_{n=1}^{N}\sum_{m=1}^{M}\overline{I_n I_m} = 2\sum_{n=1}^{N}\overline{I_n}^{\,2} + \sum_{n=1}^{N}\sum_{m\neq n}^{M}\overline{I_n I_m} = \sum_{n=1}^{N}\overline{I_n}^{\,2} + (\sum_{n=1}^{N}\overline{I_n})^2$$

$$= \sum_{n=1}^{N}\overline{I_n}^{\,2} + \overline{I_{overall}}^{\,2} \tag{1.15}$$

Thus, the standard derivation of overall is:

$$\sigma_{overall}^{\,2} = \sum_{n=1}^{N}\overline{I_n}^{\,2} \tag{1.16}$$

And SCR is:

$$\text{SCR} = \frac{\sigma_{overall}}{\overline{I_{overall}}} = \frac{\sqrt{\sum_{n=1}^{N}\overline{I_n}^{\,2}}}{\sum_{n=1}^{N}\overline{I_n}} \tag{1.17}$$

when each independent speckle pattern has same average intensity, the above equation can be simplified as:

$$\text{SCR} = \frac{1}{\sqrt{N}} \tag{1.18}$$

This is a very important conclusion. That N independent speckle patterns overlap with each other on intensity, if they have equal average intensity, the SCR of the system after overlapping will drop to $\frac{1}{\sqrt{N}}$. This conclusion can be used in the design of speckle reduction in laser projection systems.

1.2.3 Speckle Reduction in Laser Projection

As speckle degrades projection image quality seriously, it has to be reduced. Many methods have been proposed recently. Before discussing in any detail methods to reduce speckle, it is very helpful to have an overview of ideas in speckle reduction.

Most methods of speckle reduction in laser projection are contributed to by three methods, i.e. wavelength diversity, polarization diversity and angle diversity, which can be expressed as [17]:

$$\text{SCR} = \frac{1}{R} \qquad (1.19)$$

$$R = R_\lambda R_\sigma R_\Omega \qquad (1.20)$$

where R_λ is the wavelength diversity of the system. If the light source is an ideal monochromic laser with a single wavelength, the value of R_λ is 1. In other cases, the R_λ is always a value bigger than 1. For example, when two monochromic lasers with a sufficiently large difference in wavelengths are used, R_λ is $\sqrt{2}$.

R_σ is contribution from the polarization diversity of the screen. For a depolarized screen, this value is equal to $\sqrt{2}$ and for a polarization maintained screen, the value is 1. It is well known that for a polarized maintained screen which is mostly used in 3D projection, laser projection will generate more speckle than conventional screen.

R_Ω is the reduction factor contributed to from the spatial diversity. When using

time-varying components like a vibrating diffuser, a rotating lightpipe and rotating lens array, a large R_Ω can be generated. In other words, R_Ω reduces the speckle by generating multiple independent speckle patterns simultaneously or within the integration time of detector/ audience. The overlapping of these speckle patterns can greatly reduce the speckle as discussed in Section 1.2.2. However, in a practical laser projection system, the R_Ω is limited by the optical geometry of the system and the SCR reduction will not follow $\frac{1}{\sqrt{N}}$ completely[18]. This limitation is crucial. Almost all speckle reduction methods proposed in the market using spatial diversity are seriously limited by this and cannot reduce the SCR below human perception threshold. Detailed discussion regarding this limitation will be conducted in Chapter 4.

A few examples of speckle reduction using different methods are presented here.

One idea to reduce speckle in laser projection is to provide a large wavelength diversity. Typically, there are three choices to achieve a large R_λ: a) a broadband laser b) blending of several lasers with different wavelengths and c) a combination of a) and b). This is easy to understand, a laser source with more spectrum diversity will be able to generate more independent speckle patterns on the screen, which will overlap and provide speckle reduction.

Several methods have been reported to generate broadband laser. For example, one way to achieve a broadband laser is by adding current modulation to the laser [19], because for laser diode, output wavelength at a different driving current is different. When the AC signal is applied, if the modulation frequency is high enough, the total spectrum of the laser can be considered as expanded. As shown in Figure 1.6, by driving the laser with an AC

signal from 0.1A to 0.2A, the bandwidth can be increased from around 0.2nm to 2nm. By

a combination with other speckle reduction methods, the reported overall SCR can be

reduced to less than 5%. However, the AC modulation of laser diodes results in the decrease

of overall output optical power of the laser, which will results in a dimmer projected image.

This is due to the current modulation is mostly effective when current is close to lasing

threshold where the output power is very low. Besides of this, the modulation will also

result in a low averaging output power. As the typical working current of red LD is around

330 mA for the LD used in this experiment, the overall output power of the LD is less than

30% of the CW mode. In a practical laser projection which may have an optical power

higher than 100W, this will result in hundreds of red LDs are required to provide enough

illumination, which is very expensive and impractical.

(a)   (b)
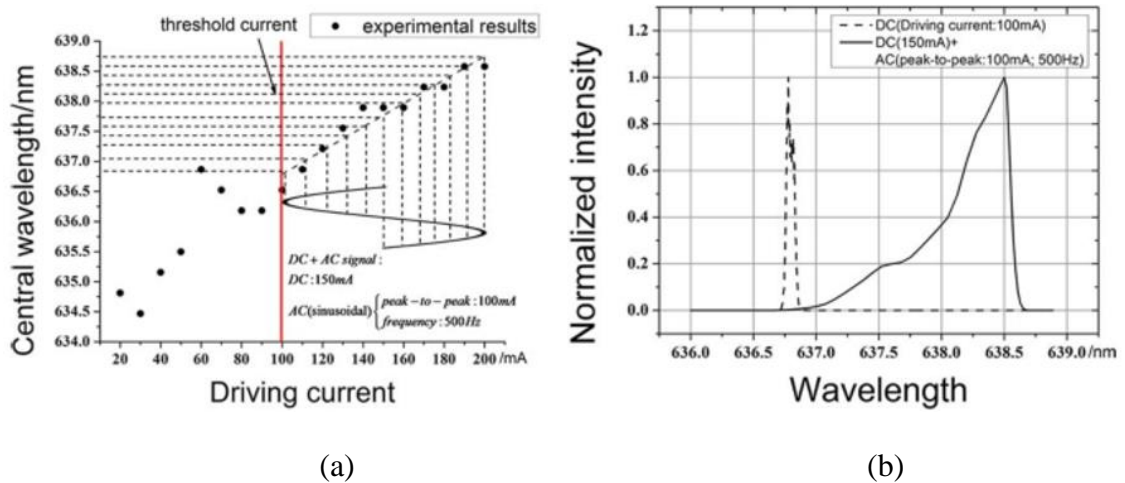
Figure 1.6 (a) The center wavelength varies with the driving current (b) the spectrum of

the output light. Note the dotted line is a measured spectrum by DC signal and solid line

is driving by a AC signal [19].

A different method is used in [20], by tailoring laser structure, a AlGaInP/GaInP quantum well laser with unevenly spaced wells combined can provide a much broad emission spectrum. The structure of the laser is shown in Figure 1.7. By unevenly spacing of the emitters as shown in Figure 1.7(b), the full width at half maximum (FWHM) spectrum width is 3.7nm, while evenly spaced laser as in Figure 1.7(a) can only provide FWHM less than 0.3nm. The SCR reported in the paper is reduced by more than four times when using tailored laser compared to conventional one. However, the tailored quantum well structure requires epitaxially grown will result in a much higher manufacture cost compared to traditional semiconductor laser diode. Also, this setup require a much larger pumping power compared to traditional cavity structure in order to get a suitable electric-optic efficiency.

As briefly presented above, the broaden of laser linewidth usually complied with issues such as decreasing of output power, increasing of manufacture cost and drop of efficiency. As a result, they are not the major stream as methods in laser speckle reduction related to wavelength diversity.

Another way is to achieve a large wavelength diversity is by providing multiple wavelengths slightly different with each other. Mitsubishi proposed a high-power intra-cavity solid-state green lasers in 2015 [21]. Two different optical crystals $ND: YVO_4$ and $ND: GdVO_4$ are used to provide the fundamental light for second harmonic generation(SHG) green light. The former can provide fundamental light at 1064nm and 1086nm, while the latter provides the fundamental light at 1062nm and 1082nm. By employing proper laser crystal and laser cavity mirror coating, the laser can emit four different wavelengths at

531nm, 532nm, 541nm and 543nm respectively. Combined with other speckle reduction methods, the minimal SCR achieved by the team is 5.6%.
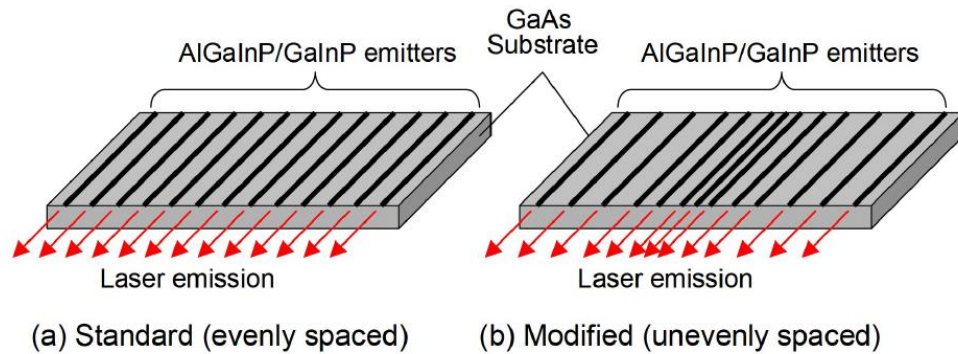
Figure 1.7 Schematic structure of a) standard-evenly spaced laser and b) modified-unevenly spaced laser [20].

Besides wavelength diversity, another type of speckle reduction is by using spatial diversity. The basic idea is to generate as many independent speckle patterns as possible within the integration time of the observer and overlap them together to create a uniform image.

For example, a deformable mirror is used in [22]. The deformable mirror is a thin reflective membrane which is also flexible. There are many independent piezo actuators underneath the membrane and they are driven at kHz frequency. When they vibrate, the ripples on the surface of the mirror are fast changing. Hence, the reflected light will be diffused at different angles and diffraction orders and changed dynamically. Figure 1.8 shows the on and off state of this deformable mirror.
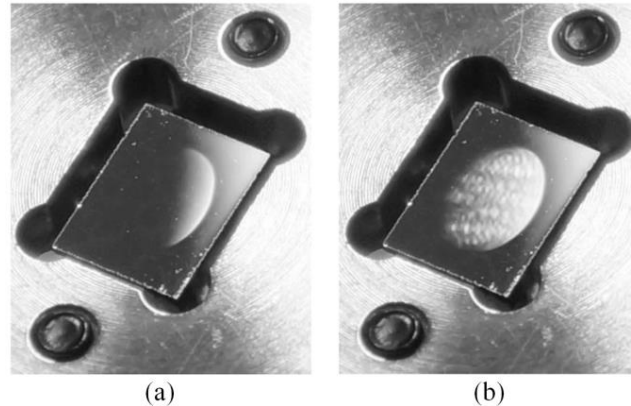
Figure 1.8 Picture (a) without and (b) with activation of the deformable mirror [22].

One advantage of this device is its surface can remain relative smooth which will prevent scattering losses. When laser light illuminate on such rapid changing random surface, many independent speckle patterns will be generated. Combined with other homogenization and beam shaping optics, a good speckle reduction effect can be provided. However, this deformable mirror is at very high cost and the overall speckle reduction is still by the limits of spatial diversity.

Besides the deformable mirror, moving/vibrating/rotating components can also be used to provide speckle reduction. For example, in [23], a rotating light pipe is used to provide speckle reduction, as shown in Figure 1.9. The light is coupled into a light pipe which is rotating fast. The output light is passed through relay lenses and a display panel and projected to the screen.

The time-varying light pipe can also generate multiple independent speckle patterns at different time. As long as it rotates fast enough, a good speckle reduction can be provided. Similar ideas other than rotating a light pipe include rotating a lens array [24] and a diffuser

[25]. A positive feature of this method is the optical penalty due to the speckle reduction is relatively low. However, it also has a big disadvantage: a mechanical rotating component is highly undesired in a practical laser projector, as it may raise serious stability issues.
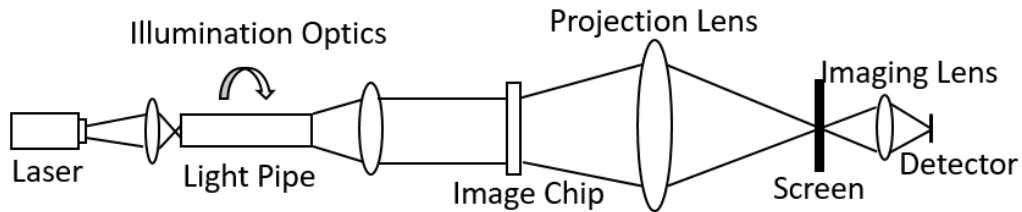
Figure 1.9 Using a rotating light pipe to reduce speckle.

Thus, method can generate multiple independent speckle patterns without a moving component, is also studied. In [26], a laser diode array is established. Each laser diode is coupled into a multimode fiber and these multimode fibers form a fiber bundle, as shown in Figure 1.10.

There are a large number of modes that can be supported in the multimode fiber. Using an approximation of ray optics, the shortest propagation time is experienced for a mode propagating along the axis of the fiber without any reflection, while the longest propagation time is expected for a mode reflecting at the interface between the core and cladding layers at the critical angle. When the optic path difference between these two modes is longer than the coherence length of the laser, these two modes are overlapped with each other on intensity bases, which is required for speckle reduction.
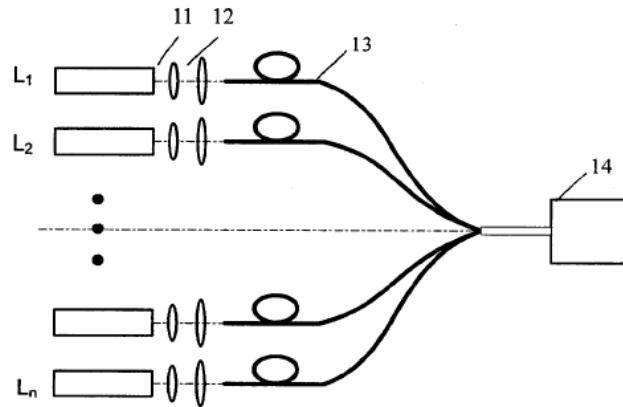
Figure 1.10 Speckle reduction using multimode fiber bundle

Other than wavelength diversity and spatial diversity, polarization diversity can also be applied to speckle reduction. However, this factor is highly limited by the application. In situations where polarized screen has to be used (like 3D movies), polarization maintained screen has to be used. Thus, no speckle reduction can be applied to this. For conventional non-polarized screen, a $\sqrt{2}$ reduction can be contributed. In [16], it is proposed that by developing a laser projector with polarization of projected light that is fast rotating between two orthogonal directions, a more effective speckle reduction can be provided from polarization diversity. However, this setup is usually very complicated and not suitable for practical use.

Several speckle reduction methods are discussed as examples above. They mostly use wavelength diversity, spatial diversity or polarization diversity to reduce speckle. However, there are also some other speckle reduction methods that may not be categorized into one of three factors, such as engineered screen which generate non-fully developed

laser speckle, random lasers that break the coherence of the laser so interference will be greatly suppressed and screen vibrating that also generate time-varying speckle patterns.

1.3. Research Motivation and Objective

In order to make laser projection commercially successful, laser speckle has to be suppressed. A compact, low-cost and low optical penalty speckle reduction system is highly desired. Though there are some existing methods that can effectively reduce the speckle level under certain conditions, it is still very challenging to find a system that satisfies requirements mentioned above. It is therefore of great interest to study and optimize speckle reduction methods and improve the speckle reduction ability and image quality of laser projection systems.

The objective of this thesis is to analyze and investigate practical solutions for a speckle free laser projection system. The laser projection system is divided into several modules and studied separately. The study includes a low speckle laser source, a projection optical engine with an integrated speckle reduction method, a low speckle micro lens array screen and a standard speckle measurement system corresponding to human perception.

1.4. Thesis Outline

This thesis is organized into six chapters. The first chapter provides a brief introduction of laser projection and the laser speckle issue. The introduction describes the physical origin of laser speckle and its statistical properties, as well as some current speckle reduction methods. This chapter also shows the motivation and objective of this thesis.

Starting from the laser source, Chapter 2 discusses speckle reduction based on wavelength diversity. The theoretical model that describes wavelength diversity in laser projection is established. The SCR of the system using wavelength diversity is simulated, based on the model and experimentally verified. The chapter also gives the guideline of optimized wavelength/power selection for lasers to provide low speckle laser projection.

Chapter 3 proposes a low-cost, high-efficiency and compact speckle reduction optical system using an electric active elastomer actuator. The theoretical analysis as well as experimental work are presented in this chapter. By combining with multimode fiber and a voice coil motor, the proposed system can greatly reduce the SCR down to 3.7%.

Chapter 4 studies an engineered screen that utilizes micro lens array(MLA) which can greatly reduce SCR. A comprehensive theoretical model has been established for the analysis and optimization of MLAs that can predict the SCR of a laser projection system using different MLA screens. The theory and calculated results agree well with the reported experimental results. This model can be used to determine a MLA cell size that can achieve an SCR below human perception.

Chapter 5 works on the standard measurement of speckle in a laser projection

system that corresponds to human perception. The measured SCR is highly dependent on measurement conditions, which include but are not limited to camera F/#, focal length, environment illumination level, and integration time. To obtain the correct SCR values that agree with the human eye, these conditions are discussed and suitable setups are proposed.

Chapter 6 provides a summary of the most important achievements of this thesis as well as potential future work.

Engineering Physics

CHAPTER 2

Speckle Reduction Based on Wavelength Diversity

2.1. Wavelength Diversity in Speckle Reduction

In the previous chapter, speckle reduction methods using wavelength diversity, spatial diversity and polarization diversity were briefly introduced. This chapter will focus on the study and optimization of wavelength diversity.

In order to suppress SCR, wavelength diversity R_λ is widely considered. This can be realized by increasing the linewidth of the laser source or by using multiple lasers with different wavelengths (i.e. wavelength blending). For example, in digital cinema laser projectors, several hundred lasers are required to achieve the required brightness [27], and the vibration technique is highly undesirable to use due to the fact that the reliability of the system is very important [28]. Therefore, a motionless de-speckle technique, such as wavelength blending (i.e. using multiple lasers with different wavelengths), has to be employed to generate a large R_λ and thus low SCR.

Although wavelength blending is a well-known technique to reduce speckle, there is no theoretical model to describe the speckle reduction effect quantitatively when multiple

lasers with different center wavelengths, wavelength gaps and line widths are used. To date, the study on the effectiveness of the wavelength blending method is mainly based on experimental investigation [29,30]. Theoretical analysis of the wavelength diversity of a single wavelength has been reported in [31]. A speckle reduction theory related to wavelength diversity has been presented in [32]. However, it is suitable only for either a light source with one single center wavelength and a Gaussian shaped spectrum or a light source with multiple longitude modes and a Gaussian shaped intensity envelope. The longitude modes were assumed to have the same linewidth and a fixed frequency or wavelength gap. Thus, there is no theoretical model that can be used to simulate and minimize SCR as a function of power ratio and wavelength gap between different lasers, which is especially important when many lasers (e.g. 100) are involved. For instance, it can be expected that when two different lasers with ideal monochromic spectras are blended, the SCR of the entire system will decrease as their wavelength difference increases and the minimum SCR will be reduced by $\sqrt{2}$. However, how far away these two wavelengths needed to be in order to achieve maximum speckle reduction is unclear.

It is worth noting that when two different lasers with the same wavelength are used, even though they are incoherent to each other, they still generate identical or nearly identical speckle patterns if they illuminate the screen from the same location. Thus, only a very limited speckle reduction effect can be expected in this case [18], which is very common when multiple lasers are coupled by a fiber bundle since all laser light comes out from the same fiber end.

In this chapter, a theoretical model is used to describe the wavelength blending

effects on speckle reduction. The minimum wavelength difference of two lasers as a function of laser linewidth to generate de-correlated speckle patterns is studied both theoretically and experimentally. The optimal power ratio between lasers that have different wavelengths and linewidths is also simulated and experimentally verified. The SCRs of a system with multiple wavelengths (more than two wavelengths) are then investigated. The number of wavelengths required for a practical laser projection system to achieve speckle free projection is analyzed. The results of this chapter have been published in [33].

2.2. Theoretical Model of Wavelength Diversity

The theoretical analysis of wavelength diversity in speckle reduction has been partially studied before. For example, Goodman [18] analyzed the relationship between SCR and the linewidth of single wavelength, and Trisnadi [17] estimated the speckle reduction effect of multiple wavelength blending. However, the model to describe the speckle reduction effect of wavelength blending has not been well studied yet. Since speckle reduction using wavelength blending is related to different wavelengths, it is convenient to discuss the question in frequency domain. Assuming that there are n different lasers, and $\hat{g}_i$ is the normalized power spectrum density function of the ith laser, which is defined as

$$\hat{g}_i = \frac{g_i(v)}{\int_0^\infty g_i(v)dv} \tag{2.1}$$

$g_i(v)$ is the power spectrum density function of the ith laser. Thus, the normalized power

spectrum density function of the entire system can be written as

$$\hat{g} = \sum_{i=1}^n C_i \hat{g}_i \tag{2.2}$$

where $\sum_{i=1}^n C_i = 1$, and C_i is the power ratio of the ith laser over the total power, which can

be expressed as

$$C_i = \frac{\int_0^\infty g_i(v)dv}{\sum_{k=1}^n \int_0^\infty g_k(v)dv} \tag{2.3}$$

the normalized power spectrum density function $\hat{g}$ includes the information on the number

of lasers, the linewidth and the power ratio of each laser. Note that the center wavelength,

linewidth, and power ratio could be different for each laser in the theoretical model

presented in this paper, which enables us to easily simulate and minimize the SCR of a

wavelength blended laser system.

Assume that the laser light directly illuminates a depolarization screen without any

other speckle reduction methods, and that the speckle is captured by a camera with a

detection lens. Let $I(x, y; v)$ be defined as the speckle intensity at point (x,y) with an

illumination frequency of v by unit radiation. $I(x, y)$ is defined as speckle intensity at point

(x,y). Thus, $I(x, y)$ can be considered as the integration of speckle intensity at frequency v

with the weight of normalized power spectrum density function. This can be expressed as

[18]

$$I(x, y) = \int_0^\infty \hat{g} \, I(x, y; v)dv \tag{2.4}$$

To obtain the expression for SCR, the average intensity and standard derivation of $I(x, y)$ are necessary. Similar to Eq.2.4, the spatial averaging of $I(x, y)$ can be expressed as

$$\overline{I(x, y)} = \int_0^\infty \hat{g}\, \overline{I(x, y; \nu)}d\nu = \overline{I(x, y; \nu)} \int_0^\infty \hat{g}\, d\nu = \overline{I(x, y; \nu)} = \bar{I} \tag{2.5}$$

Here, the order of integration and summation is interchanged. Also, as the spatial averaging of $\overline{I(x, y; \nu)}$ is independent of ν, $\overline{I(x, y)}$ equals $\overline{I(x, y; \nu)}$. Similarly, $\overline{I^2(x, y)}$ can be expressed as

$$\overline{I^2(x, y)} = \int_0^\infty \int_0^\infty \hat{g}\,(\nu_1)\hat{g}(\nu_2)\,\overline{I(x, y; \nu_1)I(x, y; \nu_2)}d\nu_1 d\nu_2$$

$$= \int_{-\infty}^{+\infty} K_{\hat{g}}(\Delta\nu)\Gamma_I(\Delta\nu)d\Delta\nu \tag{2.6}$$

where

$$K_{\hat{g}}(\Delta\nu) = \int_0^{+\infty} \hat{g}\,(\xi)\hat{g}(\xi - \Delta\nu)d\xi \tag{2.7}$$

and Γ_I is the statistical autocorrelation function of $I(x,y;\nu)$. According to the circular complex Gaussian statistics [18][34], Γ_I can be written as

$$\Gamma_I(\Delta\nu) = \bar{I}^2 * (1 + \mu(\Delta\nu)^2) \tag{2.8}$$

where μ is the complex correlation coefficient of two speckle fields with a frequency difference of $\Delta\nu$. Note that μ is not related to the laser source spectrum. It describes the correlation between two speckle fields generated by two lasers with a peak frequency gap of $\Delta\nu$. By inserting Eq.2.8 into Eq.2.6 and combining it with Eq.2.5, the standard derivation of the light field is given by

$$\sigma^2 = \overline{I^2(x,y)} - \overline{I(x,y)}^2$$

$$= \int_{-\infty}^{+\infty} K_{\hat{g}}(\Delta v)\overline{I(x,y)}^2(1+\mu(\Delta v)^2)d\Delta v - (\int_0^\infty \hat{g}\,\overline{I(x,y;v)}dv)^2$$

$$= \overline{I(x,y)}^2 \int_{-\infty}^{+\infty} K_{\hat{g}}(\Delta v)\mu(\Delta v)^2 d\Delta v \qquad (2.9)$$

Thus, the SCR of the system can be expressed as

$$\mathrm{SCR} = \frac{1}{R_\lambda} = \sqrt{\frac{\sigma^2}{\overline{I(x,y)}^2}} = \sqrt{\int_{-\infty}^{+\infty} K_{\hat{g}}(\Delta v)\mu(\Delta v)^2 d\Delta v} \qquad (2.10)$$

It worth noting that only the wavelength diversity R_λ is considered in the speckle reduction here. R_σ and R_Ω are set to 1. Using the random height screen model [18], the speckle field $\mathbf{a}(\alpha,\beta)$ is right after the screen which is given by:

$$\mathbf{a}(\alpha,\beta) = \mathbf{r}S(\alpha,\beta)e^{j\phi(\alpha,\beta)} \qquad (2.11)$$

where $\mathbf{r}$ is the amplitude reflectivity of the screen and $S(\alpha,\beta)$ is the amplitude illuminated on the screen. $\phi(\alpha,\beta)$ is the random phase resulting from the screen surface fluctuation:

$$\phi(\alpha,\beta) = \frac{2\pi}{\lambda}(-\hat{\imath}\cdot\hat{z} + \hat{o}\cdot\hat{z})h(\alpha,\beta) \qquad (2.12)$$

$\hat{\imath}$ and $\hat{o}$ are unit vectors respectively corresponding to the incident and reflected directions of the light. $\hat{z}$ is the unit vector perpendicular to the screen surface, and $h(\alpha,\beta)$ is the surface height at (α,β). Eq.2.12 can be rewritten as

$$\phi(\alpha,\beta) = \frac{2\pi}{\lambda}(-\hat{\imath}\cdot\hat{z} + \hat{o}\cdot\hat{z})h(\alpha,\beta) = ((-\mathbf{k}_i + \mathbf{k}_o)\cdot\hat{z})h(\alpha,\beta) \qquad (2.13)$$

The scattering vector $\mathbf{q}$ can be defined as

$$\boldsymbol{q} = -\boldsymbol{k_i} + \boldsymbol{k_o} = q_\alpha \hat{\boldsymbol{\alpha}} + q_\beta \widehat{\boldsymbol{\beta}} + q_z \hat{\boldsymbol{z}} = \boldsymbol{q}_t + q_z \hat{\boldsymbol{z}} \qquad (2.14)$$

where q_z is the normalized component of the scattering vector, which is given by

$$q_z = \frac{2\pi}{\lambda}(\cos\theta_i + \cos\theta_o) \qquad (2.15)$$

where θ_i and θ_o are incident angle and reflected angle, respectively.

The calculation of $\mu(\Delta v)$ has been reported in [35]. When illumination and observation angles are very close to each other, $\mu(\Delta v)$ can be expressed as

$$\mu(\Delta v) = M_h(\Delta q_z) \qquad (2.16)$$

where M_h is the first order characteristic function of the surface height fluctuations h and $\Delta q_z = \frac{2\pi|\Delta v|}{c}(\cos\theta_i + \cos\theta_o)$. For a rough surface with a height fluctuation of Gaussian distribution,

$$|M_h(\Delta q_z)|^2 = \exp(-\sigma_h^2 \Delta q_z^2) \qquad (2.17)$$

where σ_h is the standard derivation of surface height fluctuation.

Based on the above derivation, for a laser light source utilizing wavelength blending, the speckle reduction effect caused by wavelength diversity can be calculated. Using the normalized power spectrum density function $\hat{g}$ of the system and the standard derivation of the screen surface roughness σ_h, the SCR and optimal power ratio between different wavelengths can be calculated.

The above theoretical model can be used to predict the R_λ of a laser projection system using a blended system. By using a specific $\hat{g}$ that corresponds to the laser source, the R_λ can be calculated.

2.3. Simulated Results for Wavelength Diversity

With the established theoretical model, the blended laser source of the laser projection system can be optimized to have better speckle reduction. Several simulations are conducted. Different cases are studied and presented in this section. To study dependence of the SCR on wavelength difference and laser linewidth, two lasers are considered first.

2.3.1 Two Lasers with Equal Linewidth

Assume two lasers illuminate a screen from the same location and the same incident angle without using any other speckle reduction methods. If two lasers have identical spectras, even if they are incoherent, they generate the same speckle pattern if they illuminate the screen from the same location with the same incident angle [36]. As a result, there will be no speckle reduction when these two speckle fields are overlapped with each other on the intensity base.

When the wavelengths of these two lasers have a certain difference, different speckle patterns will be generated as the wave front experiences different random phase terms when they are reflected by a screen. The bigger this wavelength difference, the more de-correlated these two speckle patterns will be. When the wavelength difference is big enough to generate two completely de-correlated speckle patterns, maximum speckle

reduction by the wavelength diversity is achieved. Thus, the SCR of the system is related to the wavelength difference between lasers.

The theory was first tested by blending two ideal monochromic lasers, assuming that the lasers have the same output power but different wavelengths. Thus, the normalized power spectrum density function $\hat{g}$ is

$$\hat{g} = \frac{1}{2}[\delta(v - v_a) + \delta(v - v_b)] \tag{2.18}$$

where v_a and v_b are frequencies corresponding to each wavelength.

Bringing $\hat{g}$ into Eq.2.7, the $K_{\hat{g}}(\Delta v)$ can be written as

$$K_{\hat{g}}(\Delta v) = \int_0^{+\infty} \frac{1}{4}[\delta(v - v_a) + \delta(v - v_b)][\delta(v - v_a - \Delta v) + \delta(v - v_b - \Delta v)] \, dv \tag{2.19}$$

Note that only when $\Delta v = 0$, $\Delta v = v_a - v_b$ or $\Delta v = v_b - v_a$, $K_{\hat{g}}(\Delta v)$ is non-zero. Thus, $K_{\hat{g}}(0) = \frac{1}{2}$, $K_{\hat{g}}(v_a - v_b) = K_{\hat{g}}(v_b - v_a) = \frac{1}{4}$. Bringing the results into Eq.2.16 and using Eq2.5-2.10, we obtain

$$SCR = \sqrt{\frac{1}{2}M_h(\Delta q_z(0))^2 + \frac{1}{4}M_h(\Delta q_z(v_a - v_b))^2 + \frac{1}{4}M_h(\Delta q_z(v_b - v_a))^2}$$

$$= \sqrt{\frac{1}{2} + \frac{1}{2}\exp[-\sigma_h^2(\frac{4\pi|v_a - v_b|}{c})^2]} \tag{2.20}$$

where the assumption $\cos\theta_i = \cos\theta_o = 1$ is used.

When two wavelengths are far away from each other, $|v_a - v_b|$ is very large and $\exp[-\sigma_h^2(\frac{4\pi|v_a - v_b|}{c})^2]$ is close to 0. Therefore the SCR calculated from Eq.2.20 approaches to $1/\sqrt{2}$, which corresponds with the well-known result of two ideal monochromic lasers with different wavelengths and equal intensity.

As the theory is first verified in an ideal case, two more practical cases are studied. Figure 2.1 shows the simulated SCR as a function of the wavelength difference between (a) two diode pumped solid state (DPSS) green lasers, and (b) two semiconductor green laser diodes (LDs), respectively. In the simulations, only the wavelength diversity effect was considered. Thus, according to Eq.(1.19-1.20), $SCR = \frac{1}{R_\lambda}$. It was assumed that the two lasers have equal intensity and a Gaussian shaped spectrum with linewidth of 0.1 nm [37] and 1.2 nm [38] for the DPSS lasers and semiconductor LDs, respectively. A screen surface roughness σ_h of 100 μm was assumed in the simulations [39].

As shown in Figure 2.1(a), with the increase of wavelength difference between the two DPSS green lasers, the SCR decreases first and then saturates. The minimum SCR equals $1/\sqrt{2}$, which agrees well with the theoretical prediction of SCR for two completely incoherent lasers. We define $\Delta\lambda_{min}$ as the wavelength difference between the two lasers when the SCR drops down to 99% from its maximum to saturation.

For DPSS lasers with a linewidth of 0.1 nm, the $\Delta\lambda_{min}$ is 1.0 nm, implying that, to achieve optimal speckle reduction effects, the wavelength difference between the two lasers should be set at a value larger than 1.0 nm.

On the other hand, semiconductor LDs have much broader spectrum as compared to the DPSS lasers. As a result, the dependence of SCR on the wavelength difference of the two LDs is quite different, although the trend is similar, as shown in Figure 2.1(b). The $\Delta\lambda_{min}$ is 1.5 nm implying that, to achieve optimal speckle reduction effects a larger wavelength difference is required for LDs.
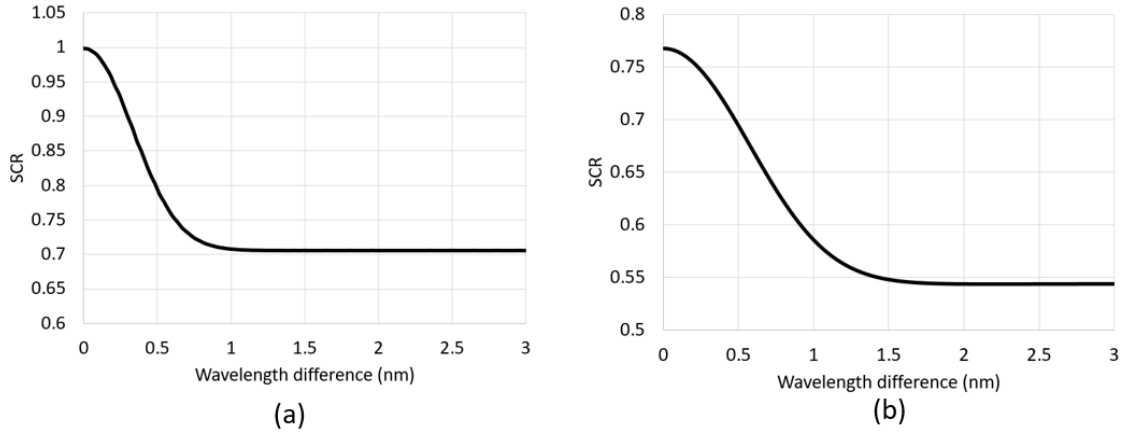
Figure 2.1 Simulated SCR as a function of the wavelength difference between a) two

DPSS lasers; b) two semiconductor laser didoes.

It is worth mentioning that, our simulated results agree with the reported results for two DPSS lasers with slightly different wavelengths [40]. In [40], it is reported that SCR of a laser source system using two DPSS lasers saturates when the wavelength difference is around 1 nm, which agrees well with our results shown in Figure 2.1(a).

To obtain a general trend, dependence of the minimum wavelength difference $\Delta\lambda_{min}$ on laser linewidth was simulated, as shown in Figure 2.2. In the simulations, two lasers with equal power and the same linewidth were assumed. The X-axis is the linewidth of the two lasers, while the Y-axis is the $\Delta\lambda_{min}$. As shown in Figure 2.2, the minimum wavelength difference $\Delta\lambda_{min}$ increases monotonically with the increase of the laser linewidth. The broader the laser linewidth, the larger the minimum wavelength difference $\Delta\lambda_{min}$ is required to achieve the optimal speckle reduction.
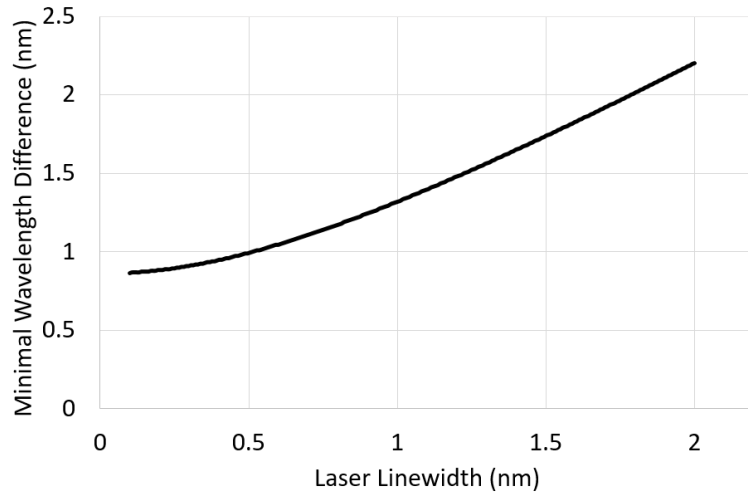
Figure 2.2 Simulated minimum wavelength difference dependence on laser linewidth for achieving the optimal speckle reduction.

2.3.2   Two Lasers with Different Linewidths

In a practical laser projection system, there are situations where different lasers with different linewidths are blended together. For example, there are two types of lasers usually used in laser projection to generate green light. One type is a diode pumped solid state (DPSS) laser, which utilizes frequency doubling and usually generates green light at around 532 nm [37]. The other type is GaN based laser diode (LD), which emits light at around 515 nm [38]. These two types of lasers are often blended together to provide speckle reduction.

Unlike the previous case where two lasers have equal linewidth, these two lasers have different linewidths. The DPSS laser has a very narrow linewidth of about 0.1 nm, while the semiconductor LD has a much broader linewidth of about 1.2 nm. They meet the

wavelength difference requirement to generate de-correlated speckle patterns. However, unlike lasers with equal linewidth that the minimal SCR will be generated when they have equal intensity, the optimized power ratio between them to generate minimal SCR is unclear. It is unknown if the minimal SCR will still be achieved when they have equal power.

To obtain the optimized power ratio between two lasers with different wavelength and linewidth, the theory described in Section.2.1 was used in the simulations, as shown in Figure 2.3 (solid curve). The X-axis shows the percentage of LD power over the total power of the two lasers, where a ratio of 0 means the light source is a pure DPSS laser, while a ratio of 1 implies the light source is pure LD. The Y-axis shows the SCR of the system. In the simulations, a Gaussian spectrum with a $1/e^2$ width of 0.1 nm and center wavelength of 532 nm was assumed for the DPSS laser. For the LD, it was assumed that the LD has several longitude modes around 520 nm, and the envelope of these modes can be roughly considered as a Gaussian function with a $1/e^2$ width of 1.2 nm. . For a white print paper, the value of σ_h is about 100 μm [39]. For a screen used for practical projection, the surface of a screen is usually more rough than a white print paper and a value of 200 μm for σ_h was used in the simulation. Considering the depolarization of the screen, the simulated SCR was divided by a factor of $\sqrt{2}$.

As shown by the solid curve in Figure 2.3, when only the DPSS laser is used, the SCR is around 69%. On the other hand, when only LD is employed, the SCR is around 37%. It is not surprising that LD gives a lower SCR as compared to the DPSS laser since LD has much wider linewidth. It is worth noting that the lowest SCR is achieved when the

power of LD over total power $P_{LD} : P_{Total}$ is around 0.8. The SCR under these circumstances is 33%. Experiment regarding this simulated results is conducted and will be presented in Section 2.3.
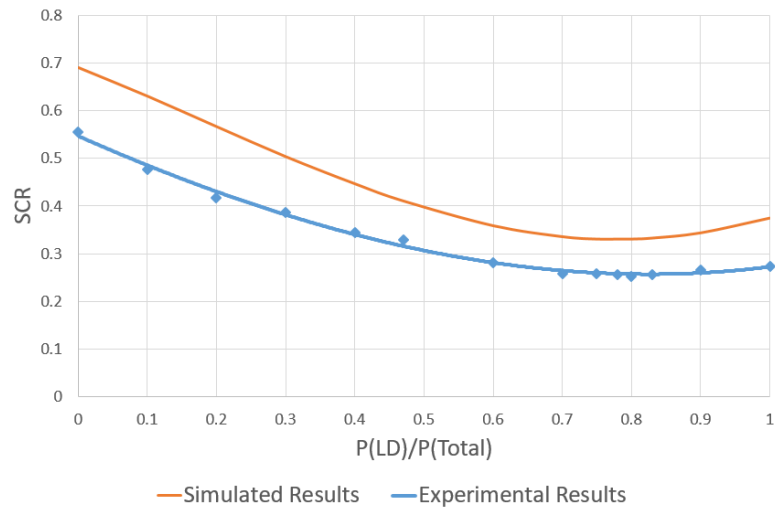
Figure 2.3 Simulated and measured SCR using wavelength blending of a DPSS green laser and a semiconductor green LD.

2.3.3   Wavelength Blending for Multiple Wavelengths

In a practical laser projection system, more than 2 lasers may be required. Therefore, the SCR of the system with multiple lasers also needs to be investigated. Wavelength blending effects of multiple lasers can be done by expanding the results obtained for two lasers and changing the $\hat{g}$ profile in the theory.

Again, two types of commonly used green lasers are studied here: semiconductor green LDs and DPSS green lasers. It was assumed that all green LDs have a Gaussian profile with a linewidth of 1.2 nm and green DPSS lasers have a Gaussian profile with a

linewidth of 0.1 nm.

In the simulations, for simplicity, the factors of speckle reduction due to the spatial diversity and polarization diversity were not considered and wavelength diversity was the only factor that contributes to speckle reduction. It was assumed that all lasers have equal intensity and the same wavelength difference between two adjacent lasers. Figure 2.4 shows the simulated SCRs as a function of wavelength difference between the two adjacent lasers for a) three lasers; b) five lasers; c) seven lasers; d) nine lasers. The X-axis is the wavelength difference between the two adjacent lasers, and the Y-axis is the simulated SCR of the wavelength blended light source. The solid and dashed lines correspond to simulated results of green DPSS lasers and LDs, respectively.

As shown in Figure 2.4, it is found that, first, even if multiple lasers are used, if they have exactly same wavelength and linewidth, there is no speckle reduction. This correlates well with the reported result [40]. Second, the SCRs reach a minimum value when the wavelength difference is bigger than 0.9 nm and 1.2 nm for the green DPSS laser and LD respectively. Third, when the wavelength difference is limited and a relatively large number of lasers is used, the speckle level of the DPSS lasers and LDs is similar, which can be seen in Figure 2.4(c) and (d). At first sight, this seems contradictory to the conventional impression since DPSS lasers have higher SCR as compared to that of the LDs. This can be explained as DPSS lasers reach minimum SCR much faster than that of LDs when the wavelength difference is increased, as shown in Figure 2.4(c) and (d). As a result, even if DPSS lasers have a higher initial SCR, they can still achieve a similar SCR level in this case.

The minimum number of lasers required to achieve a speckle free projection system can be obtained based on the simulation shown in Figure 2.4. For example, it has been reported in [41] that by using a single DPSS laser combined with multimode fiber, diffuser, light pipe and depolarized screen, the SCR of the system can be reduced to 9.6%. According to Eq.(1.19-1.20), and using $R_\lambda = 1$ for a single DPSS laser [17], the value of $R_\sigma R_\Omega$ for this system can be deduced for a de-polarized screen, i.e. R_σ is $\sqrt{2}$ [18] and $R_\Omega = 1/(R_\lambda R_\sigma) = 10.42$.
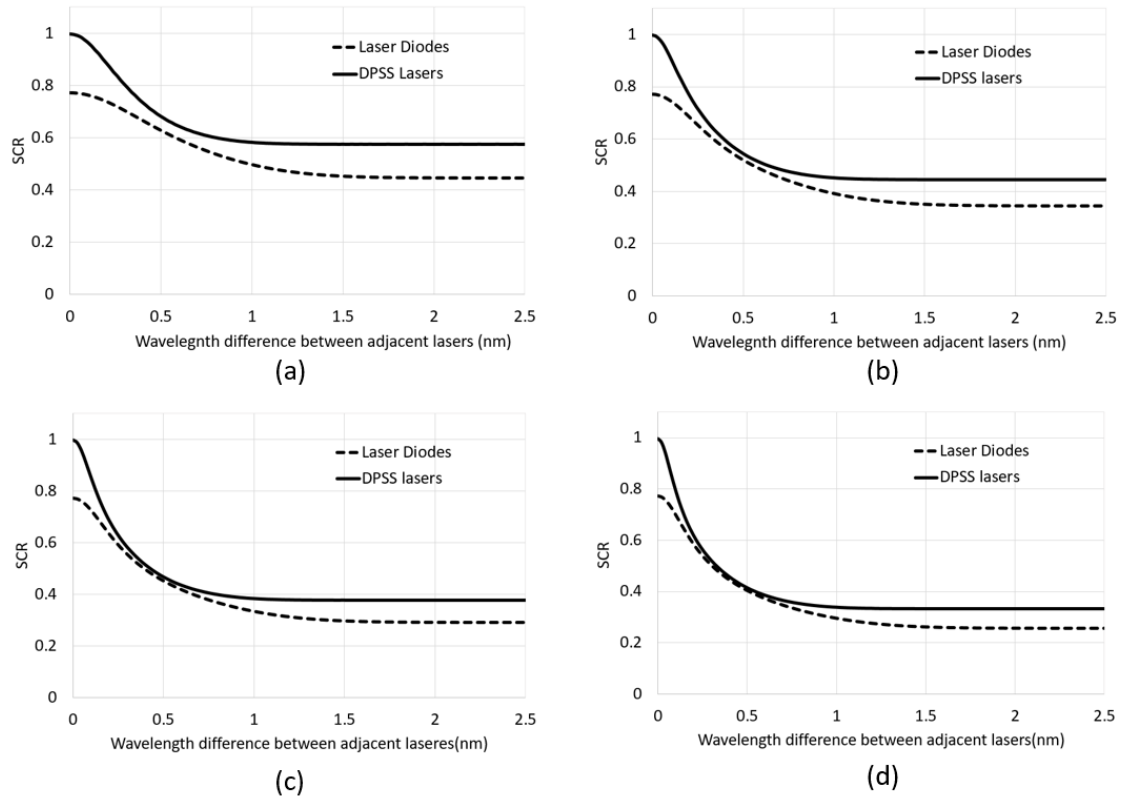
Figure 2.4 SCR as a function of wavelength difference between adjacent lasers. a) three lasers; b) five lasers; c) seven lasers; d) nine lasers.

To achieve speckle free projection (e.g. SCR $< 4.6\%$) [42], sufficient wavelength diversity

has to be provided. According to Eq.1.19-1.20, the minimum R required to achieve SCR of 4.6% is 21.74. As a result, for the system mentioned above, R_λ bigger than 2.09 is necessary. If the system use a polarization maintained screen (i.e. $R_\sigma = 1$) for the purpose of 3D display, the R_λ must be even larger, which is $2.09 \times \sqrt{2} = 2.95$. R_λ of 2.09 and 2.95 corresponding to SCR of 67.66% and 47.85% respectively. Based on the simulations shown in Figure 2.4, for DPSS lasers, at least three lasers with sufficient wavelength difference are required for a depolarized screen or five lasers for a polarized screen. For LDs, the numbers reduce down to two and three, respectively.

2.4. Wavelength Blending Experiments

In order to verify simulated results, several experiments regarding wavelength blending are conducted. Also, a low-speckle laser projection system with optimized wavelength blending laser source is presented in this section.

2.4.1 Lasers with Equal Linewidth

To verify the simulated results, dependence of SCR on the difference of two green LD wavelengths was measured using the setup shown in Figure 2.5. In the experiments, two semiconductor LDs were used. The temperature of each semiconductor LD was

controlled by an independent thermoelectric cooler (TEC), which was used to change the center wavelength of the LDs. Since the center wavelength of the green LDs increases with the increase of temperature, the wavelength difference between the two LDs can be changed by tuning the temperature of the TECs [43].

To eliminate any possible uncertainties, the temperature of LD1 was fixed at the high-end of the operation temperature range suggested by the LD manufacturer (45 ℃), while the temperature of LD2 was swept from low-end to high-end (from 7 ℃ to 45 ℃). The output powers of the two LDs were kept equal in the measurements. The output beams of the LDs were coupled into a vibrating multimode fiber bundle and then illuminated on a de-polarized screen. A monochromic camera was set 3 meters away from the screen. The camera lens was F/16 and had a focal length of 50 mm, which corresponds to the ratio of human vision [44].
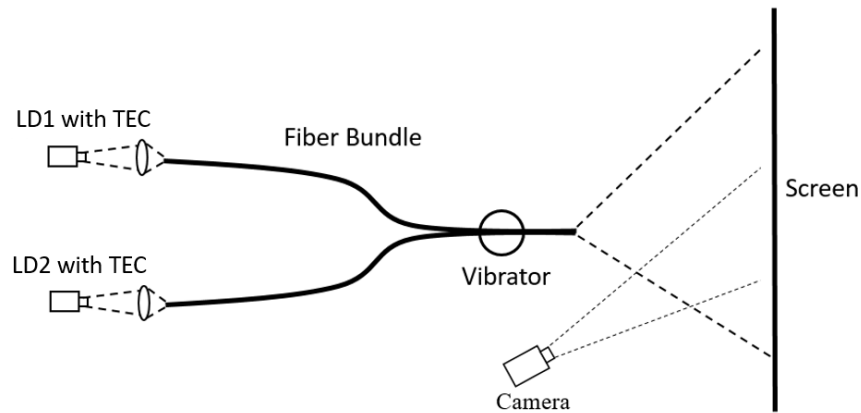
Figure 2.5 Experimental setup used to verify the theory on wavelength diversity

To make sure that the measured speckle reduction effect is mainly caused by the wavelength blending of the two LDs, dependence of SCR on wavelength tuning by changing the TEC temperature was measured for LD2 first, as shown in Figure 2.6(a). The X-axis is the center wavelength of the LD2 and the Y-axis is the measured SCRs. It can be seen that the SCR of the system remain relative stable when LD2 is set at a different temperature/wavelength. An average value of 13.7% will be used for LD2 in the following discussion.

(a)   (b)
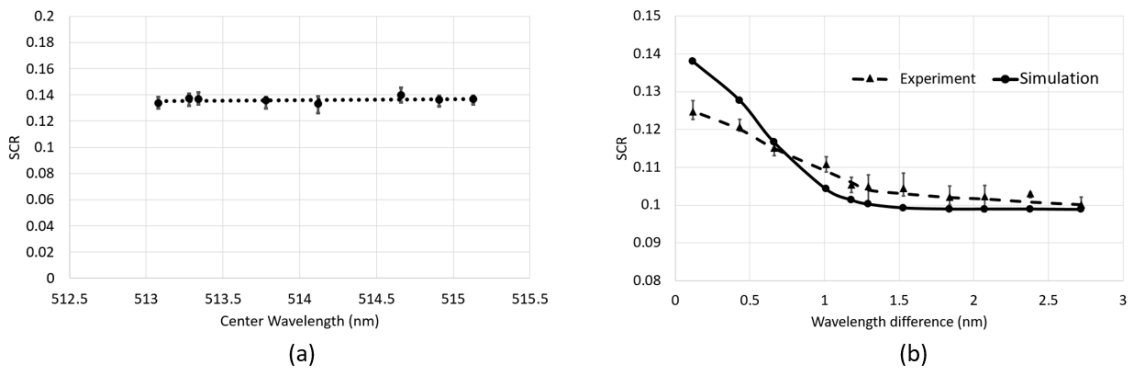
Figure 2.6 Measured SCR (a) for LD2 at different center wavelengths, and (b) for two LDs with LD1 fixed at 515.1 nm and LD2 changed from 512.5 nm to 515.1 nm.

The X-axis in Figure 2.6(b) is the wavelength difference between the two LDs and the Y-axis is the SCR. The solid curve corresponds to theoretical simulations, while the dashed curve indicates a curve fitting the measured data. It is worth noting that the values of SCR in Figure 2.6 include contributions from all of the three speckle reduction methods (i.e. wavelength diversity, spatial diversity and polarization diversity), which can be seen from the experimental setup shown in Figure 2.5. Thus, we have to consider their effects

on the simulations. As shown in Eq.1.19-1.20, the spatial diversity and polarization diversity are independent of the wavelength diversity. As a result, the simulation results shown in Figure 2.6(b) can be obtained simply by reducing proportionally the values shown in Figure.2.1(b) from 76% to 13.7% at the left end of the simulated curve. As shown in Figure 2.6(b), the measured SCR drops with the increase of wavelength difference between the two LDs and the SCR reaches the minimum value when the wavelength difference reaches to 1.5nm, which agrees well with the theoretical simulations.

The measured SCR is smaller than the calculated value when the wavelength difference is zero, as shown in Fig 2.6(b). There are several reasons that could contribute to this result. First, in the simulations, two LDs were assumed to have exactly the same spectrum shape with the same linewidth of 1.2 nm. However, in the experiments, we found that the spectrum shapes of the two LDs were not identical. As a result, when the wavelength difference is small (e.g. zero wavelength difference), the light from the two LDs do not provide a high degree of overlapping in the spectrum domain. This spectrum mismatching generates a larger wavelength diversity effect as compared to the theoretical prediction, which can result in a lower SCR. Second, laser beams were delivered from a fiber bundle in the experiments. The output beams of the two LDs from the fiber bundle were arranged close to each other but not from exactly the same location. As a result, the two LDs illuminate the screen with slightly different illumination angle. Based on [18], even when the two lasers have the same wavelength, different illumination angles generate two slightly different speckle patterns, which can also result in a slight speckle reduction.

2.4.2 Lasers with Different Linewidths

To verify the theoretical simulations of blending two lasers with different linewidths, experiments using the setup shown in Figure 2.7 were conducted. A DPSS laser at 532 nm (Nanjing CQ Laser Tech.) with a linewidth of about 0.15 nm and a semiconductor LD (NDG7475 Nichia) at 520 nm and a linewidth of 1.5 nm were used in the experiments. The two laser beams were combined using a polarizing beam splitter (PBS). A convex lens was used to enlarge the laser spot and throw the light on to a screen. The screen is not sensitive to orientation and the incident linearly polarized laser light is depolarized after diffused from the screen. A monochromic camera with a pixel size of 4.40 μm × 4.40 μm was used to capture the speckle pattern. The frame rate was set at 1/15s. The camera was set 3 meters away from the screen. The camera lens was set to a focal length of 50 mm with F/16, which gave a diameter of around 3.2 mm. It is noted that it is very important to make sure the camera setup correspond to the perception of the human eye in a projection environment since it is well known that the camera setup can greatly change the measured SCR value [45]. An improper setup might give a lower SCR that would not accurately reflect the speckle level of the system.

The SCR values were calculated from the captured images, following the suggestion from [46]. The measured speckle is shown as dots in Figure 2.3 as well so that theoretical simulations can be easily compared with the experimental results. It can be seen that a minimal SCR is achieved when $P_{LD} : P_{Total}$ is equal to 0.8, which agrees very well

with simulated results. The experimental SCRs are lower than the simulated results. The reason for this is that camera pixels have a finite size and there is a spatial averaging effect, which reduces the measured SCR [47]. This effect becomes more obvious as the speckle level increases. This also explains why on the left side of the figure, the differences between the experimental and theoretical results are larger.
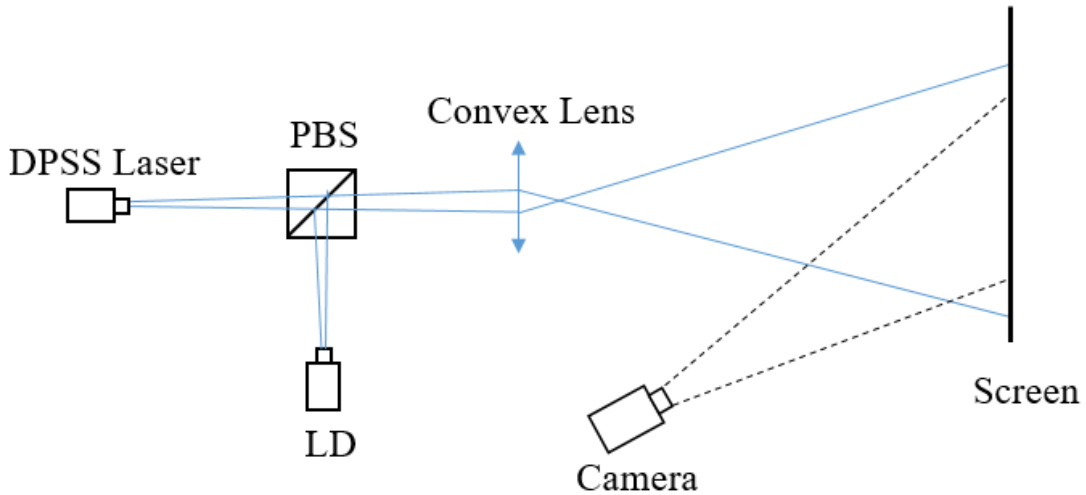
Figure 2.7 Experimental setup to verify the presented theoretical model using lasers in wavelength blending

2.5. Discussion and Conclusion

In this chapter, a theoretical model to calculate the SCR of a wavelength blended light source has been presented. The model has been verified by wavelength blending using a) two semiconductor laser diodes with equal power at different wavelengths and b) a semiconductor laser diode and a DPSS laser with fixed wavelengths and varying power

ratio.

The model can be used to select the optimal laser wavelengths and power ratio between different lasers. The minimal wavelength shifts between two adjacent wavelengths to generate de-correlate speckle patterns as a function of the laser linewidth are calculated, which can provide a guideline in the selection of lasers to generate optimized wavelength blending for speckle reduction. This minimum wavelength difference $\Delta\lambda_{min}$ is strongly dependent on laser linewidth. The broader the laser linewidth, the larger the minimum wavelength difference $\Delta\lambda_{min}$ is. It has been shown that the minimum wavelength difference $\Delta\lambda_{min}$ is 1.0 nm and 1.5 nm for the green DPSS lasers and green semiconductor LDs, respectively.

Wavelength blending effects on the number of lasers used in combined laser sources has also been studied. It has been shown that, by combining wavelength diversity, spatial diversity and polarization diversity, speckle free projection can be achieved. Assuming the wavelength difference is larger than the minimum wavelength difference $\Delta\lambda_{min}$ and a depolarized screen is used, the minimum number of lasers required to achieve speckle free projection is three and two for green DPSS lasers and semiconductor LDs, respectively. For a polarized screen, these numbers increase to five and three for green DPSS lasers and semiconductor LDs, respectively. The results presented in this paper can provide a guideline on laser selection the in design of speckle free laser projection systems.

CHAPTER 3

Speckle Reduction Based on Spatial Diversity

3.1. Spatial Diversity in Speckle Reduction

In order to reduce speckle in laser projection system, besides wavelength diversity, spatial diversity is also considered as a major factor to fulfill the purpose. The spatial diversity has been briefly discussed in Chapter 1. In this section, a more detailed discussion and comparison will be made.

Before more detailed discussion regarding speckle reduction using spatial diversity, we need to look at the working principle of laser projections. Unlike wavelength diversity, speckle reduction using spatial diversity is closely related to projection method.

For laser based projections, there are usually two different types of projection: a) whole frame laser projection and b) laser scanning projection.

The whole frame projection system projects an entire frame to the screen at once. The laser beams of three primary colors red, green and blue are expanded, reshaped and homogenized first, then illuminate on three 2D spatial light modulators or one modulator depends on the design. Figure 3.1 is a schematic diagram of a conventional whole frame projection system [48].
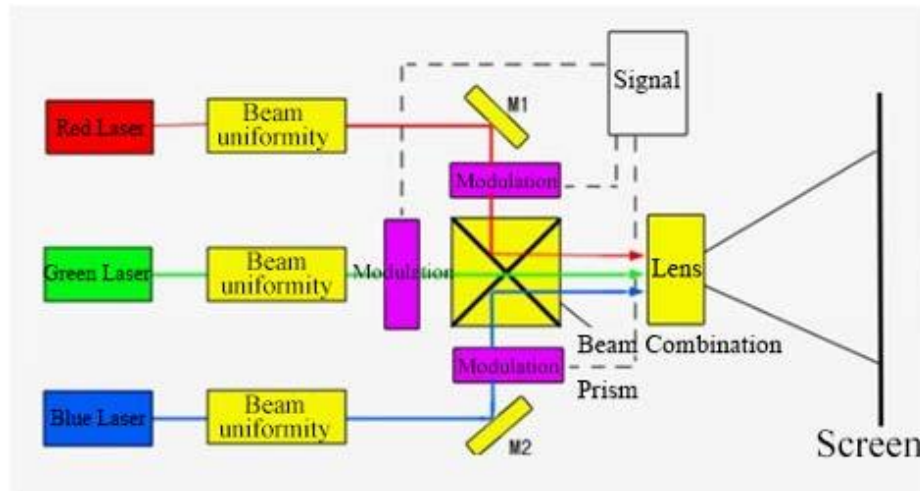
Figure 3.1 A conventional whole frame laser projection system [48]

As shown in Figure 3.1, the whole frame laser projection system has several important modules: 1) laser light source; 2) beam uniformity components; 3) spatial light modulator(s) and 4) beam combiner and projection lenses. There are typically three types of spatial light modulators: digital light processing (DLP) [48], liquid crystal on silicon (LCoS) [49] and liquid crystal device (LCD) [50]. DLP and LCoS are reflective devices. Most LCDs are transmittance devices, though there are few reflective LCDs as well [51]. They can modulate the reflective/transmitted intensity and color of the light beam that corresponds to the targeted image. The modulated light field can be projected onto a screen and then observed by the audience.

In Figure.3.1 three LCDs are used to modulate the light. In some systems, only one modulator is used as red, green and blue primary lasers are modulated in time-sequential manner [52-54]. Colorful images can also be produced if within one frame time of the modulator, only one color is illuminated on to the modulator.

When discussing speckle reduction within the whole frame laser projector, the methods mostly focus on light source and beam uniformity components. The laser light source is where the wavelength diversity technique applied, which has been discussed in Chapter 2. The homogenization and beam uniformity part is usually where spatial diversity technique applied. As mentioned in Chapter 1, the idea of spatial diversity is by generating multiple independent speckle patterns and overlap them together, which will generate a uniform light field with reduced speckle.
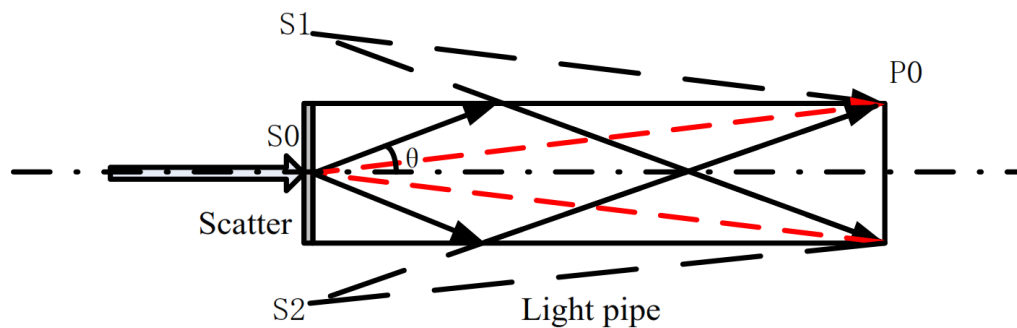
Figure 3.2 Multiple speckle patterns generated by light pipe

There are usually two methods to achieve this goal. The first is trying to generate these speckle patterns simultaneously. This can be done by using homogenization components like a light pipe [55, 56] and lens array [57]. Figure 3.2 is an example of using a light pipe to generate multiple speckle patterns. The incident laser first illuminates a diffuser, then scattered light passes through the light pipe. It is clear that the internal reflections can be considered as multiple virtual light sources illuminate from different locations and angles and they all overlap at P_0.

When the optical distance differences from different virtual light sources to the P_0 are larger than the coherent length of the laser, the overlapping on P_0 will be on intensity bases and a homogenized light field with reduced speckle can be provided.

This approach has an apparent drawback. It is difficult to generate a large number of independent speckle patterns in this case. Thus, the second option is used. By providing time varying components, these patterns can also be generated. If the patterns are generated faster than the integration time of a human eye, it will also provide speckle reduction effect. One common approach is to vibrate/rotate the diffuser [58-60]. For example, in Figure 3.2, when the diffuser moves, a different speckle pattern can be generated. If the diffuser is moving fast enough, a very large number of independent speckle patterns can be provided and a very good speckle reduction effect can be achieved.

Besides whole frame projection, the second common type of projection is laser scanning projection. The laser scanning projection utilizes the laser's characteristic of small etendue which has a very small divergence angle. When the fast scanning laser spot/line is faster than the persistence time of a human eye, two dimension images can be formed [61-63]. Unlike a conventional projection system, this type of projection usually does not use a projection lens, and is more suitable for portable, integrated display systems. Figure 3.1 is an example for a laser scanning projection system.

In Figure 3.3 two different rotating reflection mirrors are used for laser scanning. The first mirror controls horizontal scanning and rotates at a high speed while the second mirror controls vertical scanning and rotates at a relatively low speed. RGB lasers are time-sequential modulated to generate colorful image.
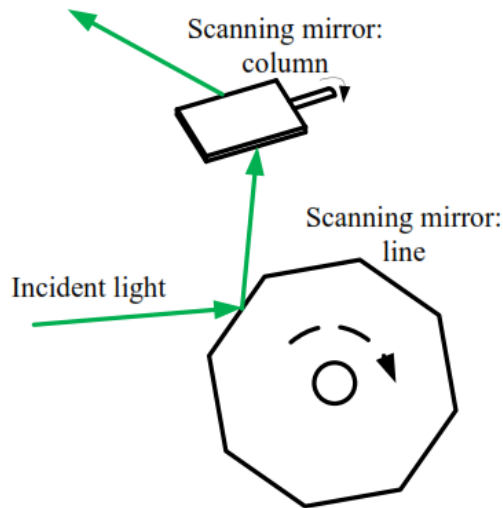
Figure 3.3 Two-dimension laser scanning projection system

The spatial diversity method for speckle reduction is not very suitable for scanning projections. First, if homogenization components like a light pipe or lens array are used, they will destroy the small divergence character of laser beams, which is unacceptable for laser scanning projection. Second, if time-varying components are used, the varying speed for laser scanning projection is much higher than whole frame projection. For example, for 3 chip LCD projection with a 50 frame rate per second, each frame has a duration of 20ms [64]. The time varying components only required to provided enough changes within 20ms. Meanwhile for laser scanning projection, the duration time of each point can easily be at ~100s ns range [65]. This requires the time varying method generates speckle patterns even faster than this period, which will be very difficult to realize in practical engineering level. These reasons seriously limit the speckle reduction in laser scanning projection. As a result,

laser scanning projection usually has much more serious speckle compared to whole frame projection. Besides this, due to safety issue, the direct scanning projection can hardly use high output power lasers. According to [66], when use Class 2 lasers for scanning projection, only less than 20 lm brightness can be provided.

As a result, the laser scanning projection is not suitable for large scale application and spatial diversity speckle reduction is mostly suitable for whole frame projection. Thus the discussion regarding spatial diversity speckle reduction will be based on whole frame projection in this thesis.

3.2. Motionless Speckle Reduction with Spatial Diversity

3.2.1 Experimental Setup of Speckle Reduction with Spatial Diversity

As discussed in Section 3.1, spatial diversity can be achieved by providing multiple speckle patterns simultaneously or by using time-varying components. Usually the former way can provide only a limited number of speckle patterns while the later one can generate a very large number of these patterns, which will provide a much better speckle reduction.

The conventional methods to provide spatial diversity using time-varying are usually achieved by moving components, such as: a vibrating diffuser, a rotating light pipe or a rotating lens array. The biggest advantage for this method is that the principle is straight

forward and it is relatively easy to implement. The speckle reduction is also very effective. However, there are also some drawbacks here. First, the mechanical moving/vibrating/rotating components may introduce instability issues into the projection system, which can hardly be acceptable for commercial projection products. Second, these mechanical moving components may require a large space and are difficult to be integrated into the system, which will cause design problems.

As a result, an integrated spatial diversity speckle reduction system with high stability is highly desired in practical laser projection systems. In this chapter, a speckle reduction system that is presented, which is compact, easy to setup, low cost and has low optical penalty.
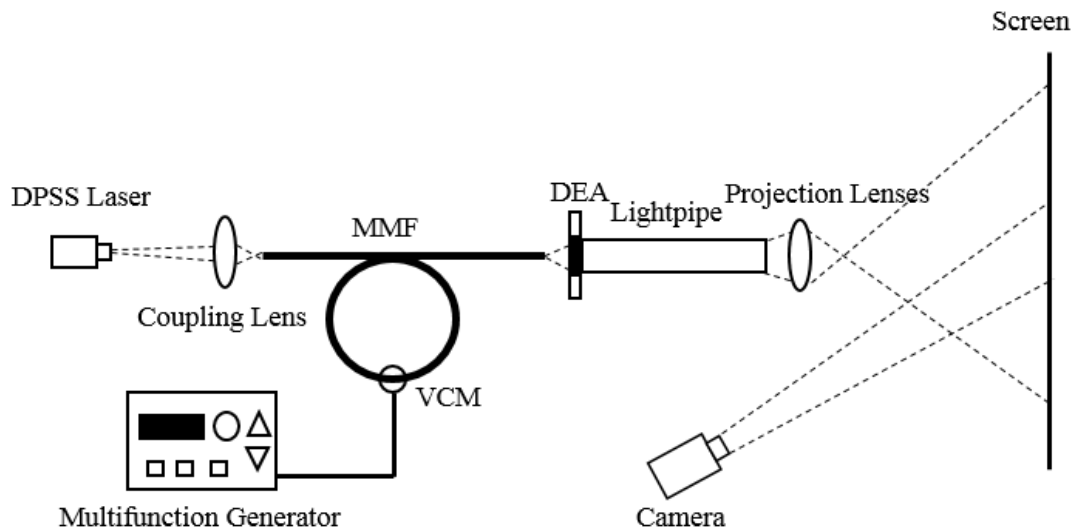
Figure 3.4 Schematic diagram of experimental setup

Figure 3.4 shows the setup used in the experiments. A frequency doubled DPSS laser from CQ Laser Technologies was used as a light source in the experiments. It emits

laser beam at 532 nm with a linewidth of about 0.1 nm. The laser beam was coupled into a multimode fiber (MMF) with a length of 2 meters. Part of the MMF was fixed on a voice coil motor (VCM), which was driven by a multifunction generator to introduce vibration in the MMF. A dielectric elastomer actuator (DEA) was placed 2 cm from the output facet of the MMF. The output light from the DEA then entered into a hexagonal lightpipe placed directly behind the device. Projection lenses were used to throw the end of the lightpipe onto a de-polarization screen. The distance between the projection lenses to the screen was 1.5 meters.
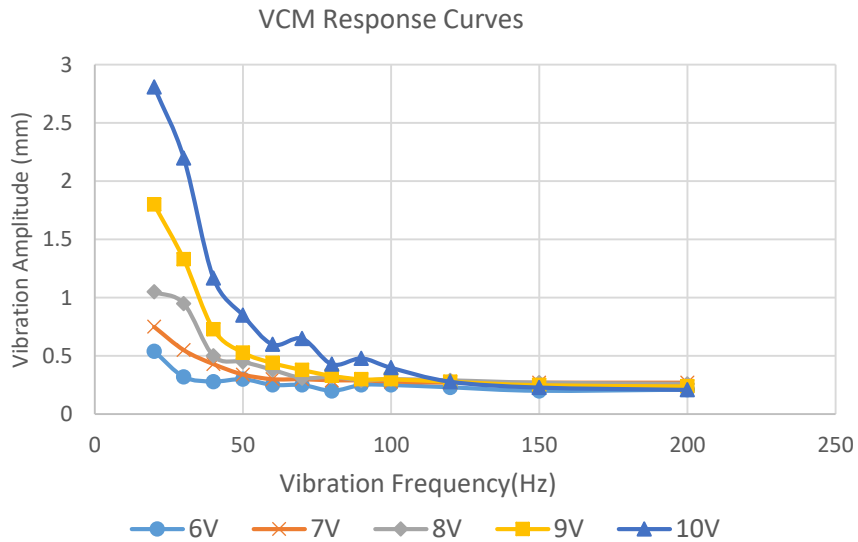
Figure 3.5 VCM response curves under a range of driving voltages

In the system described below, an optional VCM was used to vibrate the MMF, which generated a time-varying phase modulation. The diameter of the VCM was 2 cm. The amplitude-frequency relationship under a range of driving voltages (peak value) is shown in Figure 3.5.

In Figure 3.5, the X-axis is the vibration frequency of the VCM, and the Y-axis is the vibration amplitude. The driving signals used are sinusoidal and values shown above are peak voltage. In the experiments, the VCM was operated at 50 Hz and 9 V driving voltage. From Figure 3.5, the vibration amplitude of the VCM is estimated to be 0.5 mm. The vibration of VCM is optional. Also, the MMF is 2 meters long, the vibrating part can be separate away from the light engine, which will not introduce too much instability to the system.

A monochromic camera (DALSA M1600) was used as a detector. The camera was 3 meters away from the screen. The pixel size of the camera was 4.40 μm x 4.40 μm. The output image was an 8-bit grayscale image. The shutter speed was 1/15s and the camera lens had a 50-mm focal length at F/16.

Three major components are used to provide spatial diversity in the system: 1) multimode fiber, 2) dielectric elastomer actuator and 3) light pipe. They are studied independently and will be presented below.

The speckle reduction effect of the MMF is studied first. Four different MMFs with a core diameter ranging from 200 μm to 800 μm are studied and compared in the experiments. Figure 3.6 shows the measured SCR for MMFs with different core diameters with (dots) and without (squares) vibration, respectively.

In the experiments, the laser beam was coupled into an MMF with an objection lens. The MMFs were kept straight in the experiments and the output light was shone directly on the screen that was 1.5 meters away from the output facet of the MMFs. The speckle patterns were captured by the camera 3 meters away from the screen. As shown in Figure

3.6, when the MMFs remain stationary, the measured SCR drops from 54% to 44% when the core diameter increases from 200 μm to 800 μm. When the VCM was turned on, the SCR could be further reduced by introducing vibration to the MMF through a VCM, which introduces temporal diversity into the illumination light. It was found that when the MMF was coiled and consisted of two turns with a diameter of 20 cm, the VCM had the largest effect on speckle reduction and the smallest SCR was achieved. In both cases, the measured SCR from the MMF tends to saturate when the core diameter is larger than 800 μm. Considering the fact that the larger the MMFs core diameter, the higher the cost and the poorer the flexibility of the MMFs, the MMF with a diameter of 800 μm is selected for the optimized de-speckle configuration described below.
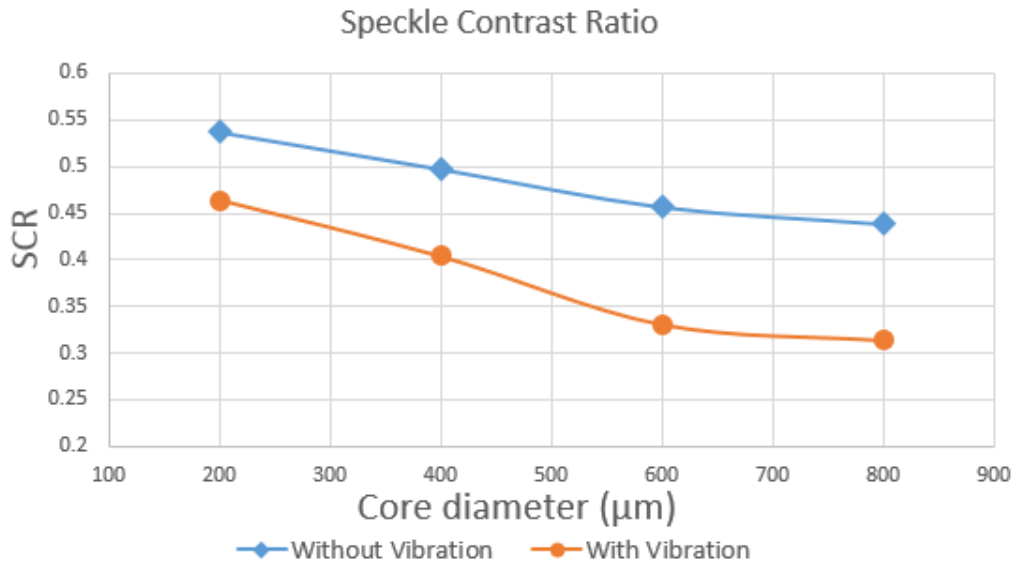
Figure 3.6 SCRs of different MMFs with and without vibration

Larger fiber core diameter can support more waveguide modes. There are several

mechanisms that contribute to speckle reduction by using an MMF that is related to its mode profiles. When the VCM is turned off, a piece of straight MMF is considered to be stationary and power distribution between different waveguide modes does not change significantly with time. Under this circumstance, the main mechanism for speckle reduction by the MMF is modal dispersion [67,68]. According to the ray optics, the shortest propagation time is experienced for a mode propagating along the axis of the fiber without any reflection, while the longest propagation time is expected for a mode reflecting at the interface between the core and cladding layers at the critical angle θ_C. The difference in propagation times between these two modes is given by:

$$\Delta t \approx \frac{L}{2cn_1}(NA)^2 \tag{3.1}$$

where L is the length of the fiber, n_1 is the refraction index of the core and NA is the numerical aperture of the fiber. The MMFs used in the experiments all have an NA of 0.37 and a length of 2 m. As a result, Δt is about 0.3 ns. The DPSS green laser used in the experiment has a wavelength of 532 nm with a spectral width $\Delta\lambda$ of 0.1nm. The coherence time of the laser source is given by $\lambda^2/c\Delta\lambda$, which is about 8 ps. Thus, the two waveguide modes described above can be considered as de-correlated and can have low temporal coherence, resulting in speckle reduction at the output end of the MMF. The MMF with a larger core diameter will provide more de-correlated modes and give a more uniform light field with little speckle. Since only the low order waveguide modes are usually excited in a straight fiber, it is necessary to bend the fiber so that high order waveguide mode can be excited. Bending MMF can change waveguide mode power distribution, and result the higher order waveguide modes being excited.

On the other hand, there are two additional mechanisms within the MMF that contribute to speckle reduction when the MMF is vibrated: phase shift and mode coupling. First, there is a phase modulation for guided modes when the VCM is turned on. Since many modes propagate along the fiber with various propagating constants, there is a phase shift between different waveguide modes. Since the phase shift is very sensitive to the ambient environment of the MMF [69, 70], the vibration caused by the VCM changes the phase shifts rapidly [71]. When the VCM is vibrating at a high frequency, the phase shifts between different modes vary on a time scale faster than the integration time of the camera. As a result, when the modes with a rapidly varying phase shift overlap at the end of the MMF, effective speckle reduction can be expected.

Second, mode power distribution is also very sensitive to vibration. The mode coupling between various waveguide modes changes when the fiber is bent and vibrated [71]. If the fiber deformation is large and fast enough to create fast-changing random mode coupling in a large range, the mode power distribution also changes randomly with time. As a result, the output pattern at the fiber end varies with time, which results in speckle reduction.

After the MMF, the second component used in the system for speckle reduction is dielectric elastomer actuator (DEA). DEAs are relatively new devices for speckle reduction. The working principle of a DEA is shown in Figure 3.7. A rigid diffuser is bonded on an electro-active polymer (EAP) membrane placed in the middle of four electrodes. When no voltage is applied to the electrodes, the diffuser is centered (Figure 3.7(a)); when the upper electrode is active, the diffuser is translated downwards (Figure 3.7(b)); when both

electrodes are active the diffuser is translated to the bottom right corner (Figure 3.7(c));

when only the left electrode is active a translation to the right results (Figure 3.7(d)). As a

result, the diffuser is set into a circular motion.
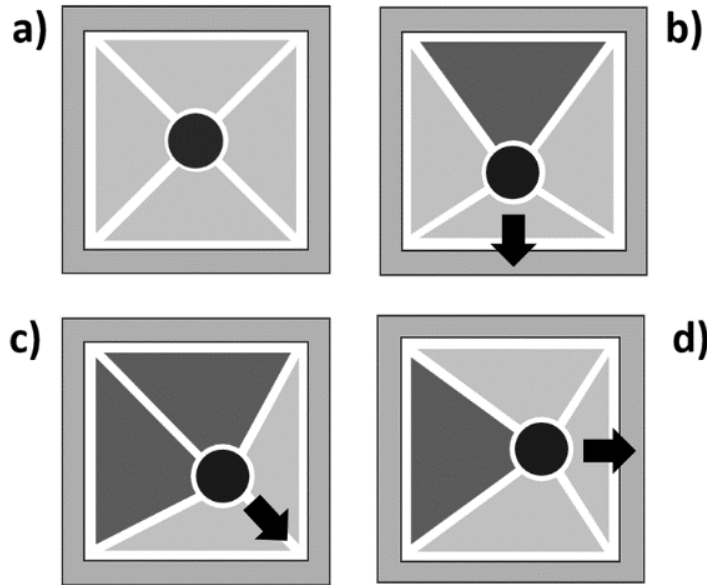
Figure 3.7 DEA Diffuser position when a) no voltage is applied to the electrodes; b) the

upper electrode is active; c) both electrodes are active; d) only the left electrode is active.

The diffuser surface contains many uncorrelated structure cells [72]. After the

moving diffuser, the light beams passing through the uncorrelated structure cells overlap

with each other and result in a time averaged, suppressed speckle pattern. By controlling

the size of the grain structure, the divergence of the diffuser can be controlled. A smaller

grain size will give a larger divergence angle. Thus, when the area of illumination is fixed

in the experiments (e.g. a circular beam spot with a diameter of 5 mm in the experiments),

the number of illuminated uncorrelated structure cells for the larger divergence angle

diffuser will be more than that for the small divergence angle diffuser. As a result, the light

from the large divergence angle DEA is more uniform than the smaller one, implying a higher speckle reduction effect.

As mentioned above, a DEA with a larger divergence angle is desired. However, in a practical optical system, there are also limitations on the DEA's divergence angle. First, as the lightpipe was used after the DEA, the divergence angle of the DEA has to be smaller than the critical angle of the light pipe in order to prevent coupling loss. For a light pipe made from N-BK7, the critical angle is 41°. Second, system étendue has to be considered in order to prevent optical loss. For a home theater projector, the commonly used LCoS panel size is 0.63" with an aspect ratio of 16:9. Incident angle on the panel is usually controlled to be less than 10° to maintain good modulation quality. The étendue of the panel can be approximated as:

$$E_P = \pi S sin^2\theta = 0.104\ cm^2 sr \tag{3.2}$$

where the S is the size of the panel and θ here is 10°. In the proposed system, the étendue is determined by the DEA. As the illumination area of the DEA is fixed (e.g. a circular beam spot with a diameter of 5 mm in the experiments), the maximum allowed divergence angle is:

$$\theta_{DEA} = sin^{-1}\left(\sqrt{\frac{E_P}{\pi A}}\right) \tag{3.3}$$

where A=0.196 cm^2. Thus, calculated θ_{DEA} is 24.3°. The DEAs with a divergence angle smaller than this value will not introduce light loss caused by étendue mismatch. Considering the above limitations, a DEA with a divergence angle of 24° was used in our experiments. In the discussion below, a DEA with divergence angle of 6° was used as a

comparison.

For other applications like cinema or conference displays, a larger display panel might be used. Thus the system étendue can be bigger and a DEA with an even larger divergence angle might be allowed.

The third component used here is the light pipe. The lightpipe is a well-known component for light homogenization. It can also be used for speckle reduction. The principle of light pipe in speckle reduction has been discussed in previous section: the overlapping of virtual images could provide a uniform light field.

For a lightpipe with a fixed incident light, the number of internal reflections is determined by the cross-section diameter and the length of the lightpipe. Generally speaking, for incident light with divergence angle of θ, which enters the lightpipe from the center of the front surface , the number of internal reflections N' is given by:

$$N' = \frac{\sin(\theta) \times L + \frac{D}{2}}{D} \tag{3.4}$$

where L is the length of the lightpipe and D is the diameter of the lightpipe. Then the round number of N' is the maximum number of reflections N that can occur within the lightpipe. As shown above, to have a large N with a fixed θ, a smaller diameter and a longer lightpipe are desired.

However, the diameter of the lightpipe cannot be too small. As the lightpipe was placed after the DEA, to prevent large coupling loss, the cross-section diameter of the lightpipe has to be controlled. As mentioned above, in our experiments, the DEA had a diameter of 5mm and a divergence angle of 24 °, and the lightpipe was placed 5 mm after

the DEA to prevent any physical contact. Therefore, the minimal required cross section diameter of the light pipe has to be $D_{min} = 5 + 2 \times 5 \times \sin(24°) = 9.1mm$. In the experiments, a lightpipe with a diameter of 10mm was chosen to avoid the coupling loss.

Limited by the cost, space and handling, the lightpipe cannot be too long either. In [73], N bigger than 4 can give very good light field uniformity. By using Eq.3.4 with a diameter of 10 mm and a divergence angle of 24 °, the desired lightpipe to achieve N equals to 5 should be no less than 12cm. In the experiments, a 15cm lightpipe was used to achieve better uniformity.

3.2.2   Experimental Results of Speckle Reduction with Spatial Diversity

The SCR values were measured using the proposed setup. It is worth noting that, first, the optimized de-speckle components were used in the experiments. As discussed in the previous section, the 800 μm MMF was used in the system. A DEA with a divergence angle of 24 ° was used to reduce speckle without étendue mismatch. Second, the speckle measurement standard recently proposed by the Laser Illuminated Projector Association (LIPA) [46] and human eye perception was considered in the measurements. The output image was captured by a camera. It is known that the camera setup can greatly change the measured SCR. A camera lens with 50 mm focal length and F/16 was chosen in the experiment. It is worth noting that these parameters result in a lens diameter of around 3.2 mm, which corresponds to the iris diameter of the human eye in a cinema environment [39]. The F/16 is chosen to match with camera pixel size, which will give a similar sampling rate

between speckle size over camera pixel size as human retina (F/8) match with visual cell size. Detailed discussion regarding camera parameter setup is in section 5.3.
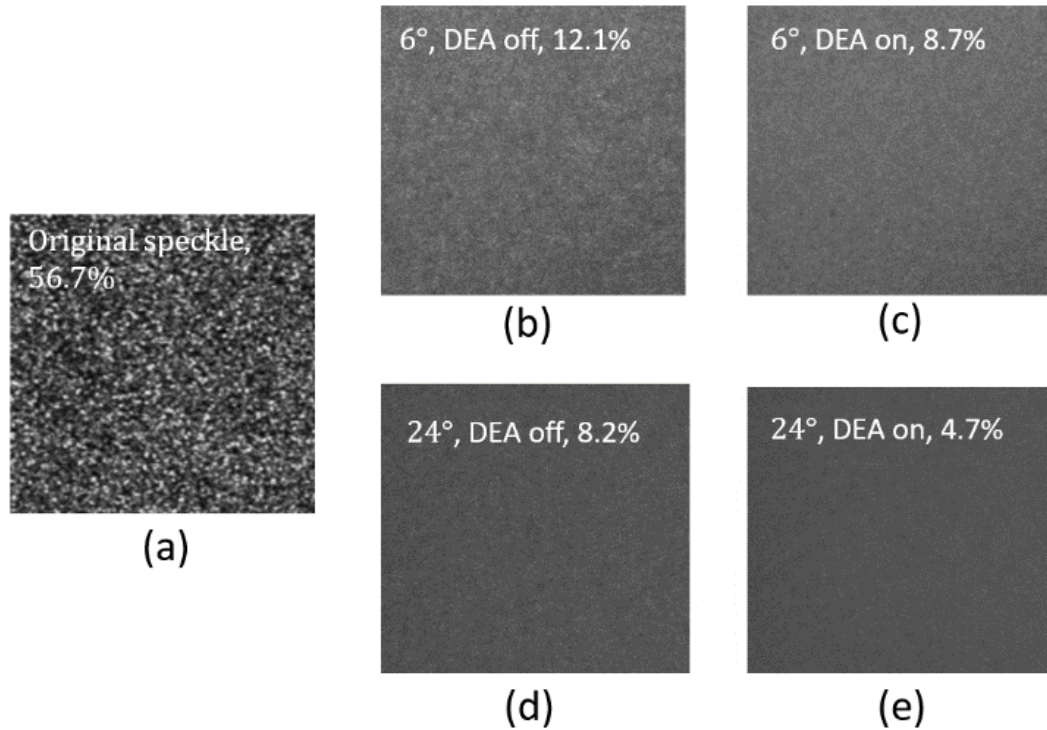
Figure 3.8 Measured speckle patterns and SCR. (a) DPSS laser light directly onto a depolarizing screen. Using a DEA with 6 ° divergence angle, the DEA was (b) inactivated and (c) activated. Using a DEA with 24 ° divergence angle, the DEA was (d) inactivated and (e) activated.

The original speckle of a DPSS laser was first measured by projecting the laser light with a beam expander directly onto the depolarizing screen. The speckle pattern is shown in Figure 3.8(a) and the SCR is 56.7%, which agrees well with the reported values [74]. The measured result is slightly lower than the theoretical SCR of $1/\sqrt{2}$ for laser projection

on a de-polarized screen. The reasons can be understood as follows: first, the DPSS laser has a finite bandwidth of around 0.1nm, which will generate less speckle than an ideal monochromic light source [33]; second, the camera used in the experiment has a pixel size of 4.4μm*4.4μm. The averaging effect caused by finite pixel size will result in a lower SCR as well [39].

Experiments were first conducted when the VCM was turned off. In this scenario, no moving component is involved in the system. The measured speckle patterns and SCR are shown in Figure 3.8(b)-(e).

Figure 3.8 (b) and (c) show the speckle patterns when a DEA device with a divergence angle of 6° was not activated and activated, respectively The measured SCRs are 12.1% and 8.7% when the DEA device was turned off and on, respectively. Therefore, with this de-speckle system setup, (56.7%-12.1%)/56.7%=78.7% and (56.7%-8.7%)/56.7% =84.7% speckle reductions from the initial value can be achieved when the DEA device is turned off and on, respectively.

When the VCM was turned on, it offers a time-varying modulation to the MMF and the speckle can be further reduced. Figure 3.9 shows speckle patterns measured under this situation.

Figure 3.9(a) and (c) show the measured speckle patterns when the DEA was not activated and the VCM was turned on. The measured SCRs are 8.5% and 6.2% for the DEA device with a divergence angle of 6° and 24° respectively, corresponding to 85% and 89.1% speckle reduction from initial speckle. Figure 3.9 (b) and (d) show the measured speckle patterns when the DEA was activated. As shown in Figure 3.9 (b) and (d), the SCR further

drops down to 6.6% and 3.7% respectively. In the last case, the DEA device with 24°
divergence angle was activated and VCM was applied. The measured 3.7% SCR is so low
that the human eye can hardly detect any speckle in the experiment.
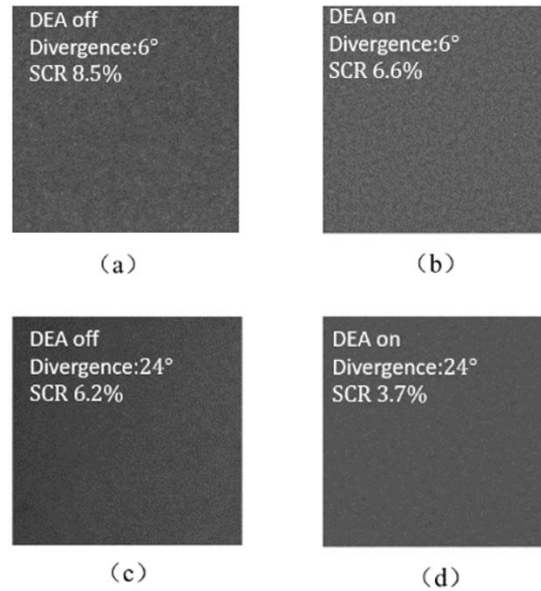
Figure 3.9 Measured speckle patterns and SCR when the VCM was turned on. Using a
DEA with 6° divergence angle, the device was not activated (a), and activated (b). Using
a DEA with 24° divergence angle, the device was not activated (c) and activated (d).

From a practical application point of view, optical power penalty (or light
transmittance) is also very important. To evaluate the optical power penalty of the de-
speckle system, optical transmittance for all the components involved in the de-speckle
system have to be considered. Table III-I shows the measured transmittance for different
DEAs without anti-reflection coating at the surfaces.

In addition, the measured coupling efficiency for the MMF is 91.8% without anti-
reflection coating at the facet of the MMF and vibration from the VCM does not introduce

any significant optical loss. For the lightpipe in combination with a DEA, besides the reflection losses at the input and output facets, the loss due to the total internal reflection has to be considered. This depends on the diffusion angle of the DEA in front of the lightpipe. The measured lightpipe transmittances are 90.0% and 88.9% without anti-reflection coating at the surfaces when the lightpipe is combined with DEAs with divergence angles of 6 ° and 24 ° respectively.

Table 3-1 Optical efficiency of different DEAs

Component	DEA (6 °)	DEA (24 °)
Transmittance	90.2%	77.6%

To summarize, when a DEA with 6 ° divergence angle is used, the transmittance of the entire de-speckle system is 0.92×0.9×0.9×100% = 73.0% (or an optical power penalty of 27.0%) without anti-reflection coating at the surfaces of the components involved. When a DEA with a 24 ° divergence angle is used, the transmittance of the de-speckle system drops down to 0.92×0.78×0.89×100% = 63.3% (or an optical power penalty of 36.7%) without anti-reflection coating at the surfaces of the components involved. Therefore, the tradeoff between SCR and optical transmittance (or optical power penalty) has to be made. By employing suitable coatings, the transmittance of the lightpipe can be higher than 0.95. Thus, the total transmittance of the system can be increased to around 77% and 67% respectively.

3.3. Discussion and Conclusion

In this chapter, a speckle reduction system mostly using spatial diversity to reduce speckle is presented. The system consists of an MMF, a VCM, a DEA and a lightpipe. The system has characteristics such as easy setup, low speckle, low optical penalty and high compatibility with a wide range of projectors. The components that provide spatial diversity used in the system have been studied, discussed and optimized individually to provide the best speckle reduction at low cost without serious light loss. It has been shown that an SCR as low as 3.7% is achieved by employing an MMF, a VCM, a DEA with a divergence angle of 24 °, and a lightpipe for a laser light from a DPSS green laser. This yields speckle which is invisible to the human eye. However, optical transmittance of 63.3% has to be accepted in this de-speckle system. It is expected that the optical transmittance can be increased to 67% and 77% by applying anti-reflection coatings on the surfaces of the components involved. It is important to use optimized de-speckle components, taking into account the balance between low SCR and high optical transmittance in designing the de-speckle system for practical applications.

CHAPTER 4

Speckle Reduction Based on Engineered Screen

4.1. Introduction

In a laser projection system, there are multiple components that play important roles related to speckle generation/reduction. In Chapter 2, low speckle laser source is discussed and in Chapter 3, low /speckle light engine is discussed. With the light engine, the modulated images will be projected on to a screen and then finally observed by an audience. As there are not too many things we can do about the audience side regarding laser speckle reduction, the last component where we could potentially apply a speckle reduction method would be the projection screen.

In recent years, one approach to reduce speckle related to screens is by employing screen vibration/rotation. For example, a screen rotation system is proposed in [75], as shown in Figure 4.1. Four off-axis motors are located at the four corners of the screen and rotate simultaneously, which will provide a rotation to the entire screen. As the screen is moving and can be considered as a time varying component, it can generate multiple independent speckle patterns and greatly reduce the speckle.

However, the drawback of such setup is clear. Stability is still one of the biggest

issues. Besides, this setup can be used for only small sized screens, when large sized screens for theaters or conferences are used, it will be almost impossible to rotate them.
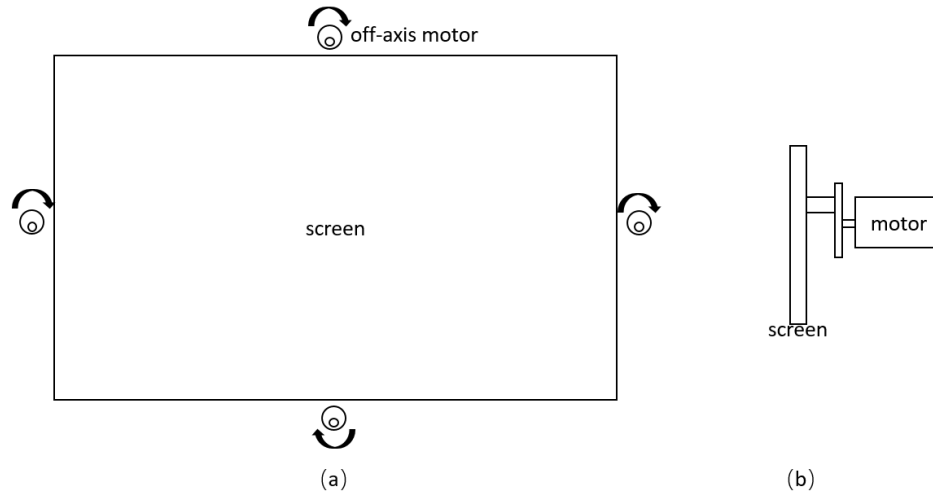
Figure 4.1 Rotating screen for speckle reduction. a) system layout and b) structure of off-axis motor.

Another similar setup is using vibrators attached to the back of the screen [76,77]. By driving these vibrators, the screen surface will also be vibrated and provide time-varying effect which can reduce speckle. However, each vibrator can only provide sufficient vibration to a small surrounding area and multiple vibrators have to be used [78]. When a large number of vibrators are used, they may form standing waves on the surface of the screen. As a result, some locations on the screen will have very limited vibrating amplitude, and speckle will be much more obvious at these areas [79]. In addition, the stability and noise caused by these motors are big issues.

As discussed above, speckle reduction related to screen moving is not the optimal

choice due to practical limitations. A specially designed screen which generate less speckle is highly desired.

4.2. Speckle Reduction Limitation with Traditional Screen

In Chapter 1 and Chapter 3, it has been briefly mentioned that the speckle reduction has an upper limit which is caused by optical layout and observation setup. This limitation is valid when a traditional projection screen is used. This chapter will detail explain the origin and results of this limitation.

In a projection system, audiences will observe the screen from multiple angles. As a result, the screen has to scatter the illumination light into a relatively large angle. Traditional screens use materials with rough surfaces which can satisfy this requirement. However, these rough surfaces will also introduce random phase term to the incident laser light and generate speckle.

Figure 4.2 is a schematic diagram of a practical laser projection system. The entire system can be simplified as several modules: laser source, homogenization components, light valve (LCD, LCoS, DLP etc), projection lens(es), screen and observers.
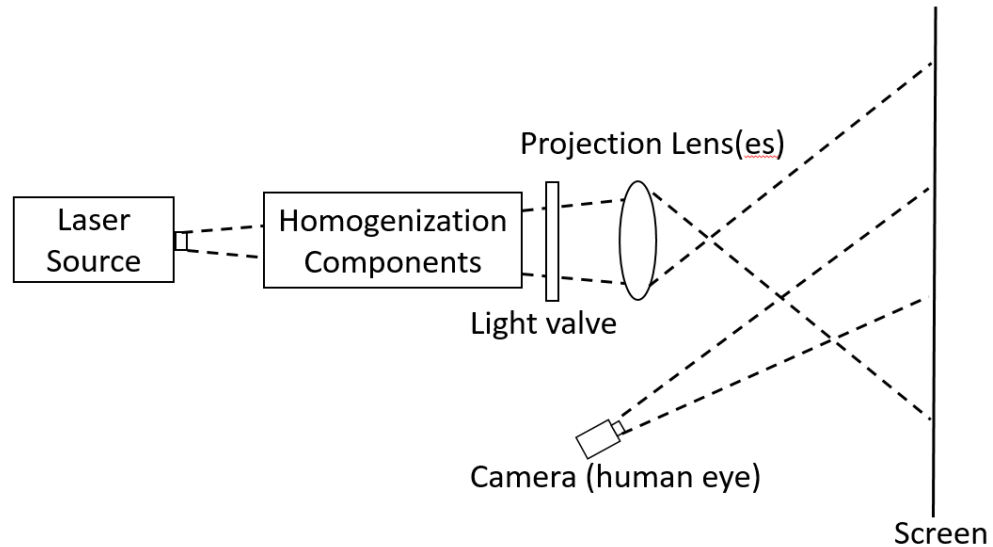
Figure 4.2 A schematic diagram of a practical laser projection system

Note that the light source can either be a laser diode (LD) or a diode pumped solid state (DPSS) laser. Multiple lasers can be used in this setup to increase wavelength diversity. The laser light emitted from the source is coupled into homogenization components, which provides multiple independent intensity patterns within the integration time of a detector that provides spatial diversity. Commonly used homogenization components can include moving/vibrating diffuser(s), rotating lightpipe and lens arrays. A single light valve or three light valves (based on the system design not shown in the figure) is/are then placed behind the homogenization system to modulate the light beam, forming images which are then projected onto a screen using a projection lens.

In a practical system, all imaging optics have a resolution limit, or diffraction limit. This limit corresponds to the minimal spot that these imaging optics can produce or identify. This limitation was first discussed by Goodman [18]. In this section, the limitation will be

discussed in detail.

Generally speaking, the diameter of minimal resolution spot (or "Airy Disk" from a more physics perspective) for an imaging system can be roughly expressed as:

$$S_{res} \approx 1.22 \frac{\lambda}{D} l \tag{4.1}$$

where λ is the wavelength of the incident light, D is the aperture diameter of the projection lens and l is the image distance.

In a practical projection system, the on-screen resolution area size of a projection lens is usually much smaller than the on-screen resolution area size of the observer (audience or camera). Only under this condition, the observers will not perceive any of the resolution spots of the projector. The detailed geometry layout is expressed in Figure 4.3 below.
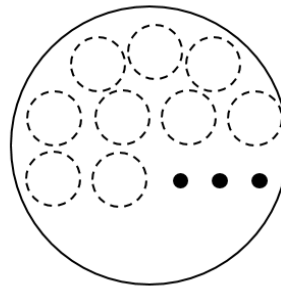
Figure 4.3 Resolution relationship between projection lens and observer

In Figure 4.3, the solid circle corresponds to the on-screen resolution area of the observer and the dotted circles correspond to the on-screen resolution areas of the projection lens. The number of on-screen resolution areas of the projection lens within one

on-screen resolution area of the observer is denoted as K.

As a result, the intensity the observer felt of one point at the imaging plane (the human retina in this case) can be expressed as:

$$I = \left| \sum_{k=1}^{K} A_k B_k \right|^2 = \sum_{k=1}^{K} \sum_{l=1}^{K} A_k A_l^* B_k B_l^* \tag{4.2}$$

where B_k represents the field of one resolution area projected onto the screen by the projection lens and A_k is a random field added to the projected field that is caused by the rough screen.

As there are homogenization components which provide spatial diversity for speckle reduction in the system, multiple independent speckle patterns will be generated within the integration time of the observer. Assuming M independent patterns can be generated, the overall intensity for one point felt by the retina can be written as:

$$I = \sum_{m=1}^{M} I_m = \sum_{m=1}^{M} \sum_{k=1}^{K} \sum_{l=1}^{K} A_k A_l^* B_k^{(m)} B_l^{(m)*} \tag{4.3}$$

where $B_k^{(m)}$ represents the field of one resolution area projected onto the screen by the projection lens for the mth speckle pattern. The summation from 1 to K represents K on-screen projection lens resolution areas that are contained within one on-screen resolution area of the detector lens.

In order to calculate the SCR of the system, the statistical properties need to be calculated. The first step is calculating the average intensity:

$$E[I|A] = \sum_{m=1}^{M} \sum_{k=1}^{K} \sum_{l=1}^{K} A_k A_l^* \overline{B_k^{(m)} B_l^{(m)*}} \tag{4.4}$$

Some assumptions need to be made for further calculation. The term $B_k^{(m)}$ can be considered as if the field was caused by a moving/rotating random diffuser. Assume that the light fields projected to different resolution areas by the projection lens are statistically independent, which means if $k \neq l$, $\overline{B_k^{(m)} B_l^{*(m)}} = 0$ [18][80]. Define when $k = l$, $\overline{B_k^{(m)} B_k^{*(m)}} = P_B$, which also implies the average intensity of illumination does not change with the time. Eq.4.4 can be rewritten as:

$$E[I|A] = \sum_{m=1}^{M} \sum_{k=1}^{K} |A_k|^2 P_B = MP_B \sum_{k=1}^{K} |A_k|^2 \tag{4.5}$$

As A_k is a random phase shift introduced to the projected field caused by the screen, it is related to the screen's properties. For conventional screens, $|A_k|^2$ can be assumed to have the same statistical property over the entire screen. Thus, the Eq.4.5 can be further simplified as:

$$E[I] = MKP_B P_A \tag{4.6}$$

where P_A is the average value of $|A_k|^2$. In order to get the standard deviation of I, the second moment is also needed:

$$E[I^2|A] = \sum_{m=1}^{M} \sum_{n=1}^{N} \sum_{k=1}^{K} \sum_{l=1}^{K} \sum_{p=1}^{K} \sum_{q=1}^{K} A_k A_l^* A_p A_q^* \overline{B_k^{(m)} B_l^{(m)*} B_p^{(n)} B_q^{(n)*}} \tag{4.7}$$

The above equation can be divided in two terms: a) $m=n$ and b) $m \neq n$. They can be written in separate forms:

$$\text{E}[I^2|\text{A}] = M \sum_{k=1}^{K}\sum_{l=1}^{K}\sum_{p=1}^{K}\sum_{q=1}^{K} A_k A_l^* A_p A_q^* \overline{B_k^{(m)} B_l^{(m)*} B_p^{(m)} B_q^{(m)*}} + \cdots$$

$$(M^2 - M) \sum_{k=1}^{K}\sum_{l=1}^{K}\sum_{p=1}^{K}\sum_{q=1}^{K} A_k A_l^* A_p A_q^* \overline{B_k^{(m)} B_l^{(m)*} B_p^{(n)} B_q^{(n)*}} \tag{4.8}$$

Again, consider the statistical property of B, the first row of Eq.4.8, non-zero terms only exist when a) $k=l=p=q$; b) $k=l$, $p=q$, $k \neq p$; c) $k=q$, $p=l$, $k \neq p$. The first row can be further written as:

$$\text{first row of Eq. 4.8} = M \sum_{k=1}^{K} |A_k|^4 \overline{|B^4|} + 2M \sum_{k=1}^{K}\sum_{p=1,p\neq k}^{K} |A_k|^2 |A_p|^2 \left(\overline{|B^2|}\right)^2 \tag{4.9}$$

And for the second row, only when $k=l$ and $p=q$ can non-zeros terms be given. Thus it can be written as:

$$\text{second row of Eq. 4.8} = (M^2 - M) \sum_{k=1}^{K}\sum_{p=1}^{K} |A_k|^2 |A_p|^2 \left(\overline{|B^2|}\right)^2 \tag{4.10}$$

Bring Eq.4.9 and Eq. 4.10 together and calculate the statistical averaging of A and the result is:

$$\text{E}[I^2] = MK\overline{|A^4|}\,\overline{|B^4|} + 2M(K^2 - K)P_A^2 P_B^2 + (M^2 - M)K\overline{|A^4|}P_B^2 + \cdots$$

$$(M^2 - M)(K^2 - K)P_A^2 P_B^2 \tag{4.11}$$

The standard deviation can be easily obtained by taking away the square of the averaging value, which is:

$$\sigma_I^2 = \text{E}[I^2] - E[I]^2 = MK\overline{|A^4|}\,\overline{|B^4|} + 2M(K^2 - K)P_A^2 P_B^2 + (M^2 - M)K\overline{|A^4|}P_B^2 + \cdots$$

$$(M^2 - M)(K^2 - K)P_A^2 P_B^2 - M^2 K^2 P_A^2 P_B^2 \tag{4.12}$$

For a traditional projection screen, its surface is random and it contributes to fully developed speckle (see Chapter 1). As a result, it follows the negative exponential

distribution and we can have $\overline{|A^4|} = 2P_A^2$.

Thus, the standard deviation is:

$$\sigma_I^2 = 2MKP_A^2\overline{|B^4|} + 2M(K^2 - K)P_A^2P_B^2 + 2(M^2 - M)KP_A^2P_B^2 + \cdots$$
$$(M^2 - M)(K^2 - K)P_A^2P_B^2 - M^2K^2P_A^2P_B^2 \tag{4.12}$$

The following discussion needs to study the property of B. Two different cases are discussed by Goodman [18]: a) the light after the homogenization system does not overfill the optic system and b) the light after the homogenization system overfills the optic system. For the first case, the light (after the homogenization components) does not over fill the projection optics. All light can be projected on to the screen. As a result, the projected light field from the projector will have a random phase (due to the homogenization components like a moving/vibrating diffuser) but with the same amplitude.

Assume the random phase has uniform statistics on $(-\pi, \pi)$. The term B can be simplified as:

$$B_k^{(m)} = e_k^{j\phi(m)} \tag{4.13}$$

As a result, we have $\langle |B|^4 \rangle = \langle |B|^2 \rangle^2 = P_B^2$. Bring this condition to Eq.4.12 and the new SCR of the system can be expressed as:

$$\sigma_I^2 = KM(M + K - 1)P_A^2P_B^2 \tag{4.14}$$

$$\text{SCR} = \frac{1}{R_\Omega} = \sqrt{\frac{\sigma_I^2}{\overline{I}^2}} = \sqrt{\frac{KM(M + K - 1)P_A^2P_B^2}{M^2K^2P_A^2P_B^2}} = \sqrt{\frac{M + K - 1}{MK}} \tag{4.15}$$

It is worth noting that only spatial diversity generated by homogenization components is considered here. The wavelength diversity and polarization diversity are set to default 1, which means no speckle reduction related to them are used.

The second case is when light after the homogenization components overfills the optic system. Under this circumstance, when the light (after the homogenization components) overfills the projection optics, each resolution cell of the projection lens undergoes a random walk of amplitudes, or in other words, the projected light field has both random amplitude and phase.

It can be assumed that the projected light field has a random phase with uniform statistics on (-π, π) and an independent Rayleigh-distributed amplitude [18][80]. As a result, the intensity of B follows the property of fully developed speckle. Based on the negative-exponential distribution of fully developed speckle, the relationship $\langle |B|^4 \rangle = 2\langle |B|^2 \rangle^2 = 2P_B{}^2$ can be used [18][80].

Thus, bringing this condition to Eq.4.12, the new SCR of the system can be expressed as:

$$\sigma_I^2 = KM(M + K + 1)P_A^2 P_B^2 \tag{4.16}$$

$$\text{SCR} = \frac{1}{R_\Omega} = \sqrt{\frac{\sigma_I^2}{\bar{I}^2}} = \sqrt{\frac{KM(M + K + 1)P_A^2 P_B^2}{M^2 K^2 P_A^2 P_B^2}} = \sqrt{\frac{M + K + 1}{MK}} \tag{4.17}$$

Combining Eq. 4.15 and Eq. 4.17, we can rewrite the SCR of the laser projection system when only spatial diversity is used:

$$\text{SCR} = \frac{1}{R_\Omega} = \sqrt{\frac{M + K \pm 1}{MK}} \tag{4.18}$$

where K is the number of projection lens resolution areas contained within one eye-resolution (or detector-resolution) area on the projection screen and M is the number of independent speckle patterns generated within the integration time of observer (eye, camera

etc). The "plus" sign corresponds to the case in which the diffused light overfills the optic system, while the "minus" sign corresponds to the case in which the diffused light does not overfill the optic system.

In most cases, K is a limited number while M can be much larger. For a practical system, K can be estimated as:

$$K = \left(\frac{l_2 \frac{\lambda}{D_2}}{l_1 \frac{\lambda}{D_1}} \right)^2 \tag{4.19}$$

where l_1 and l_2 are projection distance and observation distance respectively. D_1, D_2 are the diameter of the projection lens and the detection lens (i.e. a human eye iris) respectively. Consider the human eye iris has a diameter of 3.2mm [39] observing the projection screen from 3 meters away and the projection lens has a diameter of 10mm, projecting on to the screen from 2 meters away. The calculated K is 14.

According to Eq.4.18, when very good homogenization components are used, M can be several thousand or even larger than that [32][81]. However, the SCR of the system will not follow $\frac{1}{\sqrt{M}}$ reduction. It will approach the limitation of $\sqrt{\frac{1}{K}}$.

This result implies that the SCR of the system is limited by K, which is determined by the on-screen resolution of both the projection lens and the detector.

As a result, when a laser projection system is combined with a conventional screen, the SCR is limited by optics geometry, which is usually difficult to change, though by combining with wavelength diversity and polarization diversity, the SCR can be further suppressed. However, this will add more complexity to the system and increase the cost.

Also, for some applications like 3D projection, polarized light is required and one cannot apply polarization diversity to reduce speckle.

4.3. Speckle Reduction with Micro Lens Array Screen

As discussed in the previous section, when using a conventional screen for laser projection, the speckle reduction using spatial diversity is limited by projection optics and observation geometry. As a result, an engineered screen that can prevent the above limitation and reduce SCR is highly desired.

The physical origin of this limitation is caused by the random phase terms added by the rough surface screen. So, if there is a specially designed screen that does not introduce "that much" random phase term to the wave front of the illumination light field, there is possibility that this limitation can be prevented.

One possible solution to achieve this is by using a micro lens array (MLA) as the projection screen [82-84]. A micro lens array is similar to conventional lens array, whose surface has configuration of a large number of lenses [85]. For an MLA, the size of each lens is usually less than 1 mm while a conventional lens array can have lens size of several millimeters or even larger. Figure 4.4 is an illustration of a periodic distributed micro lens array.

Each single lens of an MLA will diverge/focus the incident beam to a large angle,

which will be perceived by observers to fulfill the observing angle requirements. Recently, MLA thin film that has a size of several tens of inches has become already available [86]. Thus, by combining with reflection coating at the back surface of the MLA, it can be used as a screen for front projection.
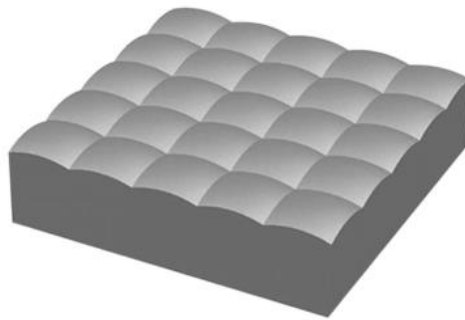
Figure 4.4 Schematic structure of micro lens array

Recently, the utilization of micro lens arrays (MLA) for projection screens has been reported [87] where the SCR as a function of the observer's on-screen resolution area and coherence area were investigated. Theoretical analysis of the SCR has been reported by Goodman when the MLA cell size is bigger than the on-screen projection resolution [18]. However, the SCR of a practical projection system, including a projection lens and a MLA screen with different lens cell size, has yet to be analyzed. There is no a solid theoretical model that specifically describes the speckle reduction effectiveness of MLAs for practical laser projection systems.

This chapter provides a theoretical model describing the mechanism of speckle reduction in a practical laser projection system using MLA technology for a screen. The

SCR of the system was simulated and compared with the published experimental results. An optimized cell size of MLA was obtained based on different laser projector conditions.

4.3.1   Theoretical Model

In this section, a theoretical model is first established to describe an MLA screen in laser projection. Most assumptions still follow Section 4.2. However, due to the special structural properties of an MLA, the statistical assumptions of the screen will be revised. As a result, the results of the SCR will also be changed.

The total intensity received by the observer is still following the Eq.4.3, and the calculation of averaging intensity can also be expressed as Eq.4.5. But the discussion of A_k needs to be revised.

As A_k is a random phase shift introduced to the projected field caused by the screen, it is related to the screen's properties. When the MLA is used as screen material, assuming that within one on-screen resolution area of the projection lens there are N (N ≥ 1) MLA cells, when the MLA cell size is bigger than the on-screen area of the projection lens, N is defined as 1. The expression of A_k can be written as:

$$A_k = \frac{1}{\sqrt{N}} \sum_{n=1}^{N} r e^{i\phi_n} \tag{4.20}$$

where r represents the reflection (or transmission for rear-projection) coefficient of the MLA. r is assumed to be of equal value for all MLA cells. Two assumptions are used here.

First, all lenses of the MLA have a similar cell size. Second, these lenses have a random height fluctuation [18]. The projected light can be diffused with a certain angle by the MLA screen. This angle is determined by the surface radius of these lenses. As a result, we can use a random phase ϕ_n to represents the phase imparted to the field reflected (or transmitted for rear projection) from the screen by the nth screen lens. The factor of $\frac{1}{\sqrt{N}}$ is introduced here to preserve finite second moments of the sum even when N approaches a very large value. As a result:

$$\overline{I_A} = \frac{1}{N}\overline{\left|\sum_{n=1}^{N} re^{\iota\phi_n}\right|^2} = \frac{r^2}{N}\sum_{n=1}^{N}\sum_{m=1}^{N}\overline{e^{\iota(\phi_n-\phi_m)}} = r^2 \tag{4.21}$$

where we assume ϕ_n and ϕ_m are random phases and uncorrelated for $n \neq m$. Bring Eq.4.21 into Eq.4.5, we have:

$$\text{E}[I] = MKP_B r^2 \tag{4.22}$$

Similarly, the second moment of *I* can be expressed as:

$$\text{E}[I^2] = MK\overline{|A^4||B^4|} + 2M(K^2 - K)r^4P_B^2 + (M^2 - M)K\overline{|A^4|}P_B^2 + \cdots$$
$$(M^2 - M)(K^2 - K)r^4P_B^2 \tag{4.23}$$

Now we need to discuss $\overline{|A^4|}$, which is given by

$$\overline{|A^4|} = \frac{r^4}{N}\sum_{n=1}^{N}\sum_{m=1}^{N}\sum_{p=1}^{N}\sum_{q=1}^{N}\overline{e^{\iota(\phi_n-\phi_m+\phi_p-\phi_q)}} \tag{4.24}$$

Due to the random distribution of ϕ and lack of correlation between them, only three terms survive the averaging operation: a) *n=m=p=q*; b) *n=m, p=q, n≠p*; c) *n=p, m=q, n≠m*. The calculated result of Eq.4.24 is given by:

$$\overline{|A^4|} = \left(2 - \frac{1}{N}\right)r^4 = \left(2 - \frac{1}{N}\right)\overline{I_A}^2 \tag{4.25}$$

By substituting Eq.4.25 into Eq.4.23, we can get:

$$E[I^2] = MK\left(2 - \frac{1}{N}\right)\overline{I_A}^2\overline{|B^4|} + 2M(K^2 - K)\overline{I_A}^2 P_B^2 + (M^2 - M)K\left(2 - \frac{1}{N}\right)\overline{I_A}^2 P_B^2 + \cdots$$

$$(M^2 - M)(K^2 - K)\overline{I_A}^2 P_B^2 \tag{4.26}$$

As a result, the standard deviation of the light field intensity is:

$$\sigma_I^2 = E[I^2] - E[I]^2 = MK\left(2 - \frac{1}{N}\right)\overline{I_A}^2\overline{|B^4|} + 2M(M^2 - M)K\left(2 - \frac{1}{N}\right)\overline{I_A}^2 P_B^2$$

$$+(M^2 - M)(K^2 - K)\overline{I_A}^2 P_B^2 - M^2 K^2 \overline{I_A}^2 P_B^2 \tag{4.26}$$

Again, to further study the SCR of the system, the statistical properties of B have to be assumed. Similarly, as in the previous section, two different cases are studied: a) the light after the homogenization system does not overfill the optic system and b) the light after the homogenization system overfills the optic system.

When light does not overfill the optic system, the assumption of Eq.4.13 can still be used and we still have: $\langle|B|^4\rangle = \langle|B|^2\rangle^2 = P_B^2$. Thus, the standard derivation and the SCR of the system can be written as:

$$\sigma_I^2 = \left[MK^2 + \left(1 - \frac{1}{N}\right)M^2 K - MK\right]\overline{I_A}^2 P_B^2 \tag{4.27}$$

$$\text{SCR} = \frac{1}{R_\Omega} = \sqrt{\frac{\sigma_I^2}{\overline{I}^2}} = \sqrt{\frac{\left[MK^2 + \left(1 - \frac{1}{N}\right)M^2 K - MK\right]\overline{I_A}^2 P_B^2}{M^2 K^2 \overline{I_A}^2 P_B^2}} = \sqrt{\frac{K + \left(1 - \frac{1}{N}\right)M - 1}{MK}} \tag{4.28}$$

The second case is that the light after the homogenization components overfill the optic system. Still, the intensity of B follows the properties of fully developed speckle with a negative-exponential distribution. Thus, there is $\langle|B|^4\rangle = 2\langle|B|^2\rangle^2 = 2P_B^2$ and the

standard derivation as well as the SCR of the system can be written as:

$$\sigma_I^2 = \left[MK^2 + \left(1 - \frac{1}{N}\right) M^2 K + \left(1 - \frac{1}{N}\right) MK \right] \bar{I}_A^{\,2} P_B^2 \tag{4.29}$$

$$SCR = \frac{1}{R_\Omega} = \sqrt{\frac{\sigma_I^2}{\bar{I}^2}} = \sqrt{\frac{\left[MK^2 + \left(1 - \frac{1}{N}\right) M^2 K + \left(1 - \frac{1}{N}\right) MK \right] \bar{I}_A^{\,2} P_B^2}{M^2 K^2 \bar{I}_A^{\,2} P_B^2}}$$

$$= \sqrt{\frac{K + \left(1 - \frac{1}{N}\right) M + \left(1 - \frac{1}{N}\right)}{MK}} \tag{4.30}$$

Eq.4.28 and Eq.4.30 are the revised SCR of the laser projection system when using spatial diversity combined with an engineered MLA screen. It can be seen that when compared to Eq.4.18, where a conventional screen is used, the results have been revised. Detailed discussion and optimization of MLA for laser projection will be presented in the following section.

4.3.2   Discussion and Optimization of MLA screen for laser projection

As presented in Section 4.3.1, Eq.4.28 and Eq.4.30 shows the effect on the MLA screen on speckle reduction. The parameter N implies the number of MLA lens cells within one resolution area of the projection lens, which provides a direct impact on the SCR of the system.

To verify the results, two extreme cases are considered: i.e. $N \to \infty$, and $N \to 1$. Still, the discussion will be divided into two cases. When light overfills the optics system and N is large, i.e. $N \to \infty$, Eq.4.30 evaluates to:

$$SCR = \sqrt{\frac{M + K + 1}{MK}} \tag{4.31}$$

which is actually the result presented in Eq.4.17. The physical meaning is fairly straight forward. When the cell size of the MLA is very small, the screen is considered as rough enough for the incident wavelength, and provides similar results to conventional projection screens.

When N=1, Eq.4.30 can be write as:

$$SCR = \sqrt{\frac{1}{M}} \tag{4.32}$$

This result indicates that the limitation of K no longer exists. Thus, the SCR of the system is determined only by the number of independent speckle patterns that can be generated within the integration time of the detector (i.e. the human eye).

When K=N=1, the projected light field illuminates only one lens cell and form only one image point on the detector sensor (retina). There is no interference in the projected light. However, the amplitude of the projected light field already undergoes a random walk and the intensity of the projected light follow the negative-exponential distribution, which can be considered as fully developed speckle.

The second case is when light after the homogenization components overfill the optic system. Similar to the previous case, when N is large, i.e. N → ∞, the Eq.4.28 can be written as:

$$SCR = \sqrt{\frac{M + K - 1}{MK}} \tag{4.33}$$

This is the result of Eq.4.15. The physical meaning is the same as that discussed above. The MLA screen can be considered as being like the conventional projection screens again when the cell size is small enough.

On the other hand, when N=1, Eq.4.28 can be write as:

$$\text{SCR} = \sqrt{\frac{K-1}{MK}} \qquad (4.34)$$

Eq.4.34 is very similar to Eq.4.32 when M is a large number (which is the usual case in practical systems). The primary difference lies in when K equals to 1. In this situation, the speckle vanishes in Eq.4.34. The reason for the difference between Eq.4.32 and Eq.4.34 is due to the fact that the projected light field does not undergo a random walk of amplitudes and the projected light field have equal intensity (no speckle). However, the screen texture will be visible to the observer now, which may cause degrading of the image quality.

It is worth nothing that in the practical systems both K and M are relatively large. Thus, Eq.4.28 and Eq.4.30 will have similar results. Also, as in the real projection systems, when homogenization components such as diffuser(s) are used, there is a high chance that not all light can be collected by the optic system. As a result, the following discussion will be mainly focused on the case in which light overfills the optic system if it is not specifically mentioned.

As presented above, M, K and N are very important when determining the SCR of the system. The M is determined by the homogenization components which provide multiple independent speckle patterns, while K and N are related to the projection optics

and the MLA cell size. In order to provide an optimized MLA for laser projection with reduced speckle, N, K and M have to be discussed.

Figure 4.5 is a schematic illustration of the on-screen relationships between the detector (i.e. the human eye) resolution area, the projection lens resolution area, and the MLA cell size with different values of N.
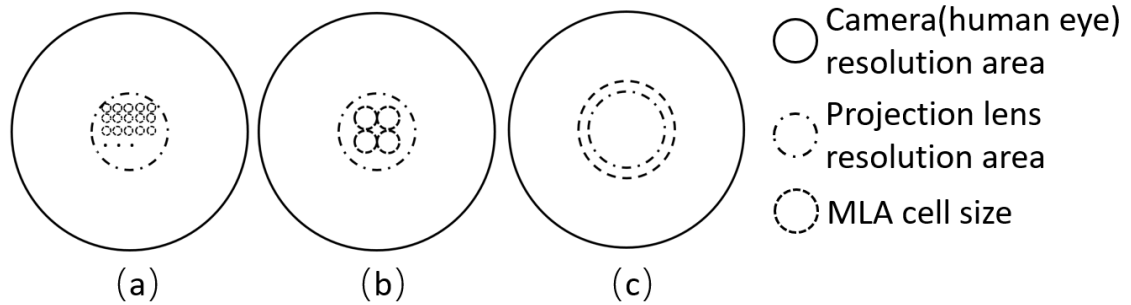
Figure 4.5 The relationship between camera resolution area, projection lens resolution area and MLA cell size for different N (a) when N→∞, (b) N is relatively small, (c) N equals 1.

The solid ring and dash-dotted ring represent the on-screen resolution area of the detector (human eye) and the projection lens respectively. The dashed ring represents the MLA cell size. It is worth noting that the minimum value of N is 1; this corresponds to an MLA cell size equal to or bigger than the projection lens resolution area. K can be calculated by Eq.4.19. It is clear that for different projectors and projection geometries, the value K can be totally different. The SCR of the laser projection system can be simulated based on N, M and K. R_λ and R_σ are still considered equal to 1 here. Figure 4.5 shows

several simulated results for a practical projection system.
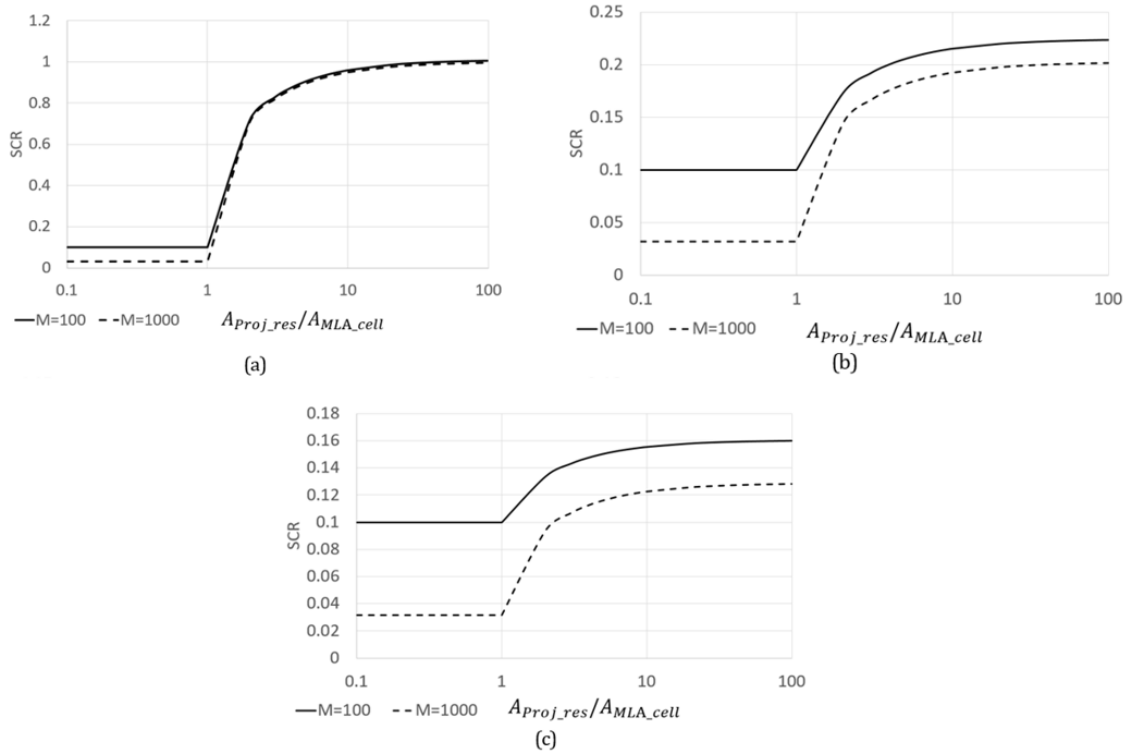
Figure 4.6 Simulated SCR as a function of cell size of MLA screen for M = 100 (solid line) and M = 1000 (dashed line). (a) K=1; (b) K=25, (c) K=64.

In Figure 4.6, the X-axis represents the ratio between projection resolution area and MLA cell size, or in other words, the value of N. The Y-axis shows the simulated SCR. Solid curves correspond to M=100 and dashed curves correspond to M=1000. It is can be seen that when the MLA cell is very small compared to the projection resolution area, the SCR is large. Conversely, when the MLA cell size is comparable to the projection resolution area, the SCR drops significantly. It is worth noting that, when the ratio between

the projection resolution area and the MLA cell size is smaller than 1, the change of the ratio will not cause any difference in the SCR. Under this circumstance, only one phase term will be introduced to the projected light field (Eq.4.20). N is defined as 1 when the MLA cell size is bigger than the on-screen area of the projection lens. With further increases to the MLA cell size, the SCR will reach a minimum value.

The simulated results show that the SCR of the system is highly related to the cell size of the MLA screen. A larger cell size will result in a lower SCR. However, there are two concerns regarding the increase in cell size. First, when cell size is greater than the projection resolution area, the SCR reaches its minimum value and will not further reduce. This agrees well with reported results from [87]. Second, the cell size has to be smaller than the detector (i.e. human eye) resolution area. Otherwise, the screen texture will be perceived by the observer, which can affect the image quality.

From Figure 4.6, it can be seen that the SCR is mostly determined by the parameter K when the MLA cell size is small (as compared to the on-screen projection resolution area). A smaller K will result in a larger SCR, which corresponds to the right side of the Figure 4.6(a), (b), (c). In the extreme case where K is equal to 1, the SCR will be close to 1, even if a large M is provided.

On the other hand, when the MLA cell size is comparable to the on-screen projection resolution area, the SCR will be affected by the value of M. A bigger M will provide a much smaller SCR. When the MLA cell size is equal to or greater than the on-screen projection resolution area, the SCR will reach a minimum value. This value is determined by M only, which agrees with Eq.4.32. As a result, without considering the

effect of $R_\lambda R_\sigma$, a sufficiently large M is needed to reduce the SCR below 4%. Based on our calculation, a minimum value of M = 625 is required to reach the SCR human perception threshold of 4% (below 4% is considered as speckle free projection).

A simulation was conducted to calculate the required MLA cell size to achieve speckle free (<4%) projection. It is worth noting that different projection systems and observation conditions will give different values for M and K. The value of K used in the simulation corresponds to a home theater environment, assuming the projection lens has a diameter of 10 mm and projects an image onto an MLA screen placed 2 meters away from the lens. The diameter of the projection lens resolution area in this scenario is 130 μm. All of the following calculations are based on these assumptions. For a larger projection environment like digital cinema theater or conference room, a different value of K will be generated. However, the calculations still follow the same process.

In order to suppress the SCR below 4% using Eq.4.30, the minimum MLA cell size corresponds to an observer viewing the projected image at different distances as shown in Table 4.1:

Table 4-1 Minimum MLA cell size (μm) required to reduce SCR below to human perception.

Observation Distance (m)	Value of M				
	< 625	625	1000	3000	10000
2	NA	130	129	128	128
4	NA	130	127	123	122
6	NA	130	122	113	110
8	NA	130	116	102	96

It can be seen from Table 4.1 that when M is too small, simply using an MLA screen will not suppress the SCR below 4%. To rectify this, the screen has to be used in conjunction with a laser projection system that has a sufficient M value. In other words, the MLA screen has to be combined with other speckle reduction methods to achieve speckle free projection. For a laser projection system with compact speckle reduction methods such as moving/vibrating diffusers, multimode fibers, light pipes and lens arrays, a M greater than 1000 is achievable [32].

When M just meets the minimum requirements, the cell size of the MLA has to be bigger than the projection resolution size, which in this case is 130 μm. With a bigger M and a greater observation distance, the minimum cell size required for the MLA decreases. When K is a small value (close to 1), from Eq.4.30 it can be seen that N has to be close to 1 in order to decrease the effect of K and get a low SCR. This is still valid even when M is very large. This explains why in Table 4.1, the minimum cell size remains almost constant when the observation distance is 2 meters (where a small K is generated), even with large values of M.

As mentioned above, the cell size of MLA also cannot be too large, otherwise the screen texture becomes visible to an audience. The upper limit is the on-screen observation resolution limit (diffraction limit) of the human eye. For the above assumed projection environment, consider the human iris has a diameter of 3.2 mm [39], they are around 400 μm, 800 μm, 1200 μm and 1600 μm when observing at 2 meters, 4 meters, 6 meters and 8 meters respectively. It also should be noted that the projection distance was set to be 2 meters away from the screen. If the projection distance is smaller or greater, the MLA cell

size requirement will also be different. By changing K in Eq.4.30, a new minimum cell size can then be calculated.

The optimization process of choosing a suitable MLA screen for a laser projection system can be divided into the following steps.

Step 1: Measure the spectrum of the laser source and obtain the value of R_λ. For a DPSS laser $R_\lambda = 1$ can be used, while for semiconductor laser diodes R_λ must be calculated using the method presented in Chapter 2.

Step 2: Calculate the resolution of the projection lens at the screen, as well as the observation resolution, to obtain the value of K. Set the calculated on-screen resolution size as the maximum cell size of the MLA.

Step 3: Choose a conventional screen which is rough (such as matte white) and project an image using the laser projector with the light source chosen in Step 1 and the geometry used in Step 2.

Step 4: Using the measured values of SCR, R_λ, K, and R_σ (which for a matte white screen is $\sqrt{2}$), the value of M can be calculated using Eq.1.19, Eq.1.20 and Eq.4.18.

Step 5: With R_λ, K, M, and R_σ (for an MLA, this value is now 1), to reduce the SCR below 4% the value of N (i.e. the minimum MLA cell size) can be calculated using Eq.1.19, Eq.1.20 and Eq.4.30 (or Eq. 4.28 if light does not overfill the system).

The above steps help to determine the cell size range of an MLA screen which can provide speckle free projection and will not be observed by an audience.

4.4. Summary

In this chapter, the potential of using MLAs for screens that reduce speckle in laser projection systems has been studied. A comprehensive theoretical model has been established for the analysis and optimization of MLAs that can predict the SCR of a laser projection system using different MLA screens. The theory has taken into account the influences of MLA cell size and on-screen projection/detection resolution area size, which has not been reported to date. The theory and calculated results agree well with the reported experimental results. This model can be used to determine a MLA cell size that can achieve a SCR below human perception. This procedure for optimizing MLA cell size and for calculating the SCR has provided a guideline for designing practical laser projection systems.

CHAPTER 5

Standard Speckle Measurement in Laser Projection

5.1. Introduction

In Chapter 1 we discussed that there are two types of speckle: objective speckle and subjective speckle. When there are no imaging optics involved, it is called objective speckle. When imaging optics are involved, it is called subjective speckle. In this case, the speckle is observed by imaging optics first, then real images are formed on image plane (for example, images observed by human eyes and then formed on the retina). It is straight foward that, subjective speckle will be highly affected by the measurement condition/setup. In a practical evaluation system for SCR, human observation results can only be used for quantitative analysis. Accurate qualitative SCR values can only be measured by instruments like cameras. There are many parameters that have a great impact on measured SCR values. This implies that even for the same laser projection system, when different measurement setups are used, totally different SCR values can be acquired. This causes great difficulty in evaluation and comparison of the effectiveness of different speckle reduction methods.

In this chapter, several parameters that affect the measured SCR will be identified

and discussed. Suitable setups that correspond to human vision perception on SCR will be discussed and chosen.

This part of the work is conducted as a part of speckle measurement metrology study of the Laser Illumination and Projection Association (LIPA).

5.2. Factors that Affect Speckle Measurement

To study the factors that affect speckle measurement in laser projection, a suitable experiment setup has to be used. In order to meet the purpose of general applications, the schematic structure shown in Figure 4.2 was used as the setup of the measurement. The following discussion will be based on this setup. The influence of camera (sensor, pixel, shutter speed etc), optics geometry (aperture, F number, focal length, distance etc) and calculation algorithm will be explained.

5.2.1   Influence of Camera on SCR Measurement

For a camera used in SCR measurement, the properties of a camera mostly focus on the following parameters: color/monochromic, pixel size, lens parameters, gain and shuttle speed.

The factor to be discussed is the color/monochromic camera. The biggest difference between a colorful camera and a monochromic camera is that the former has a Bayer filter

in front of the image sensor (CCD or CMOS) [88-89]. Figure 5.1 shows a schematic structure of the Bayer filter. The gray layer is the image sensor. The top layer is the Bayer filter. Each square corresponds to one pixel in the final image. The different color refers to the color that can pass through the filter and is accepted by the image sensor.
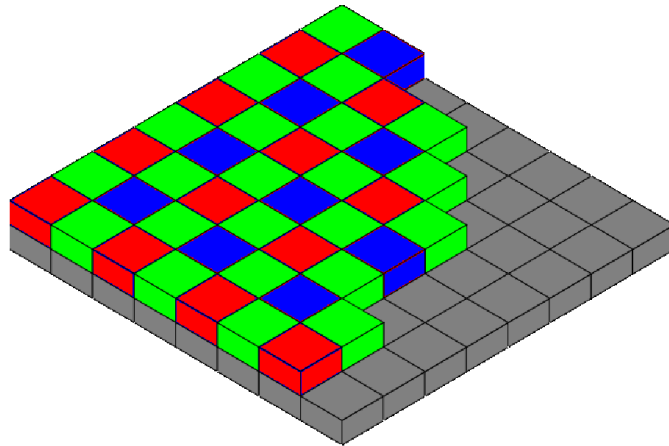
Figure 5.1 Schematic structure of Bayer filter (Source: Wikipedia)

As a color camera needs information about the red/green/blue channel to rebuild the color image, three different filters are used. Each kind of filter only allows one color to pass through. Thus, by using interpolation algorithm, the value of a certain color at those pixels which does not have corresponding filters can be calculated and the overall image will not lose too much information [90].

However, for speckle patterns, where the intensity fluctuates a lot within adjacent pixels, the interpolation algorithm will not be able to reproduce the actual intensity value accurately [91]. As a result, only monochromic cameras are suitable for the measurement of SCR.

The second factor that needs to be discussed is the pixel size of the camera sensor.

This factor is closely related to the camera lens parameters when measuring the SCR of the system. To discuss this, the average size of a speckle spot has to be studied. The average size of a speckle spot (A_C) is defined as the coherence area of a speckle spot, which can be calculated as[47,92]:

$$A_C = \frac{4\lambda^2(f/\#)^2}{\pi} \tag{5.1}$$

where λ is the wavelength of incident light and $f/\#$ is the F number of the camera lens. As shown in Eq.5.1 The F number of the camera will change the speckle size and further, it has an influence on the measured SCR as camera pixel size (A_P) is a fixed value.

Figure 5.2 Speckle patterns with different A_C a) 92 μm^2, b) 46 μm^2, c) 23 μm^2, d) 11μm^2

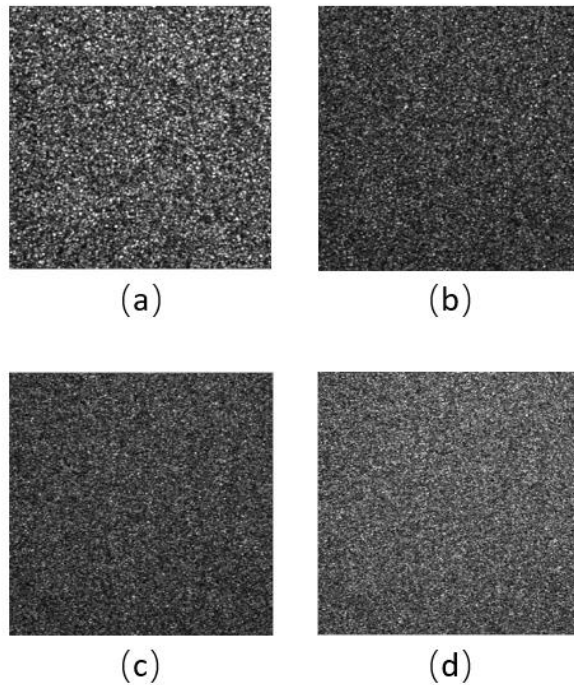When A_C is much larger than A_P, a good sampling of the actual speckle pattern can be achieved and the measured SCR will be close to real value. However, if A_C is comparable or even smaller than A_P, a smaller SCR will be obtained. This is due to the spatial integration of the camera pixel, which will provide an averaging effect which smooth out laser speckle.

One simple experiment is conducted to verify this result. A DPSS laser was used as the laser source and was directly projected onto the screen, which means there is no speckle reduction method used besides the polarized screen.

The F number of the camera changed from small to large in order to change A_C. All other parameters remained the same for all experiments. Measured speckle patterns are shown in Figure 5.2. By changing the F/# of the camera lens, the A_C is changing from 92 μm^2 to 11 μm^2. It can be seen that the speckle spot size is much bigger in Figure 5.2(a) than other the figures. The camera sensor has a pixels size of 4.4 μm * 4.4 μm. The measured SCR of four conditions are: a) 0.533, b) 0.510, c) 0.469, d) 0.414. It is clear that the measure SCR drops with the decreasing of A_C. As a result, for accurate SCR measurement, the ratio between A_C and A_P should be a similar value as the speckle size generated by the human eye over the average visual cell size.

Another issue regarding camera pixels is the fill factor of them. The fill factor of a pixel refers to the effective area of the pixel that can collect light over the entire area occupied by the pixel and interlines next to it. The CCD camera has a relative large fill factor (larger than 50%, combined with microlens array, the value can be close to 100%) and a good sampling can be achieved. However, if the fill factor is too low, interpolation

might be needed in order to get more accurate measured patterns.

The third factor regarding the camera in speckle measurement is gain boost in the camera [93]. Gain boost is often used in cameras in order to provide enough information for dark images [94]. According to Eq.1.1, when the intensity of the entire speckle field increases proportionally, which means both dark pixels and bright pixels will be boosted with same ratio, the calculated SCR will remain the same. This is due to the standard deviation and average intensity of the entire speckle field being increased with same ratio and cancelled with each other out.
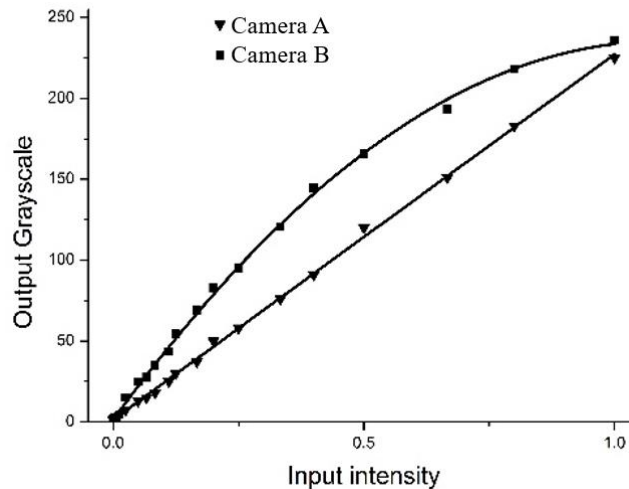

Figure 5.3 Gain curves of two different cameras

However, in conventional applications, the dark part of the image will receive higher gain in order to make it more clear. This will help images to acquire more information from objects but in SCR measurement, this may cause inaccurate values.

Figure 5.3 shows a comparison of gain curves of two different cameras measured in experiments. It is clear that camera B provides more gain when input intensity is low. This will cause brighter image with higher averaging intensity and lower SCR.

The forth factor that needs to be considered is shutter speed (integration time). This will also influence the measured SCR. Consider a laser projection system as described in Figure 4.2, when time-varying components are used to generate multiple independent speckle patterns and provide spatial diversity which reduces speckle. The number of independent speckle patterns M is determined by both the speckle reduction technique and the shutter speed (or integration time in other words). A slower shutter speed will allow a larger M to be generated [18]. Though when M is very large and a conventional screen is used, the SCR will reach a limitation and will be less likely to further reduce, the shutter speed should still be similar to the integration time of human perception, which is around 20 frame per second or 50 ms, which means the camera should use a frame rate close to 1/20s. Besides of this, as additional illumination will result in non-speckle light field intensity fluctuation, flashes cannot be used when capture speckle patterns.

5.2.2   Influence of Optics Geometry on SCR measurement

"Optics geometry" is a broad terminology. In the SCR measurement of laser projection here, it refers to the following concepts: imaging lens aperture, and imaging lens focal length, imaging distance. The projection distance of the laser projector also has an influence on the measured SCR. However, as a projector is usually fixed and less likely to

be moved for the purpose of SCR measurement, it will not be considered as a variable in the measurement.

For imaging lens aperture, focal length and imaging distance cannot be isolated and their influences on SCR measurement are discussed separately.

First factor to be discussed here is the F/# of the imaging lens. As mentioned above, this factor will decide the average speckle spot size. Combined with the pixel size of sensors, they will have an influence on the measured SCR. This phenomenon has been studied in the previous section and will not be discussed again here.

The second factor is the imaging distance. With a fixed imaging lens, when changing the imaging distance, the on-screen resolution spot size of the imaging lens changes [95]. As a result, the K value in Chapter 4 changes. For a laser projection system with very good spatial diversity which generates a large M, the SCR of the system can be simplified (assuming no wavelength diversity and de-polarized screen is used) as:

$$\text{SCR} = \frac{1}{R_\Omega R_\sigma} = \sqrt{\frac{M + K \pm 1}{2MK}} \approx \sqrt{\frac{1}{2K}} \tag{5.2}$$

Bringing Eq.4.19 in, we can get:

$$\text{SCR} \propto \frac{l_1 D_2}{l_2 D_1} \tag{5.3}$$

where l_1 and l_2 are projection distance and observation distance respectively, and D_1, D_2 are the diameter of the projection lens and imaging lens (i.e. human eye iris) respectively. The projection distance and projection lens will not be able to change. Also, the imaging lens' diameter is set to fixed value. As a result, the measured SCR should be proportional

to $\frac{1}{l_2}$ [96].

Experiments are conducted to verify this conclusion. The experiment setup is shown in Figure 5.4. A DPSS laser with CW 532 nm output is used as the light source. A rotating diffuser and light pipe are used for spatial diversity. The end of the light pipe is projected onto the screen and then captured by a camera. The observation distance of the camera is changing from 1 meters to 2 meters.
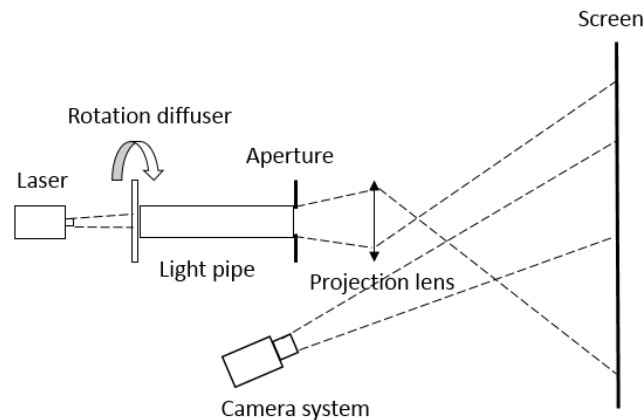
Figure 5.4 Schematic experiment setup to verify the relationship between measured SCR and observation distance [96]

The measured SCR as a function of reciprocal observation distance is presented in Figure 5.5. X-axis is the reciprocal of the observing distance and Y-axis is the measured SCR. It can be seen that the measured SCR increase from 0.13 to 0.24 when the observation distance decreases from 2 meters to 1 meter. A very good linear relationship is shown in

the measured results and Eq.5.3 is verified.

As discussed in this section, optics geometry has a very important impact on measured SCRs. By tuning the aperture/focal length of imaging optics and by changing observation distances, totally different SCR values can be acquired. As a result, a standard regarding optics geometry in SCR measurement that corresponds to human perception is very important and has to be established.
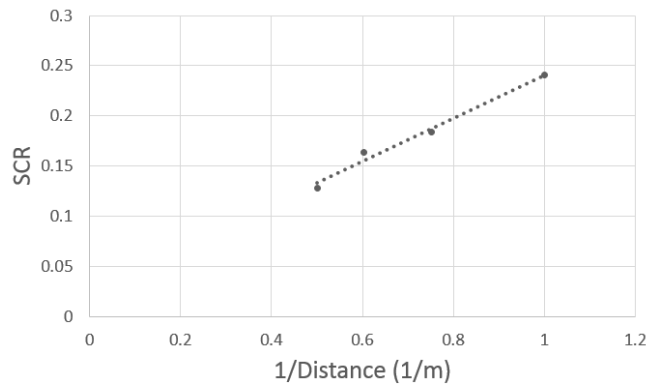
Figure 5.5 Relationship between measured SCR and reciprocal of observing distance

5.2.3   Influence of Processing Algorithm on SCR measurement

The calculation of SCR from an acquired speckle pattern seems very straight forward, which is the standard deviation over the average intensity. However, in practical applications, the SCR directly calculated by this may give inaccurate values.

There are many possible reasons. For example, hot spot phenomenon is very common in the projection field. The hot spot is a bright spot that the observer will see in

the center of his/her viewing field when looking towards a projection screen [97]. This is mostly caused by poor screen material which has higher reflectively at a small observation angle and lower reflectively at a large viewing angle. As a result of hot spot phenomenon, the center of the captured speckle pattern will be brighter than the edges. This will introduce a bigger standard derivation of the entire image which introduce higher SCR. However, this fluctuation is not caused by speckle and should be excluded.

The second phenomenon that might generate higher SCR is the non-uniform light field projected by the projector. This is mostly seen in lower-end projectors which has limited light field reshaping and homogenization. This non-uniformity will have a similar influence on SCR measurement as a hot spot, which generates inaccurate SCR.

As a result, in order to get accurate SCR, background non-uniformity has to be removed. The method that can be used is by applying a digital filter that eliminates a low frequency signal [98-99]. A Gaussian filter $g(x, y)$ is used here. The value of the filter is shown in the figure below. The filter has a size of 19*19 pixels with a standard deviation of 9.
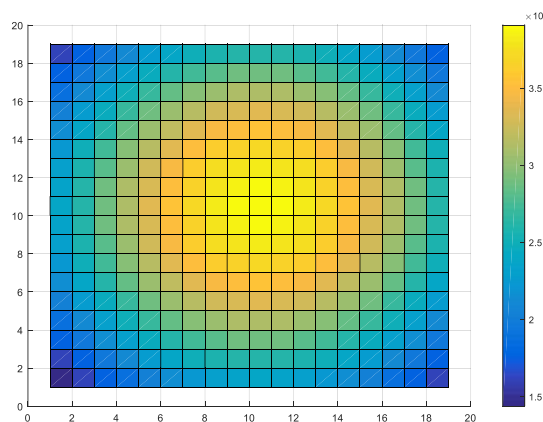
Figure 5.6 Gaussian filter used for post-processing

Assume the speckle pattern acquired by the camera is $f(x, y)$. To filter the low frequency, the convolution between $f(x, y)$ and $g(x, y)$ is first calculated. A new field $h(x, y) = f(x, y) * g(x, y)$ is a smoothed light field from $f(x, y)$. A third field $p(x, y)$ is calculated by using each element of $f(x, y)$ divided by correspond element of $h(x, y)$. This calculation will be able to remove the slowly-varying non-uniformity of the speckle pattern that will cause inaccurate SCR. Detailed code of this post processing is shown in Appendix.

Figure 5.7 shows three calculated images. The first one is the raw speckle field captured directly from the camera. There are some slow-varying non-uniformity exists over the entire image. The second image is an averaged background by using the Gaussian filter $g(x, y)$. The third image is acquired by using the element of first image divided by correspond element of the second image. The calculated SCR for the first image is 0.71 and for the last image it is 0.68. This post processing will be able to eliminate non-speckle slowly-varying components in an acquired image and provide more accurate SCR values. For a screen with good lambertian scattering (which means light scattered to all directions with equal intensity), this post processing will have a limited effect. However, for a screen which has strong specular reflection, this technic will ensure an accurate measured. SCR.
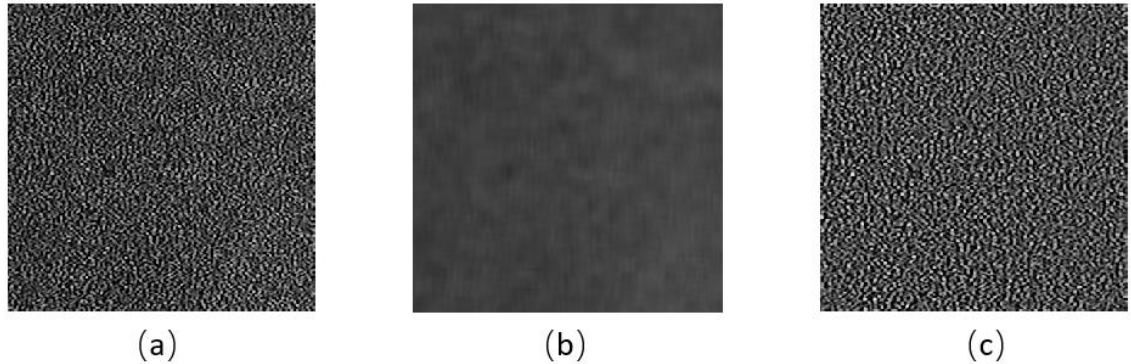
Figure 5.7 Post-processing for SCR calculation (a) original captured image $f(x, y)$ (b) slow-varying background $h(x, y)$ (c) final speckle field $p(x, y)$.

5.3. Standard Measurement Corresponding to Human Perception

It has been discussed in Section 5.2 that measurement conditions can greatly affect the measured SCR. A standard measurement system that agrees with human perception in speckle measurement is needed. In this section, such a system will be presented.

First, the projector and camera should be setup in an appropriate configuration. Figure 5.8 shows the schematic setup of them. The projector and camera should have the same incident/observation angle towards the screen, which means the projector, the center of the projected image, the center of captured image and the camera should be all located on the same line if we mirror-flip the camera to the other side of the screen, as shown in Figure 5.8. This setup assures that the camera captured the center of reflected beam, or in other

words, the center of the hot spot phenomenon generated by the screen. As the center of the hotspot has a better uniformity compared to the boundaries, this will help us minimize the effect of the hotspot phenomenon [100].
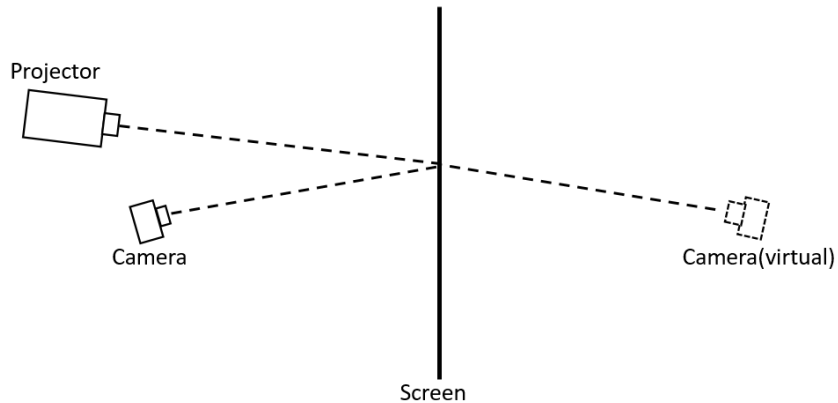
Figure 5.8 Projector and camera setup in SCR measurement.

The projector distance is determined case by case. Thus, there will be no detailed requirement on this value. However, the camera distance is very important. This has been presented in the previous section that the measured SCR will be reduced with the increase of the observing distance. To agree with a practical situation, the observation distance of the camera is set to be equal to the projected image height [46,101].

The second consideration is the camera and the imaging lens. A monochromic camera with a liner response has to be used to capture speckle patterns. There are two key points need to follow in camera selection: first, the camera lens diameter should agree with human iris diameter in order to have similar on-screen resolution; second, the sampling rate between speckle size (determined by F/# of the camera lens) and camera pixel should agree with the ratio generated by human iris and visual cell size.

A Dalsa 1600M camera will be used as an example. The camera has a pixel size of 4.4μm * 4.4 μm. As discussed in section 5.2.1, based on the discussion of speckle spot size A_C and pixel size A_P, the camera lens has to have a suitable F/# in order to get suitable ratio of A_C/A_P. We first need to study the situation of the human eye.

Generally speaking, for the adult eye in a projection environment, people consider that the iris diameter is 3.2 mm [39]. Also, the focal length of the human eye is usually considered as 22 mm. Besides this, according to [102], the average density of cone cells in the human retina near the fovea is around 191,000 cones per mm^2. Thus, the average size of a cone cell is around 5 μm^2. Based on this, the ratio between speckle size A_C over the retina cone cell size is around 3.45.

Based on this value, the lens parameters can be decided. First, the lens aperture should be similar to the iris diameter. This corresponds to the correct K value as discussed in Chapter 4. Thus, we could fix the lens diameter with a value of 3.2 mm.

Second, suitable F/# will be chosen to give a correct A_C/A_P correspond to human retinal and visual cell size. The pixel size for the camera used in experiments is 4.4 μm * 4.4 μm. In order to get the A_C/A_P value close to 3.45, by combining with Eq.5.1, the desired F/# of the camera lens should be around F/15. Combined with a lens diameter of 3.2mm, and considering the availability, the lens chosen in the experiment has a focal length of 50mm, with an aperture of 3.2mm and F/15.5. It is worth noting that, when a different camera with a different pixel size is used, the above calculation should be revised and a new camera lens should be selected.

The camera is set to have a frame rate of 15 frames per second, which is close to

human eye integration time 50 ms [103]. This will help to provide similar averaging effect as the human eye when time-varying components are used for speckle reduction.

The next factor is a post-processing algorithm. There are many methods to perform low-frequency filter over a raw image data. One of the most commonly used methods here is a Gaussian filter, which will also be used here. The processing is achieved by using a MATLAB code. A sample code is attached in the appendix of this chapter.

An experimental is presented to test this setup. The setup is shown in Figure 5.9. A DPSS laser at 532nm was used as the light source. In order to test the system, no speckle reduction components were used here. The laser beam was expanded by a convex lens and projected on to the screen directly. The Dalsa M1600 camera was used to capture the projected light field. The camera was set to F/16 with 50mm focal length as described above. The measurement distance was 2 meters.

The measured speckle pattern is post processed to remove the slow varying background. For the experiment setup shown above, the measured SCR is 56.7%. It worth noting that for a DPSS laser whose linewidth is very narrow, the wavelength diversity is almost negligible. Thus, the theoretical measured SCR should be around 70% when combined with a de-polarized screen and an ideal image sensor (with pixel size of infinitely small). The measured value is smaller than this number, mostly due to spatial averaging effect caused by the visual cell size. This measured result also agrees with the published result in [104]. Thus, this experiment setup can be considered as accurate.
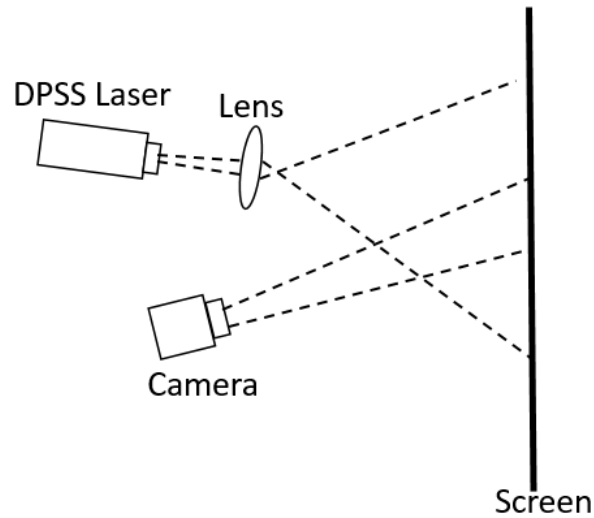
Figure 5.9 Experiment setup for standard SCR measurement.

5.4. Conclusion

In this chapter, the standard measurement of SCR for laser projection has been studied. Several factors including the camera, lens parameter, measuring distance and post-processing have been discussed. It is shown that the measured SCR is highly related to measurement conditions. An unsuitable setup will get totally different SCR values.

As the purpose of SCR measurement is to indicate the speckle level perceived by the human eye, the parameters and settings regarding the factors mentioned above are discussed and set to correspond to the human eye. One example of certain values of these parameters that can provide a measured SCR with good consistency with the subjective

perception of the human eye is presented. This measurement and processing metrology can be used to compare the speckle level of different laser projection systems. This measurement procedure can be used as a blueprint for future standardized SCR measurements for different applications including but not limited to home theater, cinema and conferences.

CHAPTER 6

Conclusion

6.1. Summary of Accomplishments

The thesis presents a study on laser speckle issued in laser display, especially focusing on the laser projection field. The achievements of this research are described in Chapters 2 – 5. The main results are summarized here.

The thesis briefly reviews the origin of the laser speckle issue in laser display. The laser projection system is divided into several components: a) laser light source, b) optic light engine, c) projection screen and d) evaluation system. The first three parts are discussed and optimized for speckle reduction in the laser projection system. The last part is discussed for standard SCR measurement corresponding to human eye perception.

In Chapter 2, laser speckle reduction by employing a low speckle laser light source is investigated. A theoretical model is established to describe the wavelength diversity and its speckle reduction effect when a blended laser light source is used. The model is verified by experiments. The model can be used to select the optimal laser wavelengths and their power ratio that generate less speckle SCR. The minimum wavelength differences $\Delta\lambda_{min}$ between two adjacent wavelengths to generate de-correlated speckle patterns as a function

of the laser linewidth are calculated. It has been shown that the minimum wavelength difference $\Delta\lambda_{min}$ is 1.0 nm and 1.5 nm for the green DPSS lasers and green semiconductor LDs, respectively. Also, in order to achieve speckle free projection, by combining with wavelength diversity, spatial diversity and polarization diversity, the minimum number of lasers required to achieve speckle free projection is three and two for green DPSS lasers and semiconductor LDs, respectively. These two values change to five and three when a polarized maintained screen is used.

In Chapter 3, a speckle reduction optic system is presented. The system consists of a multimode fiber, a voice coil motor, a dielectric elastomer actuator and a lightpipe. The dielectric elastomer actuator is integrated into a laser projection system for speckle reduction for the first time. The system can provide very good speckle reduction with low optical penalty, low cost and straight-forward configuration. An SCR as low as 3.7% is achieved in the system.

In Chapter 4, an engineered screen that utilizes a micro lens array (MLA) is studied for the purpose of speckle reduction in laser projection. The theoretical limitation of speckle reduction when using a conventional screen is presented in this chapter. A theoretical model that can describe the speckle reduction effect of MLA is established. By using MLA as a screen and taking into account the influence of on-screen projection/observation resolution area size, the SCR of the system can be greatly reduced. This model can be used to predict the SCR of the system and determine the MLA cell size that can achieve speckle free projection. A procedure for designing an MLA screen in a laser projection system has been presented as well.

Chapter 5 discussed standard measurement setup for SCR. Multiple factors including the camera, lens parameter, measuring distance and post-processing and their influence on SCR measurement are studied. As measured SCR is highly dependent on measurement conditions, a standard setup that indicates human perception when observing speckle in a projection environment is proposed. The proposed setup can be used to evaluate the speckle level of different projection systems and provides accurate SCR values.

As presented above, this thesis studied multiple components of laser projection regarding the speckle issue. The three components of low speckle laser source, optic system with integrated speckle reduction methods and engineered low speckle screen, can be combined and provide a speckle free laser projection system. Also, the standard SCR measurement system can be used to evaluate speckle levels of laser projection systems. A complete study of the speckle issue in laser projection is presented in this thesis.

6.2. Suggestions for Future Work

Despite the achievements presented in this thesis, there are still many things that remain to be done to further reduce the speckle level and improve the performance of laser projections.

On low speckle laser source aspect, though guideline of wavelength and power selection have been proposed, lasers with the desired wavelengths at low cost are still an issue. For example, there are very limited choices for DPSS green lasers close to 532 nm.

Development work with these highly compact and low cost lasers is required.

Besides this, regarding an optic engine with integrated speckle reduction, the current setup using DEA and MMF has limited optical efficiency, which will result in a loss of lumen output. Therefore, such an optic engine with lower optical penalty is highly desired. Moreover, the DEA used has a relatively low optical damage threshold, so when high lumen output laser projectors (with optical output power higher than ~200 W) are used, there might be potential damages. Research regarding using new material with high damage thresholds for DEA should be done.

Last but not least, the integration of a low speckle laser source, a speckle reduction optic engine and a low speckle MLA screen should be done. A complete speckle-free laser projection needs to be designed and built.

References

1. Matthew S. Brennesholtz and Edward H. Stupp. Projection Displays. Wiley Publishing, 2nd edition, 2008.

2. Weichmann, Ulrich, Hermann Giese, Ulrich Hechtfischer, Gero Heusler, Achim Koerber, Holger Moench, Folke-Charlotte Noertemann, Pavel Pekarski, Jens Pollmann-Retsch, and Arnd Ritz. "UHP lamps for projection systems: getting always brighter, smaller, and even more colorful." In Liquid Crystal Materials, Devices, and Applications X and Projection Displays X, vol. 5289, pp. 255-266. International Society for Optics and Photonics, 2004.

3. Derra, Guenther, Holger Moench, Ernst Fischer, Hermann Giese, Ulrich Hechtfischer, Gero Heusler, Achim Koerber et al. "UHP lamp systems for projection applications." Journal of Physics D: Applied Physics 38, no. 17 (2005): 2995.

4. Wang, Fu-Kwun, and Tao-Peng Chu. "Lifetime predictions of LED-based light bars by accelerated degradation test." Microelectronics Reliability 52.7 (2012): 1332-1336.

5. Fournier, Florian, and Jannick Rolland. "Design methodology for high brightness projectors." Journal of Display Technology 4.1 (2008): 86-91.

6. Chellappan, Kishore V., Erdem Erden, and Hakan Urey. "Laser-based displays: a review." Applied optics 49, no. 25 (2010): F79-F98.

7. Recommendation, I. T. U. R. B. T. "2020:"Parameter values for ultra-high definition television systems for production and international programme exchange"." International Telecommunication Union, Geneva (2012).

8. Chichibu, Shigefusa F., and Shuji Nakamura. Introduction to nitride semiconductor blue lasers and light emitting diodes. CRC Press, 2014.

9. Wierer Jr, Jonathan J., Jeffrey Y. Tsao, and Dmitry S. Sizov. "Comparison between blue lasers and light-emitting diodes for future solid-state lighting." Laser & Photonics Reviews 7.6 (2013): 963-993.

10. Sugiura, Hiroaki, et al. "56.3: 65-inch, Super Slim, Laser TV with Newly Developed Laser Light Sources." SID Symposium Digest of Technical Papers. Vol. 39. No. 1. Oxford, UK: Blackwell Publishing Ltd, 2008.

11. Hirano, Yoshihito, et al. "Solid-state SHG green laser for laser TV." International Quantum Electronics Conference. Optical Society of America, 2009.

12. Tauscher, Jason, et al. "Evolution of MEMS scanning mirrors for laser projection in compact consumer electronics." MOEMS and Miniaturized Systems IX. Vol. 7594. International Society for Optics and Photonics, 2010.

13. CHRISTIE Corp. 2012. Laser Illumination Technology. http://www.christiedigital.co.uk/emea/display-technology/laser-projection/pages/default.aspx

14. Ong, Desmond C., et al. "Analysis of laser speckle severity, granularity, and anisotropy using the power spectral density in polar-coordinate representation." Optical Engineering 51.5 (2012): 054301.

15. Roelandt, Stijn, Youri Meuret, An Jacobs, Koen Willaert, Peter Janssens, Hugo Thienpont, and Guy Verschaffelt. "Human speckle perception threshold for still images from a laser projection system." Optics express 22, no. 20 (2014): 23965-23979. Goodman, Joseph W. Speckle phenomena in optics: theory and applications. Vol. 1. 2007

16. Spitzer, Frank. *Principles of random walk*. Vol. 34. Springer Science & Business Media, 2013.

17. Trisnadi, Jahja I. "Speckle contrast reduction in laser projection displays." Projection Displays VIII. Vol. 4657. International Society for Optics and Photonics, 2002.

18. Goodman, Joseph W. "Statistical properties of laser speckle patterns." In Laser speckle and related phenomena, pp. 9-75. Springer, Berlin, Heidelberg, 1975.

19. Cui, Zhe, et al. "Speckle suppression by controlling the coherence in laser based projection systems." Journal of Display Technology 11.4 (2015): 330-335.

20. Furukawa, Akio, Norihiro Ohse, Yoshifumi Sato, Daisuke Imanishi, Kazuya Wakabayashi, Satoshi Ito, Koshi Tamamura, and Shoji Hirata. "Effective speckle reduction in laser projection displays." In Emerging Liquid Crystal Technologies III, vol. 6911, p. 69110T. International Society for Optics and Photonics, 2008.

21. Yanagisawa T , Shohda F , Akino Y , Ikeda K , Shen Z , Yamamoto S , et al. De-speckle effects resulted by wavelength multiplexing of intra-cavity solid-state green lasers Laser display and lightning conference Japan; 2015.

22. F. Shevlin, "Speckle Reduction With Multiple Laser Pulses," in 2nd Laser Disp. Conf. LDC'13, Yokohama Jpn. Apr 23 - Apr 24 (2013).

23. Sun, Mingjie, and Zukang Lu. "Speckle suppression with a rotating light pipe." Optical Engineering 49, no. 2 (2010): 024202.

24. Kasazumi, Ken'ichi, Yasuo Kitaoka, Kiminori Mizuuchi, and Kazuhisa Yamamoto. "A practical laser projector with new illumination optics for reduction of speckle noise." Japanese journal of applied physics 43, no. 8S (2004): 5904.

25. Kuratomi, Yuhei, Kazuo Sekiya, Hiroaki Satoh, Tatsuhiro Tomiyama, Tohru Kawakami, Baku Katagiri, Yoshito Suzuki, and Tatsuo Uchida. "Speckle reduction mechanism in laser rear projection displays using a small moving diffuser." JOSA A 27, no. 8 (2010): 1812-1817.

26. Yong Bi, Zuyan Xu, Taofang. A lighting system with speckle reduction. CN patent, 200610079034X.

27. Zhang, Yunfang, et al. "Demonstration of a home projector based on RGB semiconductor lasers." Applied optics 51.16 (2012): 3584-3589.

28. Ouyang, Guangmin, Zhaomin Tong, M. Nadeem Akram, Kaiying Wang, Vladimir Kartashov, Xin Yan, and Xuyuan Chen. "Speckle reduction using a motionless diffractive optical element." Optics letters 35, no. 17 (2010): 2852-2854.

29. Son, Seong-Jin, Do-Kyeong Ko, and Nan Ei Yu. "Study of an optical device based on a quasi-phase-matching method for speckle noise reduction for laser display." Journal of the Korean Physical Society 69, no. 5 (2016): 756-761.

30. Kuksenkov, Dmitri V., Rostislav V. Roussev, Shenping Li, William A. Wood, and Christopher M. Lynn. "Multiple-wavelength synthetic green laser source for speckle reduction." In Nonlinear Frequency Generation and Conversion: Materials, Devices, and Applications X, vol. 7917, p. 79170B. International Society for Optics and Photonics, 2011.

31. Svensen, Øyvind, Xuyuan Chen, and Muhammad Nadeem Akram. "Speckle reduction in laser projection displays through angle and wavelength diversity." Applied optics 55, no. 6 (2016): 1267-1274.

32. Manni, Jeffrey G., and Joseph W. Goodman. "Versatile method for achieving 1% speckle contrast in large-venue laser projection displays using a stationary multimode optical fiber." Optics express 20, no. 10 (2012): 11288-11315.

33. Ma, Qianli, and Chang-Qing Xu. "Wavelength blending with reduced speckle and improved color for laser projection." Optics and Lasers in Engineering 97 (2017): 27-33.

34. Middleton, David, and Institute of Electrical and Electronics Engineers. An introduction to statistical communication theory. Piscataway, NJ: IEEE press, 1996.

35. Chen, Xuyuan, Øyvind Svensen, and Muhammad Nadeem Akram. "Speckle reduction in laser projection using a dynamic deformable mirror." Optics express 22, no. 9 (2014): 11152-11166.

36. Yamada, Hirotaka, Kengo Moriyasu, Hiroto Sato, and Hidekazu Hatanaka. "Effect of incidence/observation angles and angular diversity on speckle reduction by

wavelength diversity in laser projection systems." Optics express 25, no. 25 (2017): 32132-32141.

37. Gan, Yi, Yang Lu, Qingyang Xu, and Chang-Qing Xu. "Compact integrated green laser module for watt-level display applications." IEEE Photonics Technology Letters 25, no. 1 (2013): 75-77.

38. Miyoshi, Takashi, Shingo Masui, Takeshi Okada, Tomoya Yanamoto, Tokuya Kozaki, Shin-ichi Nagahama, and Takashi Mukai. "510–515 nm InGaN-based green laser diodes on c-plane GaN substrate." Applied Physics Express 2, no. 6 (2009): 062201.

39. Cui, Zhe, Anting Wang, Qianli Ma, and Hai Ming. "Analysis of the speckle properties in a laser projection system based on a human eye model." JOSA A 31, no. 3 (2014): 616-620.

40. Yanagisawa T , Shohda F , Akino Y , Ikeda K , Shen Z , Yamamoto S , et al. De-speckle effects resulted by wavelength multiplexing of intra-cavity solid-state green lasers Laser display and lightning conference Japan; 2015.

41. Ma, Qianli, Chan-Qing Xu, Adrian Kitai, and David Stadler. "Speckle reduction by optimized multimode fiber combined with dielectric elastomer actuator and lightpipe homogenizer." Journal of Display Technology 12, no. 10 (2016): 1162-1167.

42. Roelandt, Stijn, Youri Meuret, An Jacobs, Koen Willaert, Peter Janssens, Hugo Thienpont, and Guy Verschaffelt. "Human speckle perception threshold for still

images from a laser projection system." Optics express 22, no. 20 (2014): 23965-23979.

43. Miyoshi, Takashi, Shingo Masui, Takeshi Okada, Tomoya Yanamoto, Tokuya Kozaki, Shin-ichi Nagahama, and Takashi Mukai. "510–515 nm InGaN-based green laser diodes on c-plane GaN substrate." Applied Physics Express 2, no. 6 (2009): 062201.

44. Campbell, F. W., and R. W. Gubisch. "Optical quality of the human eye." The Journal of physiology 186, no. 3 (1966): 558-578.

45. Janssens, Peter. "Laser projector speckle measurements." In 29th International Display Research Conference. EURODISPLAY 2009, pp. 5-7. 2009.

46. Laser Illumination and Projection Association. "Recommend practice: measurement of speckle in laboratory conditions". 2015.

47. Roelandt, Stijn, Youri Meuret, Gordon Craggs, Guy Verschaffelt, Peter Janssens, and Hugo Thienpont. "Standardized speckle measurement method matched to human speckle perception in laser projection systems." Optics express 20, no. 8 (2012): 8770-8783.

48. Zhe Cui, "Analysis of the scientific problems in laser-based display technology", Doctor dissertation, University of Science and Technology of China, 2015.

49. Hornbeck, Larry J. "The DMD TM projection display chip: a MEMS-based technology." Mrs Bulletin 26, no. 4 (2001): 325-327.

50. Tan, Kim L., Karen D. Hendrix, Markus Duelli, David M. Shemo, Aurelie Ledeur, Jerry Zieba, and Mike Greenberg. "64.2: Design and Characterization of a

Compensator for High Contrast LCoS Projection Systems." In SID Symposium Digest of Technical Papers, vol. 36, no. 1, pp. 1810-1813. Oxford, UK: Blackwell Publishing Ltd, 2005.

51. Levis, Maurice E., and Helen Gourley. "LCD projection system with polarization doubler." U.S. Patent 5,884,991, issued March 23, 1999.

52. Bruzzone, Charles L., David JW Aastuen, Roger J. Strharsky, Stephen K. Eckhardt, Michael F. Weber, and Gary T. Boyd. "Reflective LCD projection system using wide-angle Cartesian polarizing beam splitter." U.S. Patent 6,486,997, issued November 26, 2002.

53. Hornbeck, Larry J. "Current status of the digital micromirror device (DMD) for projection television applications." In Electron Devices Meeting, 1993. IEDM'93. Technical Digest., International, pp. 381-384. IEEE, 1993.

54. Evans, Allan, Grant Bourhill, and Marina V. Khazova. "Time-sequential colour projection." U.S. Patent 7,404,644, issued July 29, 2008.

55. Li, Lin, Jeffrey Brian Sampsell, Jagtar Singh Saroya, and George Stuart Vernon. "Single panel color video projection display using reflective banded color falling-raster illumination." U.S. Patent 6,870,581, issued March 22, 2005.

56. Slobodin, David E. "Segmented light pipe apparatus and method for increasing luminous efficiency of single light-valve, color video projection displays." U.S. Patent 6,334,685, issued January 1, 2002.

57. Brukilacchio, Thomas J., and Charles A. Demilo. "Light emitting diode projection system." U.S. Patent 7,832,878, issued November 16, 2010.

58. Pan, Jui-Wen, Chih-Ming Wang, Hsiao-Chin Lan, Wen-Shin Sun, and Jenq-Yang Chang. "Homogenized LED-illumination using microlens arrays for a pocket-sized projector." Optics express 15, no. 17 (2007): 10483-10491.

59. Kubota, Shigeo, and Joseph W. Goodman. "Very efficient speckle contrast reduction realized by moving diffuser device." Applied optics 49, no. 23 (2010): 4385-4391.

60. Pan, Jui-Wen, and Chi-Hao Shih. "Speckle reduction and maintaining contrast in a LASER pico-projector using a vibrating symmetric diffuser." Optics express 22, no. 6 (2014): 6464-6477.

61. Yurlov, Victor, Anatoly Lapchuk, Sangkyeong Yun, Jonghyeong Song, and Haengseok Yang. "Speckle suppression in scanning laser display." Applied optics 47, no. 2 (2008): 179-187.

62. Akram, M. Nadeem, Vladimir Kartashov, and Zhaomin Tong. "Speckle reduction in line-scan laser projectors using binary phase codes." Optics letters 35, no. 3 (2010): 444-446.

63. Wallhead, Ian, Roberto Ocaña, and Paula Quinzá "Designing a laser scanning picoprojector. Part 1: characteristics of the optical displaying system and color-management-related issues." Applied optics 51, no. 20 (2012): 4803-4809.

64. Ware, Colin, and Ravin Balakrishnan. "Reaching for objects in VR displays: lag and frame rate." ACM Transactions on Computer-Human Interaction (TOCHI) 1, no. 4 (1994): 331-356.

65. Brainard, David H., Denis G. Pelli, and Tom Robson. "Display characterization." Signal Process 80 (2002): 2-067.

66. Buckley, Edward. "Eye‑safety analysis of current laser‑based scanned‑beam projection systems." Journal of the Society for Information Display 18, no. 11 (2010): 944-951.

67. Manni, Jeffrey G., and Joseph W. Goodman. "Versatile method for achieving 1% speckle contrast in large-venue laser projection displays using a stationary multimode optical fiber." Optics express 20, no. 10 (2012): 11288-11315.

68. Mehta, Dalip Singh, Dinesh N. Naik, Rakesh Kumar Singh, and Mitsuo Takeda. "Laser speckle reduction by multimode optical fiber bundle with combined temporal, spatial, and angular diversity." Applied optics 51, no. 12 (2012): 1894-1904.

69. Povilus, Alexander P., Spencer E. Olson, Rahul R. Mhaskar, Boon-Keng Teo, Jeffrey R. Guest, and Georg Raithel. "Time averaging of multimode optical fiber output for a magneto-optical trap." JOSA B 22, no. 2 (2005): 311-314.

70. Kajenski, Peter J., Peter L. Fuhr, and D. R. Huston. "Mode coupling and phase modulation in vibrating waveguides." Journal of lightwave technology 10, no. 9 (1992): 1297-1301.

71. Ha, Woosung, Sejin Lee, Yongmin Jung, Jun Ki Kim, and Kyunghwan Oh. "Acousto-optic control of speckle contrast in multimode fibers with a cylindrical piezoelectric transducer oscillating in the radial direction." Optics express 17, no. 20 (2009): 17536-17546.

72. Graetzel, Chauncey, Marcel Suter, and Manuel Aschwanden. "Reducing laser speckle with electroactive polymer actuators." In Electroactive Polymer Actuators and Devices (EAPAD) 2015, vol. 9430, p. 943004. International Society for Optics and Photonics, 2015.

73. Bowron, John W., and Reginald P. Jonas. "Off-axis illumination design for DMD systems." In Design of Efficient Illumination Systems, vol. 5186, pp. 72-83. International Society for Optics and Photonics, 2003.

74. Chen, Xuyuan, Øyvind Svensen, and Muhammad Nadeem Akram. "Speckle reduction in laser projection using a dynamic deformable mirror." Optics express 22, no. 9 (2014): 11152-11166.

75. Shin, Sung Chul, Sin Sung Yoo, Sang Yeon Lee, Chan-Young Park, So-Yeon Park, Jae Wook Kwon, and Seung-Gyu Lee. "Removal of hot spot speckle on laser projection screen using both the running screen and the rotating diffuser." Displays 27, no. 3 (2006): 91-96.

76. Tu, Shih-Yu, Hoang Yan Lin, and Min-Ching Lin. "Efficient speckle reduction for a laser illuminating on a micro-vibrated paper screen." Applied optics 53, no. 22 (2014): E38-E46.

77. McKnight, Douglas J., and Kevin Curtis. "System and method for vibrating screens to reduce speckle." U.S. Patent 9,897,819, issued February 20, 2018.

78. Curtis, Kevin, David A. Coleman, and Gary D. Sharp. "Speckle reduction using screen vibration techniques and apparatus." U.S. Patent 8,724,218, issued May 13, 2014.

79. Curtis Kevin, Coleman Dave, McKnight Doug, Sharp Gary. "Screens for laser projection" Real D, 2015

80. Svensen, Øyvind, Xuyuan Chen, and Muhammad Nadeem Akram. "Speckle reduction in laser projection displays through angle and wavelength diversity." Applied optics 55, no. 6 (2016): 1267-1274.

81. Suzuki, Koji, Tatsuo Fukui, Shigeo Kubota, and Yasunori Furukawa. "Verification of speckle contrast measurement interrelation with observation distance." Optical Review 21, no. 1 (2014): 94-97.

82. Hedili, M. Kivanc, Mark O. Freeman, and Hakan Urey. "Transmission characteristics of a bidirectional transparent screen based on reflective microlenses." Optics express 21, no. 21 (2013): 24636-24646.

83. Freese, Robert P., David Reed, and Dale S. Walker. "Micro-lens array based light transmitting screen with tunable gain." U.S. Patent 6,829,087, issued December 7, 2004.

84. Freese, Robert P., David Reed, and Dale S. Walker. "Micro-lens array based light transmitting screen with high resolution and low imaging artifacts." U.S. Patent 6,816,306, issued November 9, 2004.

85. Sales, Tasso RM. "High-contrast screen with random microlens array." U.S. Patent 6,700,702, issued March 2, 2004.

86. Kim, Hyeon-Don, Gun-Wook Yoon, Jeongho Yeon, Joo-Hyung Lee, and Jun-Bo Yoon. "Fabrication of a uniform microlens array over a large area using self-aligned

diffuser lithography (SADL)." Journal of Micromechanics and Microengineering 22, no. 4 (2012): 045002.

87. Pauwels, Jaël, and Guy Verschaffelt. "Speckle reduction in laser projection using microlens-array screens." Optics express 25, no. 4 (2017): 3180-3195.

88. Bayer, Bryce E. "Color imaging array." U.S. Patent 3,971,065, issued July 20, 1976.

89. Toi, Takao, and Mutsumi Ohita. "A subband coding technique for image compression in single CCD cameras with Bayer color filter arrays." IEEE Transactions on Consumer Electronics 45, no. 1 (1999): 176-180.

90. Malvar, Henrique S., Li-wei He, and Ross Cutler. "High-quality linear interpolation for demosaicing of Bayer-patterned color images." In Acoustics, Speech, and Signal Processing, 2004. Proceedings.(ICASSP'04). IEEE International Conference on, vol. 3, pp. iii-485. IEEE, 2004.

91. Qianli Ma and Chang-qing Xu. "Influence of Camera on Speckle Contrast Measurement" Laser Display Conference, Yokohama, Japan, 2015.

92. Dainty, J. Christopher, ed. Laser speckle and related phenomena. Vol. 9. Springer science & business Media, 2013.

93. Yang, Owen, and Bernard Choi. "Laser speckle imaging using a consumer-grade color camera." Optics letters 37, no. 19 (2012): 3957-3959.

94. Holm, Jack M. "Strategy for pictorial digital image processing." U.S. Patent 6,249,315, issued June 19, 2001.

95. Born, Max, and Emil Wolf. Principles of Optics: Electromagnetic Theory of Propagation, Interference and Diffaction of Light. Pergamon Press, 1959.

96. Ma, Qianli, ChangQing Xu, and Hai Ming. "Viewing angle dependence of speckle contrast ratio in laser projection system." In Advances in Display Technologies V, vol. 9385, p. 938507. International Society for Optics and Photonics, 2015.

97. Lin, Hoang Yan, Wann-Diiang Tyan, and Ying Tsung Lu. "High-gain wide-viewing-angle null-hot-spot optical diffuser useful for display screen application." In Display Devices and Systems, vol. 2892, pp. 64-72. International Society for Optics and Photonics, 1996.

98. Burt, Peter J. "Fast filter transform for image processing." Computer graphics and image processing 16, no. 1 (1981): 20-51.

99. Deng, Guang, and L. W. Cahill. "An adaptive Gaussian filter for noise reduction and edge detection." In Nuclear Science Symposium and Medical Imaging Conference, 1993., 1993 IEEE Conference Record., pp. 1615-1619. IEEE, 1993.

100. Katagiri, Baku, Tetsuya Miyashita, Takahiro Ishinabe, and Tatsuo Uchida. "Novel screen technology for high‐contrast front‐projection display by controlling ambient‐light reflection." Journal of the Society for Information Display 11, no. 3 (2003): 585-590.

101. Kilpi, Katriina, Wendy Van den Broeck, and An Jacobs. "Design of a large-scale subjective test in the cinema." In Integrated Network Management (IM 2013), 2013 IFIP/IEEE International Symposium on, pp. 1340-1345. IEEE, 2013.

102. Curcio, Christine A., Kenneth R. Sloan, Robert E. Kalina, and Anita E. Hendrickson. "Human photoreceptor topography." Journal of comparative neurology 292, no. 4 (1990): 497-523.

103. Wandell, Brian A. Foundations of vision. Vol. 8. Sunderland, MA: Sinauer Associates, 1995.

104. Yu, Nan Ei, Ju Won Choi, Heejong Kang, Do-Kyeong Ko, Shih-Hao Fu, Jiun-Wei Liou, Andy H. Kung et al. "Speckle noise reduction on a laser projection display via a broadband green light source." Optics express 22, no. 3 (2014): 3547-3556.